Imperial College London
Department of Electrical and Electronic Engineering
Control and Power Research Group

Modelling and Analysing the Flexible Operation of Interconnectors in the Multi-Service Electricity Market

Qingwen Pang

Supervisor: Prof. Goran Strbac

Co-supervised by: Dr. Antonio De Paola
Dr. Vincenzo Trovato

A thesis submitted to
Imperial College London
For the degree of Doctor of Philosophy
September 2023

Declaration of Originality

I hereby declare that the content contained within this thesis is the results of my own work, and that any ideas or quotations from other works are appropriately referenced.

Copyright Declaration

The copyright of this thesis rests with the author. Unless otherwise indicated, its contents are licensed under a Creative Commons Attribution-Non Commercial 4.0 International Licence (CC BY-NC).

Under this licence, you may copy and redistribute the material in any medium or format. You may also create and distribute modified versions of the work. This is on the condition that: you credit the author and do not use it, or any derivative works, for a commercial purpose.

When reusing or sharing this work, ensure you make the licence terms clear to others by naming the licence and linking to the licence text. Where a work has been adapted, you should indicate that the work has been changed and describe those changes.

Please seek permission from the copyright holder for uses of this work that are not included in this licence or permitted under UK Copyright Law.

Qingwen Pang

19^{th} July, 2023

Abstract

This thesis addresses the challenges posed by the increased penetration of renewable energy sources, particularly the reduction in system inertial response, which affects post-fault frequency dynamics. The research focuses on integrating interconnectors as alternative flexibility providers alongside traditional synchronous generators. A novel modelling setup is introduced for interconnectors that allows them to provide both energy and inertia-dependent primary frequency response simultaneously, marking a significant shift from traditional operations that only manage energy flow. The thesis also explores the economic and operational impacts of these multi-service interconnectors within competitive market environments. It contrasts two market paradigms: a centralized approach, where the interconnector is operated to minimize system operational costs, and a market-based approach, where the interconnector functions as profit-maximizing, privately-owned asset. The advantages of the multi-service model across these market paradigms are analyzed and compared using common market indicators such as social welfare and interconnector revenues.

The research further employs a sampling-based methodology to evaluate system performance under varying conditions, specifically analyzing the impact of wind and demand variability on interconnector operations. Additionally, the thesis explores the impact of incorporating ancillary services from different system layers on interconnectors. It investigates the synergy and interaction between Demand Side Response (DSR) from Thermostatically Controlled Loads (TCLs) and flexible interconnectors to achieve enhanced system performance under proposed market paradigms. The research finally extends to more complex network topologies, such as multi-area systems in a meshed network, exploring both regulated and market operations. Using the enumeration method to capture the market behaviour and estimate the market equilibrium, it offers insights into the planning, operation, and market strategies for interconnectors in realistic power system topologies, highlighting their potential to enhance the security and efficiency of low-carbon power systems.

Publications

Journal Papers:

Q. Pang, A. De Paola, V. Trovato and G. Strbac, "Value of Interconnectors Operating in Simultaneous Energy-Frequency Response Markets," *IEEE Transactions on Power Systems*, vol. 37, no. 5, pp. 3381-3393, 2022.

Q. Pang, V. Trovato, A. De Paola and G. Strbac, "Market-Based Operation of Interconnectors in a Multi-Area Power Network With Meshed Topology," *IEEE Transactions on Energy Markets, Policy and Regulation*, vol. 2, no. 1, pp. 79-91, March 2024

Conference Paper:

Q. Pang, A. De Paola, G. Strbac and V. Trovato, "The impact of variable wind and demand levels on the flexible operation of interconnectors in Great Britain," *2022 IEEE 7th International Energy Conference (ENERGYCON)*, Riga, Latvia, 2022, pp. 1-7

Acknowledgements

First and foremost, I would like to express my deepest gratitude to my supervisor Professor Goran Strbac for his persistent guidance, insightful suggestions and constant encouragement throughout my PhD journey. His constructive instruction, illuminating discussion and, most importantly, unwavering support, contributed significantly to my professional growth.

I would also like to extend my sincerest thanks to my co-supervisor, Dr. Antonio De Paola, and Dr. Vincenzo Trovato. Their expertise and willingness to assist have been invaluable in overcoming challenges that I encountered in my research. All their constructive inspirations from the start of my PhD, critical questions and insightful feedback during the research, and their thorough guidance in my work and final writing, have directly impact the quality and rigor of this thesis.

I am also immensely grateful to my colleagues in Control and Power Group at Imperial College London. The good research atmosphere and supportive community, played a significant role in my research life. Special thanks my colleagues in Room 1111. Our friendly and supportive environment, the brainstorming discussions have make the research hours rewarding and enjoyable.

Beyond the professional sphere, I am thankful for my friends, Meng Zhang, Yian Jin, Xiaoyu Chen, who have stood by me through this whole journey. Their unwavering faith, emotional support and companionship are immeasurable and crucial part of not just my PhD journey but my personal well-being.

Last but not least, my profound gratitude goes to my family and my parents, Yunsheng Pang and Shuying Wang. Their enduring love and belief in me are always my constant source of strength and motivation. They've stood by me through every trough and peak, providing the endless patience and guidance whenever I felt disheartened or lost. This journey would not have been possible without their love, encouragement and supports.

Contents

Abstract **7**

Acknowledgements **11**

List of Acronyms **18**

List of Figures **27**

List of Tables **31**

1 Introduction **33**

1.1 Background and Thesis Context 33

1.1.1 Decarbonization and Challenges in the Power System 33

1.1.2 Requirements for Flexibility 34

1.1.3 Value of Electricity Interconnectors: Current Practice 37

1.1.4 Market Reformation 39

1.2 Problem Statement and Research Scope 40

1.3 Original Contributions 41

1.4 Thesis Outline 43

2 Value of Interconnectors Operating in Simultaneous Energy-Frequency Response Markets **47**

2.1 Introduction . . . 48

2.2 Modelling the Inertia-Dependent Frequency Response . . . 51

2.2.1 Dynamics of Frequency Evolution and Security Standards . . . 51

2.2.2 Frequency Response Constraints . . . 53

2.3 Simultaneous Exchange of Energy and Frequency Response through the Interconnectors . . . 56

2.3.1 Technology Discussion and Assumptions . . . 56

2.3.2 Model setup . . . 58

2.3.3 Traditional Centralized Approach (CA) . . . 59

2.3.4 Model Assumptions of the UC Problem . . . 60

2.3.5 CA Formulation . . . 60

2.4 Case Study . . . 64

2.4.1 Base Case . . . 66

2.4.2 Impact of Varying Interconnector Capacity . . . 66

2.4.3 Impact of Varying Wind Capacity . . . 68

2.5 Conclusion . . . 69

2.6 Future Works . . . 70

3 Market-Based Operation of the Multi-Service Interconnectors **72**

3.1 Introduction . . . 73

3.2 Market Approach (MA) . . . 75
3.2.1 Analytical Formulation for Area A and B . . . 77
3.2.2 Analytical Formulation for Interconnector . . . 77
3.2.3 Model Framework and Implementation Scheme . . . 81
3.3 Case Studies . . . 82
3.3.1 Base Case - Comparisons between CA and MA . . . 83
3.3.2 Impact of Varying the Interconnector Capacity . . . 87
3.3.3 Increasing Synchronous Generation Costs in France . . . 88
3.3.4 Changing the Maximum Infeed Loss in GB . . . 90
3.4 Conclusion . . . 91
3.5 Future Works . . . 92
3.5.1 Incorporating the Cost of Losses . . . 93
3.5.2 Impact of Outages . . . 94

4 Assessment of the Impact of Wind and Demand Variability on the Flexible Operation of Interconnectors 96

4.1 Introduction . . . 97
4.2 Model Formulation . . . 98
4.2.1 Centralized Approach (CA) and Market Approach (MA) . . . 99
4.3 Assessment Methodology . . . 99
4.4 Case Studies . . . 103
4.4.1 Seasonal and yearly aggregated results . . . 103

4.4.2 Yearly-aggregated results under CA and MA . . . 105

4.4.3 Correlation Assessment . . . 107

4.5 Conclusion . . . 110

4.6 Future Works . . . 110

5 Flexible Operation of Multi-Service Interconnectors with Thermostatically Controlled Loads 113

5.1 Introduction . . . 114

5.2 Modelling and Control of the Aggregated Thermostatically Controlled Loads . . . 117

5.2.1 Aggregated TCL Modelling . . . 117

5.2.2 Demand Side Response Formulation of TCLs . . . 120

5.3 Optimal Scheduling of Multi-Service Interconnector and TCLs . . . 122

5.3.1 Centralized Approach (CA) Formulation . . . 123

5.3.2 Market Approach (MA) Formulation . . . 126

5.4 The Implementation of the MA . . . 129

5.5 Case Studies . . . 131

5.5.1 Base Case . . . 133

5.5.2 Comparison Between Models with/without Flexible TCLs . . . 135

5.6 Conclusions . . . 137

5.7 Future Works . . . 138

6 Market-Based Operation of Interconnectors in a Multi-Area Power Network with Meshed Topology **140**

6.1 Introduction . . . 141

6.2 Modelling and Assumptions . . . 144

6.3 Formulation . . . 147

6.3.1 Centralized Approach (CA) . . . 148

6.3.2 Market Approach (MA) . . . 150

6.4 Numerical Solution . . . 153

6.5 Case Studies . . . 157

6.5.1 Focus on the France-Ireland Link - Base Case . . . 159

6.5.2 Operation of Link1 and Link2 under MA . . . 162

6.5.3 The Value of Providing Inter-Area FR . . . 163

6.6 Discussions . . . 165

6.7 Conclusions . . . 165

6.8 Future Works . . . 167

7 Conclusions and Future Works **170**

7.1 Conclusions . . . 170

7.2 Future works . . . 175

Bibliography **177**

List of Acronyms

RES Renewable Energy Sources

OCGT Open Cycle Gas Turbines

CCGT Combined Cycle Gas Turbines

HVDC High Voltage Direct Current

ENTSO-E European Network of Transmission System Operators for Electricity

IEM Internal Energy Market

LCC Line Commutated Converter

VSC Voltage Source Converter

PWM Pulse Width Modulation

IGBT Insulated gate-controlled transistors

FR Frequency Response

SQSS Security and Quality of Supply Standard

RoCoF Rate of Change of Frequency

QSS Quasi-Steady-State

UC Unit Commitment

CA Centralized Approach

MA Market Approach

LP Linear Programming

PDFs Probability Distribution Functions

DSR Demand Side Response

TCLs Thermalstatically Controlled Loads

MPI Multi-Purpose Interconnector

Nomenclature

Chapter 2 & Chapter 3

τ	Index of generation technologies
k	Index of power system
$\mathcal{G}$	Set of generators
ξ_t	Set of decision variables
$\alpha_{k,\tau}$	No load cost of generation technology τ in area k (£/MWh)
$\beta_{k,\tau}$	Linear production cost of generation technology τ in area k (£/MWh)
$\gamma_{k,\tau}$	Quadratic production cost of generation technology τ in area k (£/MW^2h)
r_τ	FR headroom of technology τ
s_τ	FR/dispatch level slope of generation τ
L_k	System demand at area k [MW]
Δt	Time step duration [h]
G_τ^{max}	Total installed capacity of technology τ [MW]
D_k	Load damping parameters (s)
ν_k	Time parameter in RoCoF constraints [Hz]
f_k^{roc}	Frequency parameters in RoCoF constraints [Hz]

σ_k Delivery time of FR [s]

Δf_k^{qss} Maximum frequency deviation requirement at quasi-state-state [Hz]

Δf_k^{max} Maximum frequency deviation requirement at Nadir [Hz]

Δf_k^{nadir} Frequency deviation at Nadir [Hz]

ΔG_k Maximum infeed loss in area k [MW]

$h_{k,\tau}$ Inertia constant of technology τ in area k [s]

h_k Inertia of the infeed generation loss in area k [s]

F^{max} Total capacity of interconnector [MW]

$H_{k,\tau}$ Commitment decisions of technology τ in area k [p.u.]

$P_{k,\tau}$ Power output of generation technology τ at area k [MW]

$R_{k,\tau}$ Frequency response reserved by generation technology τ at area k [MW]

F^p Power flow on the line [MW]

F^r Power headroom reserved for frequency response on the line [MW]

π_k Price of power in area k [£/MWh]

ρ_k Price of FR in area k [£/MWh]

$\delta\pi$ Price differentials of power [£/MWh]

$\delta\rho$ Price differentials of FR [£/MWh]

$\hat{R}_k$ Aggregated FR in area k, [MW]

$\hat{H}_k$ System post-fault inertial response [MWs^2]

φ_k Optimized unit commitment cost in Area k [£]

φ_{INT} Optimized interconnector revenues[£]

Chapter 4

m Index of seasons

s Index of sample

j Index of historical year

N_a Number of sampled elements in each of four seasons

N Sample size

φ_s MA solutions under MA in sample s [£]

ϕ_s CA solutions under MA in sample s [£]

SD Sets of demand samples

SD Sets of wind generation samples

$S\tilde{D}$ Sets of demand samples

$S\tilde{W}$ Sets of wind generation samples

$\Delta\pi$ Price differentials of power [£/MWh]

$\Delta\rho$ Price differentials of FR [£/MWh]

Chapter 5

τ Index of generation technologies

k Index of power system

x Index of for individual TCL device

$\mathcal{S}$ Set of discrete energy level of TCLs

ξ_t Set of decision variables

T_{off} Ambience temperature [$^{\circ}C$]

T_{on} Asymptotic cooling temperature [$^{\circ}C$]

η Thermal time constant of the TCL [h]

S_A^{TCL} Aggregated TCLs energy level at area A [MWh]

P_A^{TCL} Aggregated TCLs power consumption at area A [MW]

R_A^{TCL} Aggregated TCLs frequency response at area A [MW]

$\hat{S}_{A,max}^{TCL}$ Maximum energy of the aggregated TCLs at area A [MWh]

$\hat{S}_{A,min}^{TCL}$ Minimum energy of the aggregated TCLs at area A [MWh]

$\hat{P}_{A,max}^{TCL}$ Maximum power consumption of the aggregated TCLs at area A [MW]

$\hat{P}_{A,min}^{TCL}$ Minimum power consumption of the aggregated TCLs at area A [MW]

w Time window (s)

ϵ Tolerance value for convergence check

λ Coefficient of penalty term

$\alpha_{k,\tau}$ No load cost of generation technology τ in area k (£/MWh)

$\beta_{k,\tau}$ Linear production cost of generation technology τ in area k (£/MWh)

$\gamma_{k,\tau}$ Quadratic production cost of generation technology τ in area k (£/MW^2h)

r_τ FR headroom of technology τ

s_τ FR/dispatch level slope of generation τ

L_k System demand at area k [MW]

Δt Time step duration [h]

G_{τ}^{max} Total installed capacity of technology τ [MW]

D_k Load damping parameters (s)

ν_k Time parameter in RoCoF constraints [Hz]

f_k^{roc} Frequency parameters in RoCoF constraints [Hz]

σ_k Delivery time of FR [s]

Δf_k^{qss} Maximum frequency deviation requirement at quasi-state-state [Hz]

Δf_k^{max} Maximum frequency deviation requirement at Nadir [Hz]

Δf_k^{nadir} Frequency deviation at Nadir [Hz]

ΔG_k Maximum infeed loss in area k [MW]

$h_{k,\tau}$ Inertia constant of technology τ in area k [s]

h_k Inertia of the infeed generation loss in area k [s]

F^{max} Total capacity of interconnector [MW]

$H_{k,\tau}$ Commitment decisions of technology τ in area k [p.u.]

$P_{k,\tau}$ Power output of generation technology τ at area k [MW]

$R_{k,\tau}$ Frequency response reserved by generation technology τ at area k [MW]

F^p Power flow on the line [MW]

F^r Power headroom reserved for frequency response on the line [MW]

π_k Price of power in area k [£/MWh]

ρ_k Price of FR in area k [£/MWh]

$\hat{H}_k$ System post-fault inertial response [MWs^2]

Chapter 6

i Index of power systems

m Index of interconnectors

x Index of generation technologies

$\mathcal{N}$ Set of power systems

$\mathcal{M}$ Set of interconnectors

$\mathcal{X}$ Set of generation technologies

Ψ_{CA} Set of decision variables under CA

Ψ_{MA} Set of decision variables under MA

$\mathbf{A}$ Incidence matrix of network topology

$c'_{i,x}$ No load cost of generation technology τ in area i (£/MWh)

$c''_{i,x}$ Linear production cost of generation technology x in area i (£/MWh)

$c'''_{i,x}$ Quadratic production cost of generation technology x in area i (£/MW^2h)

r_x FR headroom of technology x

s_x FR/dispatch level slope of generation x

L_i System demand at area i [MW]

Δt Time step duration [h]

$\bar{G}_x$ Total installed capacity of technology x [MW]

D_i Load damping parameters (s)

ν_i Time parameter in RoCoF constraints [Hz]

f_i^{roc} Frequency parameters in RoCoF constraints [Hz]

σ_i Delivery time of FR [s]

Δf_i^{qss} Maximum frequency deviation requirement at quasi-state-state [Hz]

Δf_i^{max} Maximum frequency deviation requirement at Nadir [Hz]

Δf_i^{nadir} Frequency deviation at Nadir [Hz]

ΔG_i Maximum infeed loss in area i [MW]

$h_{i,x}$ Inertia constant of technology x in area i [s]

h_i Inertia of the infeed generation loss in area i [s]

$\hat{F}_m$ Total capacity of interconnector m [MW]

$H_{i,x}$ Commitment decisions of technology τ in area i [p.u.]

$P_{i,x}$ Power output of generation technology τ at area i [MW]

$R_{i,x}$ Frequency response reserved by generation technology x at area i [MW]

π_i Price of power in area i [£/MWh]

ρ_i Price of FR in area i [£/MWh]

$\hat{H}_i$ System post-fault inertial response [MWs^2]

F_m^p Power flow on the line m [MW]

F_m^r Power headroom reserved for frequency response on the line m [MW]

Θ_m Congestion surplus function of the line m [MW]

y Step in iteration

Θ_m Congestion surplus function of the line m [MW]

List of Figures

2.1 Post-fault frequency dynamics. 52

2.2 Schematics of the two-area power system connected by an interconnector. 58

2.3 Response characteristics of the synchronous generator. 62

2.4 GB (A) and France (B) generation mix and demand profile under CA. 65

2.5 The capacity repartition of the interconnector under the multi-service model and energy-only model. 67

2.6 The capacity repartition of the interconnector under cases with different GB wind installation level (a) 40GW (b) 80GW (c) 100GW. 69

3.1 Implementation scheme of the MA. 76

3.2 Schematic representation of the resolution procedure for the MA approach and of the key interactions between the decision variables. 82

3.3 GB and France generation mix and demand profile under MA. 84

3.4 The capacity repartition of the interconnector in the CA and MA. 84

3.5 Electricity and FR price differentials in the CA and MA scenarios. 85

3.6 Energy price differentials for different generation cost in France (MA). 89

3.7 Capacity allocation of the interconnector for different cost parameters of thermal generation in France (MA). 89

3.8 Interconnector capacity allocation in the MA case, for different values of maximum infeed loss in GB and for increasing values of system inertia. 90

4.1 Comparison of demand levels (top) and wind half-hourly generation (bottom) between France and GB. Red and blue traces represent the half-hourly average values for France and GB, respectively. The blue boxes correspond to the 25^{th}-75^{th} percentiles of the GB profiles, whose minimum and maximum half-hourly values are indicated in black. 100

4.2 Hourly frequency plot of GB net demand (demand minus wind generation) in the considered dataset. 100

4.3 Line capacity allocation in CA, MA for different GB net demand level. 106

4.4 Electricity and FR price differentials between GB and France in CA and MA for different GB net demand level. 106

4.5 Line revenue and operational cost differentials between CA and MA for different levels of GB net demand. 109

4.6 Line revenue and operational cost differentials between CA and MA for different levels of energy capacity withdraw in MA. 110

5.1 Schematics of the two-area interconnected power system with DSR. 123

5.2 Interactions among market participants in MA 127

5.3 Wind and Demand Profiles in GB (A) and France (B). 132

5.4 The capacity repartition of the interconnector in the CA and MA. 134

5.5 Power and FR services allocation profile of TCLs. 134

5.6 The power and FR prices in GB under CA and MA. 134

5.7 The energy profile of TCLs 135

5.8 The capacity repartition of the interconnector in the model with/without TCLs. 136

6.1 Schematics of the multi-area power system with a mesh topology. 145

6.2 Interactions between the integrated power system and the independent merchant interconnector (taking Link3 as example) under the MA. 153

6.3 Graphical representation of the proposed enumeration approach for the calculation of the approximate market solution. 155

6.4 Graphical representation of the considered GB-Ireland-France case study. 157

6.5 Wind and demand profiles in areas (a) GB (b) France (c) Ireland. 158

6.6 Daily variations in system operational cost (blue), link 1 revenue (red), link 2 revenue (black) and link 3 revenue (grey) between MA and CA. The numbers represent percent variations. 160

6.7 Interconnector capacity allocation for (a) Link1 (b) Link2 (c) Link3. 161

6.8 Electricity and FR availability price differentials between linked areas (a) Link1 (France-GB) (b) Link2 (Ireland-GB) (c) Link3 (Ireland-France). 161

List of Tables

2.1 Generation characteristics 65

2.2 Multi-service VS. energy-Only cases comparison 66

2.3 Sensitivity analysis on the link capacity under multi-service framework 67

2.4 Sensitivity analysis on wind installation level in GB 68

3.1 Base case results 85

3.2 Multi-service VS. energy-only exchange over the interconnector 86

3.3 Results of sensitivity study on interconnector capacity 87

3.4 Sensitivity to the thermal generation cost in France 88

3.5 Sensitivity to the maximum infeed loss in Great Britain 90

4.1 Seasonal wind and net demand level 104

4.2 Operational cost and line revenue results under MA 104

4.3 Yearly aggregated results under CA and MA 105

4.4 Correlation of wind and demand with computed metrics 109

5.1 TCL parameters 132

5.2 Model with/without TCLs 136

6.1 Characteristics of synchronous and wind generation 158

6.2 Daily system results 160

6.3 Market-based operation on different lines 162

6.4 System results in Case A and Case B relative to base case 164

Chapter 1

Introduction

1.1 Background and Thesis Context

1.1.1 Decarbonization and Challenges in the Power System

Climate change has increasingly raised the global concerns and attentions which urge governments around the world to take initiatives and implement effective decolonization actions to reduce the CO_2 emissions. The IPPC global report, released in 2019, amplified this urgency, signaling a transformative moment in our collective approach to the environment [1]. In response, the European Commission (EC) has committed to a significant reduction in greenhouse emission, targeting at least 55% reduction by 2030 compared to the baseline level in 1990, and realizing no net emissions of greenhouse gases by 2050 [2]. Meanwhile, the UK, having made remarkable progress in mitigating greenhouse gas emission since 1990, aims to achieving climate-neutral by 2050, which is in line with the EU target [3]. The 26^{th} UN Climate Change Conference of the Parties (COP26) which is held in Glasgow in 2021, accentuated the importance of the world reaching Net Zero emission by 2050. The goal is pivotal to limit the global temperature rises within 1.5 degree, the benchmark that is set out in Paris Agreement [4].

The energy supply sector in Great Britain (GB) was the predominant contributor to greenhouse gas emissions until 2016, with the high combustion of fuels in electricity generation. After the

improvement in technology, the accelerated growth of renewable generation, and the transition to low-carbon content fuels, e.g., gas, the emission from the energy supply sector have drastically reduced by 70% between 1990 and 2022. It was estimated that the energy supply sector accounts for 21% GB's emission in 2020 [5]. However, this transformation was accompanied by a concerning rise in the transport sector. Since 2016, the transport emission has overtaken the energy supply sector and become the primary contributor to emissions. Alarmingly, there has been a stagnation in the reduction in this sector, with only 5% reduction of emissions between 2019 and 1990 [5].

To address these challenges, the Climate Change Committee (CCC) raised the climate ambitions for the GB, particularly targeting the electricity sector to attain net-zero emission by 2035. The CCC lays out that the decarbonization of the heat and transportation sector will be supported by the carbon-zero electricity system. Consequently, a surge of approximate 50% in electricity demand is anticipated over the next 15 years, which poses substantial challenges for the future electricity grid.

In this context, the off-shore wind has emerged as the backbone of the GB electricity system, expanding from the initial promise of 40GW in 2030 to 100GW or more by 2050 [6]. Such an influx of clean electricity can significantly contribute to the high emission sectors, including energy supply and transportation.

1.1.2 Requirements for Flexibility

The transition towards Renewable Energy Sources (RES) based electricity sector signifies the major shift from the current fossil-fuel based paradigm. However, the inherent characteristics of these two power sources introduce fundamental changes in the power system operation. Conventional generations, characterized by synchronous generators, stores substantial kinetic energy within their rotating mass. This kinetic energy provides the system with rotational inertia that is a crucial aspect in supporting system stability. Conversely, RES, particularly wind and solar generations, interface with the grid through power electronic converters. Under standard configurations, this setup either lacks rotational inertia or decouples its inertia from

the grid, which impedes the provision of inertial response to the system during load changes and other disturbances [7]. The average annual inertia has fallen by 40% in the last decade due to the replacement [8].

The resulting low inertia poses several challenges to the power system operation. One of the primary concerns is related to the frequency stability. The system characterized by insufficient inertia witnesses accelerated frequency dynamics, leading to large post-fault frequency deviations and associated rates of change [9]. Such dynamics can trigger undesirable events, including unexpected load-shedding due to large frequency deviation, or the disconnection of generators through the Rate of Change of Frequency (RoCoF) sensitive protection scheme, which would further exacerbate the issue [10]. As a consequence, the requirement for system flexibility increase, particularly for the services related to system balancing.

The security and reliability of the power system require the balance between the supply and demand to maintain the system frequency as close as possible to its nominal level (50 or 60 Hz). In GB, the National Grid Electricity System Operator (ESO) bears the responsibility to ensure the adequate generation on standby to maintain the system frequency at 50Hz with a permissible deviation of 1% under any credible circumstances that may cause frequency variations. Various circumstances necessitate different types of frequency responses. These services can be classified into dynamic frequency services, which is refers to the continuously provided service that is procured to manage the second-by-second system frequency variation, and the non-dynamic response, which is typically the service that is triggered by predefined frequency thresholds [11].

Tradition real-time system balancing services are carried by the flexible synchronous generators running part-loaded, which significantly undermines both the production efficiency and the cost efficiency. Such inefficiencies are further exacerbated during the off-peak hours, particularly when compounded by a high penetration of RES. In addition, the non-renewable, low-carbon technologies, like nuclear plants, play a significant role in electricity sector, primarily to meet the emission targets. Despite their contribution, these technologies lack the operational flexibility that is inherent to the existing gas turbine units, such as Open Cycle Gas Turbines (OCGT) and

Combined Cycle Gas Turbines (CCGT). If such flexible conventional generation remains the only source of response services, the cost of integrating RES will rise, simultaneously limiting the ability of the system to accommodate RES output. Therefore, it becomes imperative to explore alternative and cost-efficient means for maintaining system balance and stability.

Many studies have explored the challenges arising from the growing penetration of variable RES, emphasizing the increasing demands for flexibility and stability issues that future power systems will face [12] [13] [14]. Work [15] examined the potential solutions from the emerging flexible technologies in the future GB power system, and broadly classified the primary sources of ancillary services into four categories from different system layers:

a. Generation side: the enhanced flexibility from the synchronous generator (shorter required commitment time, lower minimum stale generation, and higher maximum response capability), coupled with the investigation into the feasibility of RES in providing ancillary services (frequency response provision from variable speed wind turbines), are identified as possible solutions to address the increased operational challenges.

b. Networks: cross-border interconnectors, which connect electricity systems of neighbour countries, enhance system security by offering pathways to access more efficient resources and services across an expanded geographical area, thereby overcoming local constraints. This work specifically evaluates the value of the flexible operation of the interconnector in ancillary service provision and evaluate their contributions to the overall stability and efficiency of the power system.

c. Demand side: under the wide concept of smart grid, the flexible demands allow consumers, ranging from industrial operation to residential households, to contribute to the ancillary provision cost effectively. Common flexible loads options, including smart home appliances, electrical vehicles with smart control strategies, flexible heat pump and HVAC loads, etc., are widely investigated and explored in demand side response (DSR) initiatives. This work adopts Thermostatically Controlled Loads (TCLs) as a particularly promising solution to augment system flexibility and contribute to the delivery of ancillary services.

d. Other technologies: such as the energy storage, which stands as the one of the most efficient and versatile solutions to provide ancillary services. The broad spectrum of the storage technology enable it to offer a range of services, from reserves, frequency supports to peak demand reduction.

1.1.3 Value of Electricity Interconnectors: Current Practice

Electricity interconnectors, which facilitate the flow of electric power between areas, present significant socio-economic value. They hold the potential to reshape the way power systems produce, transfer and consume energy, aiming to enhance system energy efficiency, reduce operational costs, strengthen system supply security and promote cost-effective integration of renewables. In this thesis, the flexible operation of the interconnector is introduced as the viable option for the power system economic and secure operation.

European Commission identified five contributions that electricity interconnectors would bring [16]:

- Price stabilization: One of the pivotal contributions of electricity connectors is the reduction in electricity prices as well as price volatility. By enabling the integration and utilization of advanced and efficient energy technologies, they allow systems to exploit more cost-efficient complementarities that exist within the diverse energy portfolios across Europe and reducing the local pressure during the event, such as demand spike.

- Optimal utilization of renewables: Interconnectors are instrumental in the effective distribution of renewable energy. They ensure that energy generated from renewable sources can be dispersed over a broader grid, mitigating the need for curtailments. The enhanced integration and utilization of renewables foster a more sustainable energy future.

- Enhanced security of supply: An interconnected energy system ensures that each area has diversified electricity sources, effectively reducing their dependency on local or indigenous production. This diversification inherently increases the security of the energy supply.

- Fostering Cooperation: Interconnectors pave the way for a more integrated electricity market across European Member States. This integration fosters cooperation, aligning policies, tariffs, and strategies, thus promoting a unified vision towards energy management.

- Industrial and Economic Opportunities: The development and maintenance of interconnectors provide a boost to the industrial sector, offering job opportunities. They reinforce the leadership of Europe in sustainable, low-carbon sectors, fostering innovation and technological advancements.

In light of above-mentioned advantages and low-carbon targets, it is imperative for Europe to intensify its inter-country electrical connectivity. The EU has set the goal for interconnection to achieve a minimum of 15% by 2030 to prompt EU nations to synergize their electricity productions [16].

For island power systems, where the operation faces higher cost and security requirement to transit to the low-carbon system due to their inherent geographic characteristics, the role of interconnectors becomes more crucial. Taking the GB as a case in point, as of 2023, the GB electricity market has 6GW interconnector capacity resorted to France, Netherlands, Belgium, Northern Ireland and Republic of Ireland [17]. The government has set the progressive roadmap, targeting an expansion of the interconnector capacity to 18GW and expects the cost saving of £20bn from 2020 to 2045 [18]. Moreover, the strategy is aligned with GB's environmental commitments. The enhanced interconnection is anticipated to substantially decrease the carbon footprint associated with Great Britain's energy consumption by facilitating the import and export of clean energy across Europe. The internal estimation indicates that the use of interconnectors linking Great Britain with Europe could lead to a reduction of 100 million tonnes of carbon emissions within Britain from 2020 to 2030, highlighting the environmental benefits of enhanced cross-border energy collaboration [18].

With the advantageous position, the Ireland has the most potent wind resources with highest average wind speed in Europe. The significant renewable potential, also introduce intricate

challenges in energy management. If left unaddressed, this issue could lead to wind curtailment, manifesting the under-utilization of wind potential, and also system instability. In this context, the interconnector has been demonstrated as the pivotal asset in Irish power system from the market perspective in lowering domestic electricity prices [19] [20]. Beyond the economic dividends, a theoretical exploration unveils the potential of interconnectors in mitigating wind curtailment scenarios [21]. The interconnector can not only optimize energy utilization but also consolidate Ireland stature in European renewable energy landscape.

1.1.4 Market Reformation

To foster the evolution of the energy system, the European Network of Transmission System Operators for Electricity (ENTSO-E) has investigated into the challenges and opportunities for the electricity system from both the operational and market viewpoints, offering a set of solutions to ensure a secure transition to low-carbon system. The fit-for-purpose market design is essential to effectively support the rapid transition of energy system.

The ENTSO-E, comprising 43 TSOs, has developed a market design vision for 2030 in response to the challenges on the congestion management issues and seek efficient solutions to reconcile the market outcome [22]. TSOs are dedicated to establishing a proficient and smoothly-operated Internal Energy Market (IEM), emphasizing the significance of cross-border trading.

Currently, two primary regulatory frameworks coexist for the development of cross-border interconnectors: the regulated model and the merchant model. In the regulated model, interconnectors are treated as part of the regulated asset base for Transmission System Operators (TSOs). Conversely, in the merchant model, a third-party developer takes on the responsibility of proposing and developing the interconnector project, often driven by higher incentives. To mitigate investment risks while maintaining attractive incentives, hybrid models like the 'Cap and Floor' regulatory framework have been proposed in some cases [23].

As of 1 January 2021, the GB is excluded from the EU's IEM, and the EU-UK Trade Cooperation Agreement has been provisionally applicable. The interconnector on the borders of

GB and Europe cannot be managed with the EU market coupling tools. This highlights the necessity for development of new arrangement for the power trading over interconnectors. In this context, the market-based operation and development of merchant interconnector can be the viable solution for the future market.

In GB, interconnectors already operate as stand-alone companies with regulatory approval, rather than centrally organized transmission infrastructures seen in other European cases. [17]. Non-regulated merchant interconnectors (e.g. ElecLink between France and GB [24]) also co-exist in the interconnector regulatory setup of the European Union. Under EU Electricity Regulation 2019/943, TSOs are expected to promote non-discriminatory, market-based solutions for the development of energy exchanges and the coordinated allocation of interconnector capacity. This includes the integration of balancing and reserve services, reinforcing the transition to the low-carbon power system [25].

1.2 Problem Statement and Research Scope

The research scope of this thesis encompasses the in-depth examination of the flexible operation of interconnector in the future low-carbon power system. In particular, this thesis is centered around the role of interconnector inhabit under different market paradigms.

Currently, the principal function of cross-border interconnectors, especially within the GB and EU regions, revolves around facilitating the energy trade. However, the potential for interconnectors to provide flexibility - crucial for the low-carbon power system, remains untapped, especially on a commercial scale. Under the prevalent deregulated market environment, it is anticipated that the capacity allocation of interconnectors will be determined by non-discriminatory, market-based solutions. These solutions are projected to integrate ancillary services, ensuring a fair and sustainable energy market.

1.3 Original Contributions

In the context of the problem background and research scope identified, the original contributions of the thesis are summarized as follows:

1) Multi-service operation model for interconnectors

The development of a novel paradigm for the operation of interconnectors, which envisages simultaneous allocation of the interconnector capacity for exchange of energy and frequency response services. The proposed framework aims at enabling the potential role of interconnectors as key assets in the safe and efficient operation of the decarbonized systems in the future. The multi-service and flexible operation of the interconnector is determined within a holistic framework that accounts for the scheduling decisions of the connected power systems under inertia-dependent FR constraints. To assess the effectiveness and economic viability of this new operational paradigm, a cost-based centralized approach (CA) is adopted as the benchmark framework. This approach establishes the lower bound of the operational cost, serving as a critical reference point. It involves an explicit evaluation of the value of energy and FR services exchanged over the interconnector. By comparing the performance and costs associated with the novel multi-service framework, a clearer and comprehensive understanding of the benefits and potentials offered by by this innovative framework can be obtained. This insight is crucial for facilitating the effective deployment and management of interconnector assets within the future modern power grids.

2) Market-based operation framework for interconnectors

Introduction of novel market-based approach (MA) to characterise the interconnector as a profit-seeking entity aiming to optimize its revenues. The interconnector in this model acts as a business entity, rather than a regulated asset. The results of this market-based operation are then systematically compared with those derived from the centralized approach. Such comparative analysis illuminates the distinct outcomes that emerge from the market-driven operational strategy of the interconnector, including key differences

of variations in pricing, efficiency, and social welfare. This MA not only outlines the economic behaviors of the interconnector as a business entity but also captures the dynamic interactions among various agents within the interconnected system. By focusing on these interactions, the MA offers novel insights into how individual interconnector economic decisions and market power influence the overall efficiency, and profitability from the benchmark centralized scheduling decision. This approach thus promises to provide a deeper understanding of the interconnected energy system's operational dynamics under market-driven incentives.

3) **Impacts of wind and demand variability on interconnector Operations**

Proposal of a sampling-based methodology that allows to assess, under the proposed multi-service operational paradigm, the impact of wind and demand variability on interconnector operation. This assessment is particularly relevant in the context of renewable energy integration, where wind variability poses a significant challenge to system stability. Pre-investigated scheduling approaches are considered: a centralized approach, and a market approach. To implement the assessment, simulations have been carried out considering randomly sampled GB wind and demand profiles. These profile sets serve as inputs to model the variability inherent in the wind production and customer demand patterns. The simulation outcomes are then analyzed based on key operational and economic metrics. By assessing these metrics, the methodology aims to provide a detailed understanding of how wind and demand variability affect interconnector performance, especially under different market paradigms.

4) **Investigating the simultaneous allocation flexibility from demand side TCLs and interconnectors**

Integration of additional layer of flexibility from the demand side. The research delves deeper into understanding the intertwined relationship and simultaneous allocation flexibility from multi-sources across the system. Considering the considerable amount of energy involved in the system and homogeneous distribution of the devices, Thermostatically Controlled Loads (TCLs) are introduced as the key provider of the Demand Side

Response (DSR). The TCLs, which include devices such as air conditioners, refrigerators, can adjust their consumption in response to the power grid status, thus helping with the grid stability. These services are assessed under both CA and MA. By examining the effectiveness of integrating demand-side flexibility via TCLs within these two operational frameworks, alongside the flexible interconnector, the research aims to offer a comprehensive understanding of how different layers of system flexibility interact under various market paradigms. The study aims to reveal the synergies that emerge from coordinating flexibility across these distinct components, enhancing the overall stability of the power system.

5) **Accommodating multi-service operational paradigm for the interconnector in multi-area power systems with a meshed network topology**

Extension of the novel modelling framework to the multi-area power systems with a meshed network. The expansion reveals the advancement in the complexity and applicability of the framework. In this extended framework, the focus is on assessing the value of the proposed multi-service framework within this complex network structure. Additionally, the self-interested behaviors of the interconnector — how it operates to maximize its own benefits while interacting with multiple systems — are analyzed. To effectively tackle the challenges presented by this complex topology, an effective enumeration method is employed. This method is crucial for solving the independent strategies of the interconnectors and for determining the market equilibrium numerically. The enumeration method allows for a detailed consideration of nonlinear interplays between relevant decision variables (in particular between prices and capacity allocation decisions) in a mesh connected topology.

1.4 Thesis Outline

The reminder of the thesis are organized into five technical chapters, in consistent with the contributions listed above.

Chapter 2 investigates the potential contribution that interconnectors can provide to efficiently support the security of interconnected power systems. The proposed modelling setup introduces a radical paradigm shift in the operation of the interconnectors and in their interactions with multiple markets. The performance of the interconnector and the operation of the connected areas is formulated as the traditional Unit Commitment (UC) problem, where the link is the regulated transmission asset and coordinated centrally with power systems to minimized the total operational cost. For the sustainable energy future, collaboration between the EU and UK is essential in the energy transition process. The EU-UK Trade and Cooperation Agreement highlights the importance of the effective cross-border trading mechanism to support the expansion and integration of the renewable energy sources. A case study of the GB-France systems is adopted in this thesis to assess the value of interconnectors in improving system efficiency and security under the multi-service paradigms.

Chapter 3 evaluates benefits and impact of this new multi-service methodology with typical market indicators (e.g. social welfare and interconnector revenues) under also a market-based framework where the interconnectors are privately-owned assets with self-interested objectives. The same case study of the GB-France systems is adopted for the comparison between the system performance under MA and CA results in Chapter 2. By modelling the interconnectors as "price-maker" instead of the regulated assets, the proposed work quantifies the potential inefficiencies of market solutions while considering key elements such as capacity withdrawing.

Chapter 4 adopts a sampling-based methodology to assess the impact of wind and demand variability on the short-term operation of the interconnectors, evaluating the sensitivities of relevant operational and economical metrics with respect to wind availability and demand levels. A comprehensive set of case studies is developed considering the GB-France interconnected systems. The study has shown that particularly relevant differences can arise between CA and MA as a result of capacity withdrawing by the interconnector when the GB net demand level is low.

Chapter 5 introduces the flexible demand, Thermostatic Controlled Loads (TCLs), to the multi-area power system connected through interconnectors. The work comprehensively an-

alyzes the synergy and distinctions between utilizing TCLs and interconnectors to provide frequency services from different levels. In the market realization setting, the traditional centralized mechanism is then extended to the market-based mechanism to integrate the flexible TCLs and interconnectors in simultaneous energy-FR markets, where the interconnector and demand side TCLs are all treated as active market participants. The case studies illustrated that the inclusion of the independent demand side participant exerted downward pressure on the marginal profit of the merchant interconnector.

Chapter 6 investigates the techno-economic benefits of interconnectors that operate in a multi-area power network and whose capacity can be utilized for simultaneous exchange of power and fast-frequency services. The centralized approach is used as benchmark against an alternative market-based paradigm where interconnectors can act as profit-seeking agents that maximize their collected congestion surplus. An effective enumeration method is adopted to numerically solve the MA problem and determine the market equilibrium solution. This methodology allows to account for all the nonlinear interplays between the relevant decision variables in a meshed network topology. This novel methodology is applied to a model of an interconnected Great Britain-France-Ireland multi-area system, quantifying the potential benefits on system efficiency of multi-service interconnectors and assessing the impact of their self-interested scheduling on the system operational costs.

Chapter 2

Value of Interconnectors Operating in Simultaneous Energy-Frequency Response Markets

This chapter investigates the potential contribution that interconnectors can provide to efficiently support the security of interconnected power systems. The proposed modelling setup introduces a radical paradigm shift in the operation of the interconnectors and in their interactions with multiple markets. The model enables a simultaneous allocation of the interconnector capacity for the exchange of energy and of inertia-dependent primary frequency response. The detailed inertia-dependent frequency response constraints are deduced and included in the UC model for the allocation of sufficient frequency response. The operation is analysed under a centralized approach where the interconnector is operated to minimize total system operational cost. A case study of the GB-France systems captures the key structural differences between the linked areas, and quantitively assesses the value of interconnectors on system efficiency and security.

2.1 Introduction

Chapter 1 provided a comprehensive overview of the background and context that motivate the thesis topics, with a particular focus on the role of the cross-border interconnector in the low-carbon power system. This chapter begins by exploring the operational capabilities of the interconnector to provide frequency services in response to challenges posed by the low-carbon system.

The decarbonization of the electricity sector plays a fundamental role towards the implementation of ambitious national and international targets on greenhouse emissions' reduction. An increasing penetration of renewable energy sources (RES) is therefore replacing conventional fossil-fuel generation [26] [27]. RES output is typically uncertain and intermittent. In addition, most of the RES are connected to the grid through power electronic converters. Under standard configurations, this setup impedes the provision of inertial response [7], paving the way to large post-fault system frequency deviations and associated rates of change [9]. As a consequence, the requirement for ancillary services, especially Frequency Response (FR), increases. If conventional generation remains the only source of response services, the cost of integrating RES will rise, while limiting the ability of the system to accommodate RES output. The interconnections between electricity systems can contribute to the mitigation of these issues. Under traditional paradigms, interconnectors have been proved to alleviate the RES uncertainty and variability by enabling energy exchanges between interconnected areas. This operation boosts the efficiency of the energy markets in the connected systems, improving the security of supply and ensuring greater flexibility [28] [20].

In traditional operation paradigms based only on inter-area energy exchanges, the interconnector does not directly tackle the security issues related to increasing RES penetration and reduced inertial response. The security and operation of interconnected low-carbon power systems could be substantially improved if the capacity of the interconnector were used not only for energy exchange but also for the provision of FR. A practical example of such valuable contribution is represented by the system split event occurred on 8 January 2021 across Continental Europe (CE) Synchronous Area (SA) [29]. In response to this event, the HVDC link between

GB SA and Nordic SA provided FR to CE SA. The Skagerrak, the 4 HVDC interconnector linking Norway and Western Denmark, designates 15% of its transmission capacity exclusively for the exchange of ancillary services [30]. However, in accordance with current practice, the capacity of the interconnector for ancillary services is utilized only after energy dispatch or reserved in advance to a certain extent, which does not adequately capture the potential value of these services. The study [23] particularly highlights the importance of integrating interconnectors into broader energy markets and the trend towards balancing traditional energy trading with ancillary service provisions. More details on the technical framework and actual control strategies to enable a regular and consistent FR provision by HVDC links are addressed in [31], [32].

An iterative solution of a unit commitment problem including interconnectors is proposed in [33]. Techno-economic challenges faced by a multi-area European power system are proved to be partially solved by HVDC interconnection in [34]. An assessment of the economic benefits of cross-border interconnections is presented in [35] for the South Asia region, demonstrating their substantial short-term operational benefits and the associated long-term investment savings. Another work in [36] highlights the significant potential benefits of interconnection in the Northeast Asia power grid, including enhancing the cost-efficiency, increase use of RES, and reducing emissions. The study indicates that planning for grid interconnection should carefully consider the balance between initial costs and future fuel price trends, which have shown to significantly impact economic outcomes. The paper [37] examines the electricity trade between GB and its neighbouring countries in 2030, assessing 20 different scenarios that varied in generation mix, capacity factors, interconnector reliability, and focusing specifically on the impact of fluctuations in import prices and interconnector capacities. Model in [38] emphasizes that trading between regional electricity markets is crucial for effective cost management in the integration of RES. The case of the GB-France interconnector is analysed in [39], where it is shown that interconnectors between the two countries can substantially reduce the aggregate system operation cost and reduce wind curtailment. Similar conclusions are reached in [40] for the interconnection links between power systems in remote islands, emphasizing the impact of interconnectors on an efficient reserve allocation between the different areas. Slightly different

conclusions are drawn in [20] for the case of the GB-Ireland interconnection, where the small marginal benefit of additional DC link capacity in terms of wind curtailment reduction is counterbalanced by a substantial improvement in system adequacy. The impact on energy prices of the GB-Ireland interconnection has also been analysed in [41]. Moreover, the paper [42] explores the role of the interconnectors in the remote islands, taking the Spanish Canary and Balearic archipelago as case study. The work highlights the crucial role of the interconnector especially in improving the grid resilience by integrating the reserve constraints. The value of a flexible operation of interconnections was investigated in [43]. The economic indicators are not directly linked to the generation decisions e.g. the system inertia. This is improved in [44] where the energy flows are related to the inertia-dependent frequency response requirements in the connected areas. Finally, a formulation of the energy market, including both AC and HVDC lines, is proposed [45].

The papers mentioned above focus mainly on the flexible operation of the interconnector for energy exchange between connected areas. This chapter aims to address this limitation and advances the state of the art through the development of a novel paradigm for the operation of interconnectors, which envisages simultaneous allocation of the interconnector capacity for exchange of energy and frequency response services. This framework enables the potential role of interconnectors as key assets in the safe and efficient operation of the decarbonized systems of the future.

The main contributions of this Chapter are summarized as follows:

a. Development of inertia-dependent frequency response constraints ensure the dynamic evolution of post-fault frequency adheres to security thresholds, including the Rate of Change of Frequency (RoCoF), nadir frequency, and Quasi-Steady-State (QSS) frequency. The process of integrating these constraints into the existing Linear Programming formulation is illustrated.

b. Derivation of the new operational paradigm includes the simultaneous allocation of capacity for both energy exchange and frequency response services. The modelling of the

multi-service and flexible operation of the interconnector is determined within a holistic framework that accounts for the scheduling decisions of the connected power systems under inertia-dependent FR constraints. A cost-based, Centralized Approach (CA) is adopted, with an explicit evaluation of the value of energy and FR exchanged over the interconnector.

c. Introduction of the novel modelling framework that accounts for key features of the interconnected systems, considering different generation mixes and including detailed inertia-dependent constraints for the allocation of sufficient frequency response. This allows to capture the key structural differences between the interconnected systems and to perform a quantitative analysis of real cases, such as the GB-France interconnection considered in case study.

This chapter is structured with analytical deduction of the inertia-dependent FR constraints, the qualitative description of the operational paradigms considered, and the setup and mathematical formulation of the centralized UC model. The performance of the proposed paradigms is evaluated in a case study of the GB-France systems. Finally, the conclusions and future potential model expansions follows.

2.2 Modelling the Inertia-Dependent Frequency Response

2.2.1 Dynamics of Frequency Evolution and Security Standards

The frequency dynamics is the significant signal indicator showing the power balance in system. Large power imbalance with no rapid, effective remedial actions will results in disastrous disconnection of demands, even cascading system blackouts.

Frequency control aims to control the evolution of frequency following contingencies within the allowed security threshold (Fig. 2.1). According to the GB Security and Quality of Supply Standard (SQSS), the standard for initial transient post-fault frequency evolution are specified in the condition of maximum infeed loss:

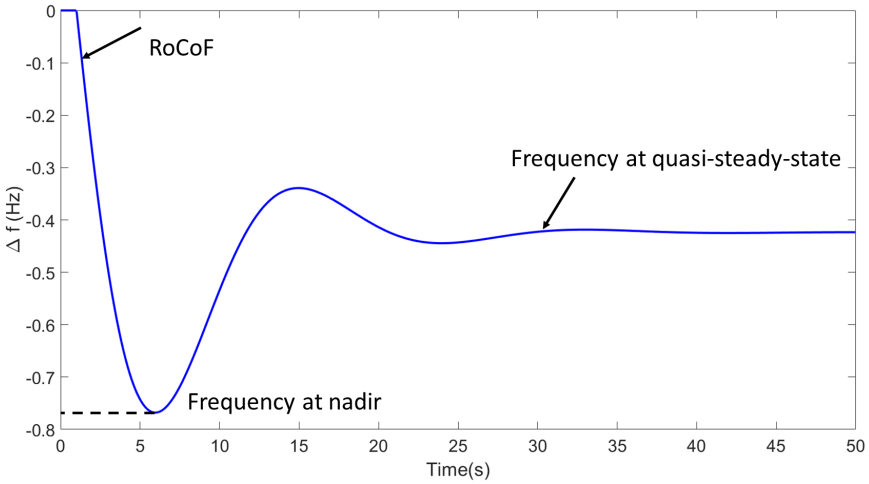


Figure 2.1: Post-fault frequency dynamics.

- The Rate of Change of Frequency (RoCoF) reaches the peak after disturbance, and is limited by the system inertia. The most sensitive value of RoCoF must be no larger than 0.125 Hz/s under any circumstances to avoid triggering the RoCoF protection mechanism. The UK national grid updates the standards for newly commissioned generation sites after July 2016 with the limit of $1Hz/s$ over $500ms$.

- The primary frequency response should limit the frequency deviation at nadir less than $0.8Hz$, preventing the undesired under frequency load shedding.

- The intermediate value of frequency at Quasi-Steady-State (QSS) should be stabilized by the further primary response to be above $49.5Hz$ within a minute.

The generalized time evolution of frequency deviation can be deduced from the swing equation, and expressed as the generation-load power mismatch:

$$2H\frac{d\Delta f(t)}{dt} + D \cdot L \cdot \Delta f(t) = \sum_{g \in \mathcal{G}} \Delta P_g(t) - \Delta P_L(t) \tag{2.1}$$

where the $H[MWs/Hz]$ is the system inertia, $D[\%/Hz]$ is the load damping coefficient, $L[MW]$ is the system demand level, $\Delta P_g(t)$ the change in generator production following the load change ΔP_L.

The governors start to respond once the power imbalance occurs. To avoid unnecessary operation, the generator governors only respond when the frequency deviation Δf exceed the frequency dead-band Δf_{DB}. The response R_g is assumed to be linearly increase with time, and modelled by the fixed slope until the response is fully delivered.

$$\Delta P_g(t) = \begin{cases} 0 & \text{,if } t < t_{DB} \\ \frac{R_g}{T_d} \cdot (t - t_{DB}) & \text{,if } t_{DB} \leq t \leq T_d + t_{DB} \\ R_g & \text{,if } t \geq T_d + t_{DB} \end{cases} \tag{2.2}$$

2.2.2 Frequency Response Constraints

Equation (2.2) models the primary frequency response, and by integrating the swing equation (2.1) the post-fault frequency evolution, and constraints related to the above-mentioned standards can be deduced. The detailed mathematical derivations are based on the work [10], and are explained as follows:

1) Rate of change of frequency (RoCoF)

The RoCoF standard specifies the maximum allowed frequency changing rate following the failure. During this initial seconds of inertia response, the governor response is not fully activated and can be neglected according to (2.2). Therefore, the frequency deviation at $t = t_{rcf}$ (usually $500ms$) can be derived by solving the swing equation, and should be limited to meet the SQSS by introducing the total system level frequency response R.

$$|\Delta f(t)|_{t=rcf} \leq \left|\Delta f_{rcf}^{max}\right| \tag{2.3}$$

$$R \cdot t_{rcf}^2 - 4 \cdot H \cdot T_d \cdot \Delta f_{rcf}^{max} - 2 \cdot \Delta P_L^{max} \cdot t_{rcf} \cdot T_d \geq 0 \tag{2.4}$$

Under the given level of maximum generation loss, the system minimum inertia should satisfy

the requirement of maximum RoCoF.

$$H = \frac{\sum_{g \in \mathcal{G}} H_g \cdot P_g^{max} \cdot N_g^{up} - \Delta P_L^{max} \cdot H_L^{max}}{f_0} \geq \left| \frac{\Delta P_L^{max}}{2\Delta f_{rcf}^{max}} \right| \tag{2.5}$$

where, ΔP_L^{max} is the maximum infeed loss, Δf_{rcf}^{max} is the RoCoF maximum requirement, H_g is the inertia constant of synchronouse generator g and H_L^{max} is the inertia of infeed generation loss.

2) Frequency at nadir

The frequency nadir is the point at which the minimum frequency is reached during the transient period. The nadir frequency depends on the inertia and governor response and load damping effect. By integrating the primary frequency response service in (2.2) into (2.1), the frequency deviation evolution can deduced:

- When $t < t_{DB}$, the frequency deviation can be computed for a specified initial condition $\Delta f(0) = 0$:
  $|\Delta f(t)| = \frac{\Delta P_L^{max}}{\tilde{D}} \cdot (1 - e^{-\frac{\tilde{D}}{2H}t})$
- When $t >= t_{DB}$, the frequency deviation can be solved as the function of t
  $|\Delta f(t)| = \Delta f_{DB} + (\frac{\Delta \tilde{P_L}}{\tilde{D}} + \frac{2RH}{T_d \cdot \tilde{D}^2}) \cdot (1 - e^{-\frac{\tilde{D}}{2H}(t - t_{DB})}) - \frac{R \cdot (t - t_{DB})}{T_d \cdot \tilde{D}}$

The time when the nadir occurs, denoted as t_{nadir} can be determined by solving $\frac{d\Delta f(t)}{dt} = 0$, and it follows that the $|\Delta f(t = t_{nadir})|$ yields:

$$|\Delta f(t = t_{nadir})| = \Delta f_{DB} + \frac{\Delta P_L}{\tilde{D}} + \frac{2 \cdot R \cdot H}{T_d \cdot \tilde{D}^2} \cdot \log\left(\frac{2 \cdot R \cdot H}{T_d \cdot \tilde{D} \cdot \Delta \tilde{P}_L + 2 \cdot R \cdot H} \right) \tag{2.6}$$

where $\tilde{D} = D \cdot L$, $\Delta \tilde{P}_L = \Delta P_L^{max} - \tilde{D} \cdot f_{DB}$. Given the criteria $|\Delta f(t = t_{nadir})| \leq \Delta f_{max}$, the constraint for the frequency deviation at the nadir condition can be formulated as:

$$\frac{2 \cdot R \cdot H}{T_d} \cdot \log\left(\frac{2 \cdot R \cdot H}{T_d \cdot \tilde{D} \cdot \Delta\tilde{P}_L + 2 \cdot R \cdot H}\right) \leq \tilde{D}^2 \cdot (\Delta f_{max} - \Delta f_{DB}) - \tilde{D} \cdot \Delta\tilde{P}_L \tag{2.7}$$

where, Δf_{max} is the allowed maximum drop of frequency of nadir, H is the system inertia, D is the damping effect and R is the system primary frequency response.

Note that, $H \cdot R = q*$ is the unique solution of the monotonically decreasing function (2.8), for any given value of $P_L, \tilde{D}, \Delta f_{DB}$ and Δf_{max}.

$$\frac{2q*}{T_d} \cdot \log\left(\frac{2 \cdot q*}{T_d \cdot \tilde{D} \cdot \Delta\tilde{P}_L + 2 \cdot q*}\right) = \tilde{D}^2 \cdot (\Delta f_{max} - \Delta f_{DB}) - \tilde{D} \cdot \Delta\tilde{P}_L \tag{2.8}$$

Hence, for any given couple of $\{H, R\}$ such that $H \cdot R \geq q*$, automatically satisfy that $|\Delta f(t = t_{nadir})| \leq \Delta f_{max}$.

$$H \cdot R \geq q* \tag{2.9}$$

The constraint (2.9) represents the bilinear term $R \cdot H$ and this particular formulation makes it a rotated Second-Order Cone constraint since R and H are strictly positive variables. This formulation, being quadratically constrained, is manageable by commercial solvers because the constraints lie within convex feasible regions. Nonetheless, to adapt the problem to fit within the frameworks of standard linear or quadratic programming, linearization techniques are commonly employed to approximate this constraint as a series of linear constraints. Considering specific points $x_i^l = \{H_i^l, R_i^l\}, \forall l \in \{1, \cdots, n_l\}$ such that $g(H_i^l, R_i^l) = q_i$, the constraint (2.9) can be linearized into (2.10).

$$g^l(H_i, R_i) = g(H_i^l, R_i^l) + g_H(H_i - H_i^l) + g_R(R_i - R_i^l) \tag{2.10}$$

3) Quasi-Steady-State frequency

The frequency recovered depends on the total delivered primary frequency response within the delivery time. Δf_{max}^{qss} is denoted as the maximum allowed quasi-steady state frequency deviation after primary frequency response action responding to the generation loss. Under the quasi-steady-state, the frequency level reaches a constant level and the RoCoF value is approximated zero. The provision of the response must hold the deviation level $|\Delta f| \leq |\Delta f_{max}^{qss}|$, which quantifies the corresponding response:

$$R \geq \Delta P_L^{max} - D \cdot P^D \cdot \Delta f_{max}^{qss} \tag{2.11}$$

As shown above, the constraints (2.4) and (2.11) are linear constraints, while the constraint (2.9) requires the proper linearization to fit in the linear programming model for the computational efficiency. For more in-depth derivations, readers may refer to [10] and [46] for further details.

2.3 Simultaneous Exchange of Energy and Frequency Response through the Interconnectors

2.3.1 Technology Discussion and Assumptions

Although the operational paradigm proposed in this work is technology-neutral, it is most likely that its technical implementation in a realistic setting would utilise HVDC lines, given their operational flexibility and their widespread use for long-distance cross-border connections. This

sub-chapter provides a detailed discussion on the technology aspects of HVDC in relation to the proposed operational framework for interconnectors.

The two technologies commonly adopted for HVDC interconnections refer to Line Commutated Converters (LCC) and Voltage Source Converters (VSC). Overall, LCC is a more mature technology and it is often used in bulk power transmission applications, given its high efficiency performance [47]. On the other hand, VSC guarantees higher controllability, with increased flexibility in both active and reactive power control. However, this is achieved at the expenses of increased converter losses [45]. The utilization of pulse width modulation (PWM) techniques in VSC to control the gate switching frequency of the insulated gate-controlled transistors (IGBT) results in higher switching losses compared to LCC. As a rule of thumb, the losses of a typical LCC converter are equal to about 0.7% of the total transmitted power, while this percentage is higher (about 2-3%) in the case of VSC systems [45].

In the context of this work, which envisages bidirectional exchange of energy and FR between the interconnected power system, the VSC technology appears to be more suitable for the following reasons:

- The application of PWM techniques on the self-commutating switches IGBT allows for flexible control of voltage and power in VSC [48].
- The VSC is capable of instantaneous power reversal within 50-100ms, without the need to change the DC voltage polarity, which is instead necessary with LCC technology [48].
- The VSC ensures faster responses compared to LCC, allowing to rapidly adjust the power output to provide frequency support [49] [50].

The VSC is more suitable for multi-terminal configurations, whereas the LCC is generally used in systems with no more than three terminals [48] [51].

Moreover, in accordance with the modelling assumptions in similar works (e.g. [52], [53]), the proposed methodology neglects the impact of HVDC losses on the social welfare and interconnector revenues. In addition, the two-area system adopted in this work lets the power flows

across the interconnector to be univocally defined. This property may no longer be maintained in presence of meshed DC-networks which require additional modelling features.

Finally, the effectiveness of the flexible interconnector is assessed based on a benchmark that assumes 100% availability, thus neglecting the impact of planned maintenance and unexpected outages.

2.3.2 Model setup

The proposed methodology focuses on multi-area power systems connected by interconnectors. A realistic example that fits in this framework is the GB power system, which can only resort to HVDC interconnectors with Ireland and Continental Europe (e.g. France) due to the long distances involved and the presence of maritime borders. Unlike with AC lines, if two power networks are only connected via DC links they are asynchronous, i.e. their frequency dynamics are decoupled.

In order to focus on the key qualitative aspects of the proposed multi-service paradigm, this work analyses the specific case of two areas connected by a single interconnector. The schematics of this setup are in Fig. 2.2. Each area is modelled as a single busbar power system, thus neglecting internal network topology constraints. Synchronous generation, RES and inflexible loads are connected to each of the two busbars.

The capacity F^{max} of the interconnector (sum of the dark and grey area in Fig. 2.2) can

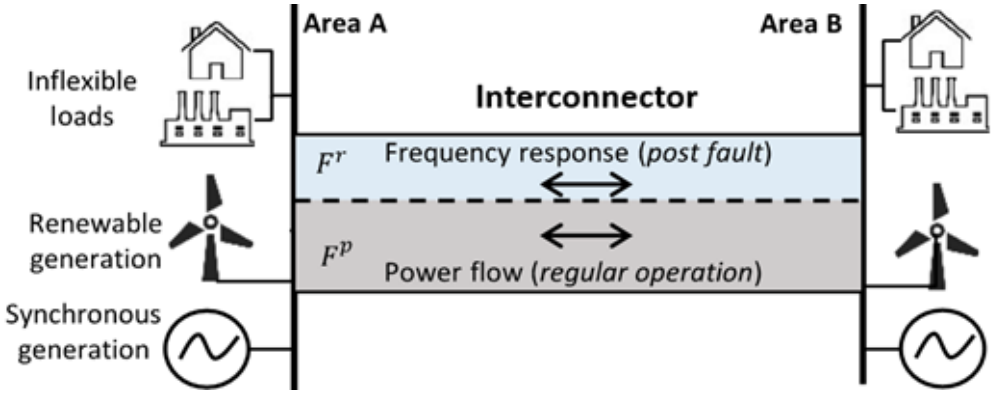


Figure 2.2: Schematics of the two-area power system connected by an interconnector.

be repartitioned to: enable bidirectional power flows F^p during regular operation (dark grey area in Fig. 2.2), and simultaneously maintain a power headroom F^r for primary frequency response (FR) [10] (light grey area in 2.2). It is worth noting that the direction of F^r can be concordant or opposite to the one of F^p. If the post-fault FR headroom is allocated in the opposite direction of the pre-fault power flow, the provision of FR will be firstly met by the reduction of power flow F^p in the opposite direction, and then by the power flow of F^r units in the required direction. Moreover, the FR service considered in this work lies in the context of short-term primary frequency control reserves [54]. Hence, the time window to evaluate the frequency dynamics after rare and severe generation outages occurring in the two areas is limited to few tens of seconds, i.e. until the frequency is stabilized at the quasi-steady-state value. The second-by-second control of frequency deviations or regulation services (i.e. automatic generation control [55], not even in place in the GB system) are out of scope in this paper. Finally, the operation of the power system under the proposed setup will be analyzed under two different approaches. This chapter focus on the system operation perspective under the new proposed simultaneous multi-service model. The analysis is carried out under the Centralized Approach (CA). In the next chapter, the work delves into the market value of the interconnector and assess its operation based on the Market Approach (MA). ‘

2.3.3 Traditional Centralized Approach (CA)

Under the CA, the operation of the different system entities in Fig. 2.2 (i.e. the areas A and B and the interconnector) is coordinated centrally in order to minimize the total operational cost or equivalently (under the hypothesis of demand inflexibility) maximize the overall social welfare. A single Unit Commitment (UC) optimization problem determines, **i).** the relevant UC generation decisions (i.e. commitment, dispatch levels and FR allocation) in Area A and Area B, and **ii).** the repartition of the interconnector capacity between F^p and F^r. Moreover, the requirements for FR are evaluated separately for each area. These are calculated against the maximum local generation outages, which are assumed to be independent of each other and non-simultaneous. In this way, each area is operated according to the typical *N-1* standard.

2.3.4 Model Assumptions of the UC Problem

The UC problems considered in this multi-service framework are formulated as deterministic, linear programming (LP) optimization problems. For each generation technology $\tau \in \{1, \cdots, \theta\}$, the size of the single plant is assumed to be significantly smaller than the total installed capacity G_{τ}^{max}. The commitment decisions can be therefore extended to the whole generation fleet by continuous variables $H_{\tau} \in [0, 1]$ which denote the online percentage of G_{τ}^{max}. The proposed LP formulation is able to properly represent the fundamental system-level scheduling requirements as presented in [56]. The cost sustained by a generator for providing FR is assumed to correspond to the opportunity cost of not providing energy. For simplicity, the inter-temporal constraints like generation ramping are not considered, allowing for addressing the dispatching problem on an instant-by-instant basis. Moreover, differently from UC problems based on mixed integer linear programming formulations [46], the LP approach allows to calculate meaningful price signals for energy (π_A, π_B) and FR headroom (ρ_A, ρ_B). These quantities are computed as the Lagrange multipliers of the relevant constraints in the UC. In fact, the LP formulation enables the Lagrange multipliers to maintain their useful economic interpretation of shadow prices, i.e. marginal savings/costs for the system following unitary variations in the constraints. More details about the mathematical implementation are in Chapter 2.3.5. It is worth emphasizing that the methodology presented in this work concerning the optimal repartition of the interconnector capacity can be easily extended to more complex UC formulations, as the fundamental interactions between the entities and the methodology for the calculation of the associated solution remain unaltered.

2.3.5 CA Formulation

As explained in Chapter 2.3.3, the optimal system operation with the CA is determined through a single UC problem. At each single time instant $t \in \{1, \cdots, T\}$, the UC minimizes the total system operational costs.

$$\min_{\xi_t}\Bigg\{\sum_{k\in\{A,B\}}\sum_{\tau=1}^{\theta}\Delta t(\alpha_{k,\tau}H_{k,\tau}G_{k,\tau}^{max}+\beta_{k,\tau}P_{k,\tau}+\gamma_{k,\tau}P_{k,\tau}^{2}\Delta t)\Bigg\}_t \tag{2.12}$$

Considering a generic time step t, let us define $\xi_t = \{H_{k,\tau}, P_{k,\tau}, R_{k,\tau}, F^p, F^r\}_t$ as the set of decision variables $\forall k \in \{A, B\}$ and $\forall \tau \in \{1, \ldots, \theta\}$. In particular, $H_{k,\tau}$ is the commitment decisions of technology τ in area k. $P_{k,\tau}$ and $R_{k,\tau}$ represent the generation dispatch level and the allocated FR, respectively. Moreover, $\alpha_{(k,\tau)}$ $[£/MWh]$ is the generation no-load cost, whereas $\beta_{k,\tau}$ $[£/MWh]$ and $\gamma_{k,\tau}$ $[£/(MWh)^2]$ are generation production costs. Without loss of generality, we assume the same number θ of generation technologies in two areas. Since the proposed UC does not include inter-temporal constraints, it can be solved independently at each time step t of length Δt across the horizon T. This allows to drop the time dependence from the notation for the remainder of this paper. The UC objective function (2.12) is subject to the following constraints, which are evaluated for $\forall k \in \{A, B\}$:

$$\sum_{\tau=1}^{\theta} P_{A,\tau} + F^p - L_A = 0 \tag{2.13a}$$

$$\sum_{\tau=1}^{\theta} P_{B,\tau} - F^p - L_B = 0 \tag{2.13b}$$

$$0 \leq H_{k,\tau} \leq 1 \tag{2.13c}$$

$$P_{k,\tau} + R_{k,\tau} \leq H_{k,\tau}G_{k,\tau}^{max} \tag{2.13d}$$

$$R_{k,\tau} \leq r_{k,\tau}H_{k,\tau}G_{k,\tau}^{max} \tag{2.13e}$$

$$R_{k,\tau} \leq s_{k,\tau}(H_{k,\tau}G_{k,\tau}^{max} - P_{k,\tau}) \tag{2.13f}$$

$$\mu_k r_{k,\tau}H_{k,\tau}G_{k,\tau}^{max} \leq P_{k,\tau} \tag{2.13g}$$

$$\hat{R}_k \geq \Delta G_k - D_k L_k \Delta f_k^{qss} \tag{2.14a}$$

$$2\Delta G_k \nu_k \sigma_k - {\nu_k}^2 \hat{R}_k - 4\Delta f_k^{roc}\sigma_k \hat{H}_k \leq 0 \tag{2.14b}$$

$$q_k - \hat{H}_k \hat{R}_k \leq 0 \tag{2.14c}$$

$$-F^{max} \leq F^p + F^r \leq F^{max} \tag{2.15}$$

The equalities (2.13a) and (2.13b) represents the supply/demand balance in each area, assuming that a positive value of F^p implies a power flow from Area B to Area A. The inequality (2.13c) implements the LP approximation of the UC problem, replacing unit commitment decisions for individual plants with the continuous variable $H_{k,z\tau}$ which represents the online percentage of the entire technology fleet. Constraint (2.13d) imposes that the sum of power generation and FR provided by each technology cannot be greater than the online capacity $H_{k,\tau}\ G^{max}_{k,\tau}$. The provision of the primary frequency response is limited by the maximum capacity of response the generator can provide, and adjustments based on the slope when the generator's output is near its highest possible levels as shown in the Fig.2.3. The inequalities (2.13e) and (2.13f) accordingly limit the amount of FR, considering a maximum headroom $r_{k,\tau} H_{k\tau} G^{max}_{k,\tau}$ (2.13e) and linking the allocated FR with $P_{k,\tau}$ through the slope $s_{k,\tau}$ (2.13f). To avoid trivial solutions that could result from the proposed LP formulation, in which the unit commitment decisions for a single unit are relaxed and extended to continuous variables for the generation fleet, the constraint (2.13g) prevents specific scenarios with large FR and no generation output, lets the generation dispatch $P_{k,\tau}$ be μ_k times higher than the FR headroom.

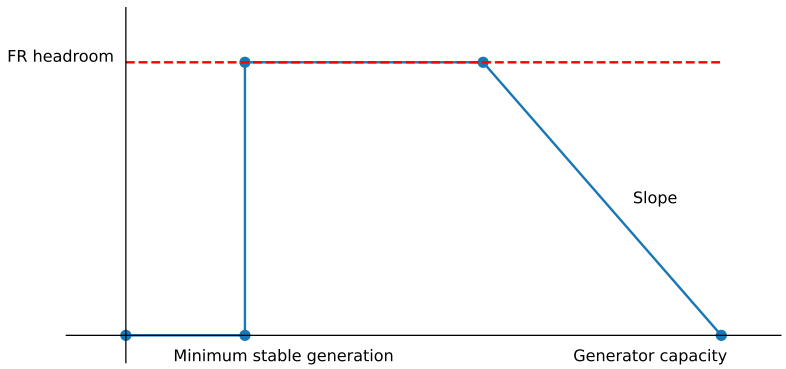


Figure 2.3: Response characteristics of the synchronous generator.

The set of constraints (2.14) derived based on the Chapter 2.2.1, ensures the post-fault security of frequency in each area following the corresponding generation loss ΔG_k. Constraint (2.14a) deals with the quasi-steady frequency deviation Δf_k^{qss}, also accounting for the contribution of the load damping D_k. The RoCoF is maintained above a secure threshold Δf_k^{roc} through (2.14b). Note that υ_k is the time interval for RoCoF calculation and σ_k the delivery time for FR [46]. Finally, (2.14c) ensures that the frequency nadir is above Δf_k^{max}. For each system condition (e.g. L_k, ΔG_k, σ_k), there is a unique value of the function $q_k = \hat{H}_k \hat{R}_k$ such that the frequency deviation at nadir Δf_k^{nad} equals Δf_k^{max}. The implementation of (2.14c) in the UC model relies on linearization techniques are described in Chapter 2.2.1 based on the work [10] and [46]. Additional information regarding the derivation and implementation of equation (2.14) can be found in reference [10].

The quantities $\hat{R}_k$ and $\hat{H}_k$ in (2.16) denote the system-level FR and total post-fault inertia, respectively, and are defined as:

$$\hat{R}_A = \sum_{\tau=1}^{\theta} R_{A,\tau} + F^r \tag{2.16a}$$

$$\hat{R}_B = \sum_{\tau=1}^{\theta} R_{B,\tau} - F^r \tag{2.16b}$$

$$\hat{H}_k = \frac{1}{f_0}(\sum_{\tau=1}^{\theta} h_{k,\tau} H_{k,\tau} G_{k,\tau}^{max} - h_k \Delta G_k) \tag{2.16c}$$

As for F^p, a positive value for F^r implies FR allocated in Area B and provided to Area A. It can be noted that $\hat{R}_A + \hat{R}_B = \sum_{\tau=1}^{\theta} R_{A,\tau} + \sum_{\tau=1}^{\theta} R_{B,\tau}$, representing the overall system FR supplied by the flexible generators from both areas, constrained by their physical limits in (2.13d)-(2.13g). Finally, (2.15) imposes feasibility limits to repartition of the interconnector capacity.

In this CA formulation, the prices π_k and ρ_k (for electricity and FR, respectively) in area k are defined according to the classical notion of shadow prices. In particular, the electricity prices π_A and π_B correspond to the Lagrange multipliers associated to power balance constraints (2.13a)

and (2.13b). Similarly, the FR prices ρ_A and ρ_B are determined as the Lagrange multipliers of the active constraint in (2.14), evaluated for $k = A$ and $k = B$, respectively.

2.4 Case Study

This section compares the key features and outcomes of the CA under the multi-service framework and under traditional energy-only framework in some relevant case studies. A 24h optimization horizon is chosen for the simulations, considering $T = 48$ time periods and $\Delta t = 30$ min as time step. In the simulation environment, the Area A represents the aggregate GB system, whereas Area B mimics the power network in France. The generation mix in the two systems reflects typical 2030 low carbon scenarios, with the main characteristics of the generation presented in Table 2.1. Taking into account the realistic generation mix in France and GB, along with their traditional operational characteristics associated with technologies, two different technologies are summarized and considered in both areas: synchronous generation (τ=1), is able to provide inertial and frequency response (such as gas and nuclear), and wind generation (τ=2), which does not provide any ancillary service [56], [46]. Table 2.1 shows that the total generation capacities in GB and France are similar. However, the partition between the synchronous and wind technologies are noticeably different, in line with actual trends [39]. Wind integration in GB is higher than that in France, which instead relies more on synchronous generation.

Relevant parameters and the operational characteristics of the synchronous generators are taken from [57], [46]. The wind and load profiles utilized for the two areas are presented in Fig. 2.4 as the blue area and purple line, respectively. They are taken from [10], [58], and refer to a typical winter week day.

The other relevant system parameters are D_k=1/50s, ν_k=0.5s, f_k^{roc}=0.5Hz (for both areas) σ_A=10s, σ_B=15s, Δf_A^{qss}=0.5Hz, Δf_B^{qss}=0.2Hz and ΔG_A=1.8GW and ΔG_B=1.5GW [44], [52]. The capacity of the interconnector is set to F^{max}=5GW, on the basis of existing interconnector projects and planned new developments by 2030 [34]. The values of the parameters above

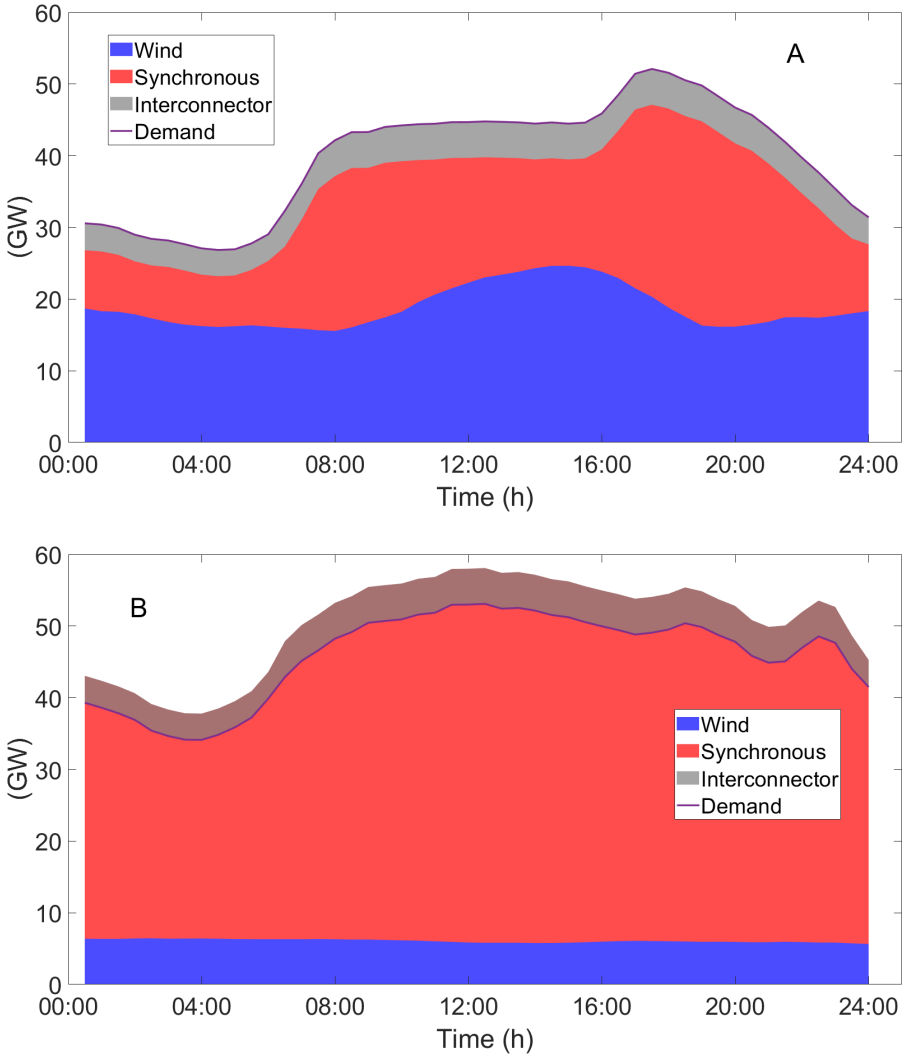


Figure 2.4: GB (A) and France (B) generation mix and demand profile under CA.

Table 2.1: Generation characteristics

	Synchronous		Wind	
	GB(A)	France(B)	GB (A)	France (B)
Capacity $G_{k,\tau}^{max}$ [MW]	65000	85000	40000	15000
FR headroom r_τ	0.1	0.1	-	-
FR slope s_τ	0.4	0.3	-	-
Constant of inertia $h_{k,\tau}$ [s]	4	6	-	-
No load cost,$\alpha_{k,\tau}$ $[£/MWh]$	7	3.5	0.5	0.5
Cost,$\beta_{k,\tau}$ $[£/MWh]$	25	10	1	1
Cost,$\gamma_{k,\tau}$ $[£/MW^2h]$	2.5e-3	5e-4	2.5e-4	2.5e-4

are used in the Base Case (BC), whose results are presented in 2.4.1. Simulations have been implemented in MATLAB R2019a on Intel® i7-8565U CPU, 1.80GHz processor with 64GB RAM.

2.4.1 Base Case

The generation/demand balance for France and GB under CA is presented in Fig. 2.4. It is worth highlighting the different generation mix in the two systems, with greater penetration of wind in GB and a larger contribution of synchronous generation (particularly nuclear) in France.

Table 2.2: Multi-service VS. energy-Only cases comparison

	Energy+FR	Energy-only
System operational cost ($M£$)	151.80	151.98
Congestion surplus ($M£$)	12.02	11.18
Average line utilization for energy (%)	92.88	98.38
Average line utilization for FR (%)	7.12	0
Average line utilization (%)	100	98.38

This basic case starts from comparing the system performance and interconnector behaviour under the traditional energy trading only model and the proposed multi-service model that includes the simultaneous exchange of energy and FR service. Table 2.2 offers the comparison metrics. With the introduction of FR services over the interconnector, there is a slight improvement in the overall social welfare in this case. This is achieved by utilizing the more cost-efficient FR resources instead of the expensive local services, thereby reducing the total system operational cost by approximately 0.15% . However, the efficiency of the link utilization has been improved, from 98.38% in the energy-only case to 100% after providing FR services. As shown in Fig.2.5, the residual part of the interconnector capacity in the energy-only case between 02:00-07:00 has been fully used under the multi-service framework, and the capacity is optimally allocated between F^p and F^r.

2.4.2 Impact of Varying Interconnector Capacity

The base case study is carried out under the realistic scenario where the links capacity between GB and France is only 5GW. In the context of the integrated Europe market, future will see rapid progress in the construction of cross-border interconnectors. The multi-service paradigm has been further analysed under scenarios with various interconnector capacity levels in this

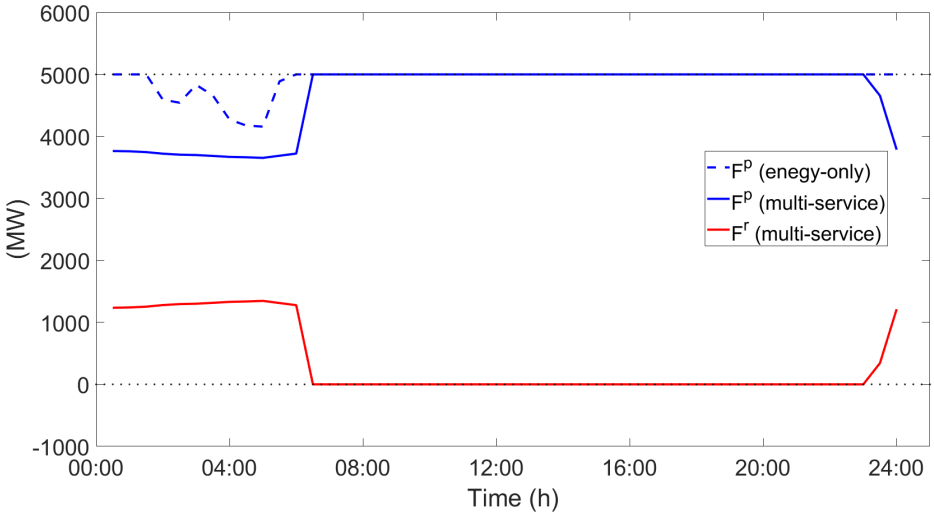


Figure 2.5: The capacity repartition of the interconnector under the multi-service model and energy-only model.

section. The simulation results have been summarized in Table 2.3. Compared to the separated system operation (0GW case), the system operational cost can be substantially reduced with the support of the interconnector. The cost of operation is the highest, up to 167.22£, when there is no link between the two areas, and can be reduced to the minimum possible value of 136.5£ in the cases where there is no more congestion over the link (30GW and 50GW cases). The cost saving can be up to around 20% with the support from the multi-service interconnector. However, this value in social welfare does not monotonically increase with the interconnection capacity. The same operational costs are observed in the case with 30GW and 50GW link capacity. The zero congestion surplus under these two cases indicates that the prices of both services between two areas have become equal, and no area holds the price advantages over the other. Electricity and FR services have been optimally dispatched for the whole interconnected power system. Once the maximum social welfare is achieved, any additional expansion of the interconnector is redundant.

Table 2.3: Sensitivity analysis on the link capacity under multi-service framework

	0GW	2GW	5GW	10GW	30GW	50GW
System operational cost ($M£$)	167.22	160.2	151.80	142.73	136.50	136.50
Congestion surplus ($M£$)	0	6.42	12.02	12.64	0	0
Average line utilization (%)	-	100%	100%	100%	57.84%	34.71%

2.4.3 Impact of Varying Wind Capacity

This section answers the question that how the interconnector contribute to the system under the high-wind penetrated, low-inertia scenarios. Table 2.4, compared the system performance between the model with energy-only interconnector the model with multi-service interconnector under different GB wind installation levels. The link capacity continues to be assumed at the constant value of 5GW.

Firstly, the low carbon power system with higher wind penetration is characterized with the benefit of low operational cost from the total system perspective, while this advantage is further amplified if the interconnector can function as the additional FR provider. From the Table 2.4, the operational cost is reduced by 38.5% in the multi-service model when the installed wind capacity increases from 40GW to 100GW, while the corresponding saving in the energy-only model is 35%. The congestion surplus collected by the interconnector may drop in the high wind scenarios, as the cheaper wind production reduces the marginal production cost of electricity in GB, possibly leading to the decline in the price spread between the linked systems.

The case studies give the numerical comparison between the GB wind curtailment levels from the current setup to the future high-wind setup. The contributions from the multi-service link increase when more wind production is available. Particularly in the case with 80GW wind capacity, with the facilitation of the interconnector providing FR service, the GB system can almost avoid wind-curtailment and improve the total social welfare from the low carbon system.

Table 2.4: Sensitivity analysis on wind installation level in GB

		40GW	80GW	100GW
System operational cost ($M£$)	Energy+FR	151.80	100.04	93.36
	Energy only	151.98	104.06	98.72
Congestion surplus ($M£$)	Energy+FR	12.02	3.34	4.26
	Energy only	11.18	3.84	5.19
Average daily wind curtailment (%)	Energy+FR	0	0.4	14.83
	Energy only	0	7.61	19.13

Fig. 2.6 displays the outcomes of interconnector capacity allocation results under these three scenarios. In the base case setup where GB has the installed wind capacity of 40GW, both

the energy service and the FR are imported from France to GB due to the more economical electricity prices stemming from the low-cost nuclear plants and the cheaper FR prices benefit from the higher penetration of synchronous generators. With the progress in GB wind installation, reduced energy prices in GB reverses the direction of the power flow during the low net demand hours. In the scenarios where GB has 80GW of installed wind capacity, the French system imports electricity from GB for the majority of times over the day. Increasing in the installed wind capacity (100GW) amplifies this trend. Due to the increasing reliance on the wind generation, the low-inertia power system in GB system highlights the enhanced requirements for FR via the interconnector, which helps to mitigate potential curtailment in the wind generation.

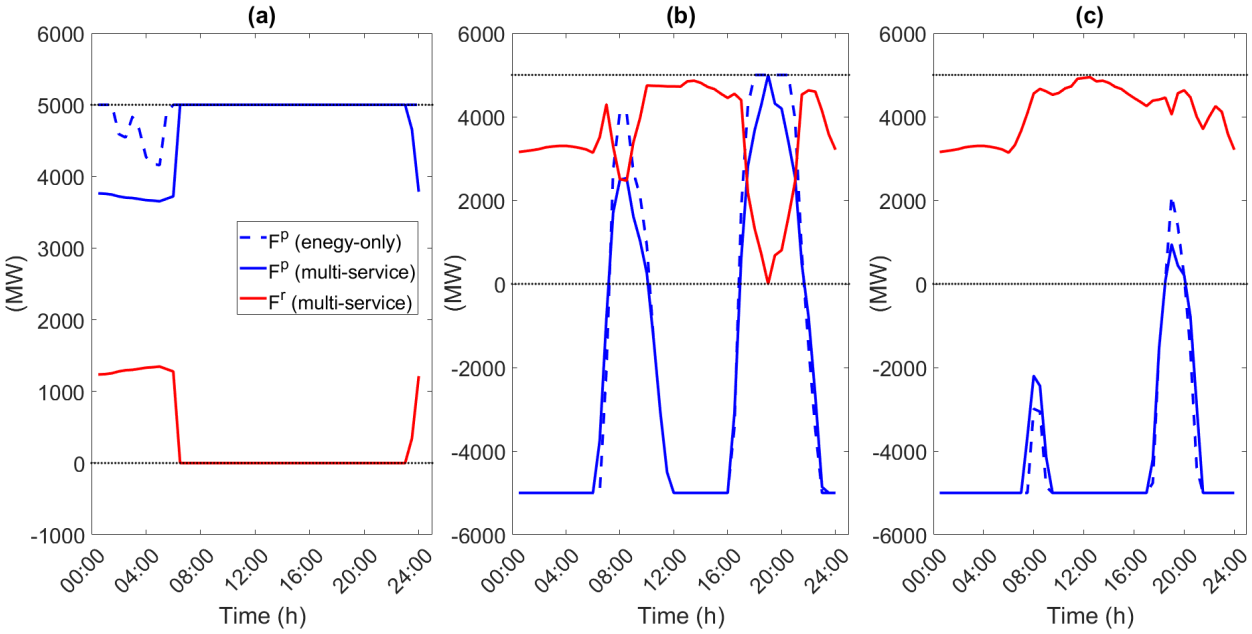


Figure 2.6: The capacity repartition of the interconnector under cases with different GB wind installation level (a) 40GW (b) 80GW (c) 100GW.

2.5 Conclusion

This chapter models and analyses the multi-service framework of the interconnector. Under this setup, the interconnector accommodates the service of delivering FR in addition to its primary function of transmitting electricity. By employing the advanced HVDC technology, the flexible

controllability in the power and rapid response enable the feasibility of the frequency support from the future cross-border interconnector.

The framework is assessed under the standard centralized scheduling method, considering the value in providing FR services from the system perspective. Case studies take the interconnector linked GB-France power system, offering a comprehensive analysis of the contribution under various scenarios. By leveraging these functionalities on the interconnector, the multi-service interconnector has been demonstrated in overall system benefits, link efficiency, especially under the high RES future scenarios.

The multi-service framework is developed by including the scheduling model with inertia-dependent constraints, serving as the benchmark model for the further investigation in the following Chapters. Another significant research topic is in the realm of regulatory framework. The next chapter focuses on the realm of regulatory frameworks for the multi-service interconnector. An alternative market-based method is proposed for the conventional centralized coordination method, moving the pathway towards the more liberalized market.

2.6 Future Works

This chapter explored the multi-service framework for the interconnector. Building upon this line of research, the discussion on the flexibility of the interconnector can be extended to encompass additional levels, including reserve services and enhanced frequency response, among others. Furthermore, to advance the development of a flexible interconnector, a deeper examination of technology feasibility and the implementation of effective control mechanisms are necessary. These elements are crucial for optimizing the interconnector's functionality and ensuring its adaptability to changing energy demands and market conditions.

Chapter 3

Market-Based Operation of the Multi-Service Interconnectors

Following the investigation in Chapter 2 on the role of flexible cross-border interconnectors involved in improving power system efficiency, this chapter delves into the benefits and impacts of the proposed multi-service operational framework under another market paradigm: a market-based scheduling approach. In the proposed market approach, the interconnectors are privately-owned assets with self-interested objectives, instead of the regulated assets to optimize the whole social welfare in the centralized approach. The solution of the market approach is characterized as the Nash Equilibrium of a competitive game. By modelling the interconnectors as "price-makers", the proposed work quantifies the potential inefficiencies of market solutions while considering the interconnector market driven behaviour such as capacity withdrawing. The same case study of the GB-France systems is adopted to quantitatively analyse and compare the system and market outcome between the traditional centralized approach and the proposed market approach by adopting typical market indicators (e.g. social welfare and interconnector revenues).

3.1 Introduction

Beyond the initiative aim at improving the system efficiency for the environmental and energy concerns, the governments globally tend to take steps towards the deregulation of the electricity market and encourage competitive practice. Within the deregulated context, it becomes essential to investigate the business strategies and models of various market stakeholders. A significant advantage of a decentralized market framework is its flexibility, which guarantees compatibility with emerging technologies. This adaptability facilitates the integration of increasingly prevalent flexibility resources, such as demand response, energy storage, enabling them to independently determine their optimal strategies for offering services [59].

The model in Chapter 2 advances the operational paradigm of the interconnector for the future low-carbon power system by including the FR service exchange alongside its primary function of energy exchange. Except the operational paradigm, analytical and qualitative advancements in market paradigms and clearing models are also required to effectively integrate multi-service provision of interconnectors in system operation. This chapter advances the research by examining potential market designs for the multi-service interconnector within a competitive market environment.

Sufficient interconnector capacity is crucial for the goal of establishing a single EU electricity market, as outlined in Directive 96/92/EC. EU legislation permits two types of projects of new interconnector instruction, public and private. These include regulated projects carried out by ENTSO, and projects implemented by commercial investors [60]. The EU acknowledges the importance of interconnectors as a promising solution to the energy trilemma and promotes the development and reliance on private and non-regulated merchant interconnectors [61].

There were many studies have discussed about the merchant approach to the transmission asset development. The benchmark study [62] expands the scope of the competitive electricity market by incorporating market-based investments in the transmission sector. The work conducted by Joskow in [52], evaluated the merchant transmission investment model in comparison to the monopoly issue in electric transmission, discussing both the advantages and disadvantages of

the regulated and merchant models. Paper [63] summarizes and compares the challenges and outcomes associated with two different approaches to transmission development: merchant and regulated transmission. It indicates the higher efficiency shown in the market approach than the regulatory ones and also highlights the importance of the regulation in creating the supportive environment that promotes transparency and competition. The work in [64] presents a specific structure that incorporates a merchant framework, enabling the inclusion of generation companies in transmission investment. A game-theoretic model is employed to determine the equilibrium of merchant strategies among various generation companies. The analysis indicates that the potential for increased profits from generation can significantly motivate investment in transmission. Works in [65] and [66] explored the similar topic by incorporating generation into the transmission planning model.

Currently, electricity interconnectors already operate in GB as stand-alone companies with regulatory approval, rather than centrally organized transmission infrastructures [17]. Non-regulated merchant interconnectors (e.g. ElecLink between France and GB [24]) also coexist in the interconnector regulatory setup of the European Union. However, further significant progress is required. The above-mentioned research primarily focuses on the long-term planning of the interconnector, with less emphasis on the short-term operational aspects. According to EU Electricity Regulation 2019/943, the TSOs are expected to promote non-discriminatory market-based solutions for the development of energy exchanges and a coordinated allocation of the interconnector capacity, considering also the integration of balancing and reserve services [25].

Compared to centralized paradigms, market solutions can offer better scalability, improved efficiency with partial information and higher robustness [67]. On the other hand, it is necessary to investigate whether they also introduce a relevant reduction in social welfare, which might be caused by the decision by the privately-owned interconnectors to withdraw capacity for higher revenues. Analyses on this topic would constitute a stepping stone for a revision of the current regulatory framework and a full implementation of a combined energy-FR operational paradigm [16].

The main contributions of this Chapter are summarized as follows:

a. Introduction of the novel market-based approach to characterise the interconnector as a profit-seeking entity aiming to optimize its revenues. The interconnector acts as a business entity, rather than a regulated asset. This proposed market approach captures the economic behaviours of the different agents within the interconnected system and provides novel insights into their interactions.

b. Incorporate the market-based framework into the multi-service framework outlined in the Chapter 2. The framework discusses the interactions among the independent players in the competitive market. Moreover, the market-based operational paradigm has been developed under the same hypotheses and assumptions of the centralized one, allowing a quantitative assessment of the contribution of the interconnectors to the overall social welfare and of the potential inefficiencies introduced by the market-driven behaviour.

This chapter is structured with the proposal of the market-based model for the multi-service interconnector, including an analytical derivation of the formulation. It characterizes the market outcome as the Nash equilibrium and outlines the final implementation scheme. The case study compares this model within both centralized and market-based frameworks, consistent with the discussions in Chapter 2. Additionally, the chapter concludes with further discussions on the transmission loss and availability of the interconnector and potential future works.

3.2 Market Approach (MA)

Under the MA, the two areas and the interconnector forming the system in Fig. 2.2 are modelled as separate independent entities. Their operation is the result of market interactions as illustrated in Fig. 3.1. In particular, the optimal generation decisions relevant to Area A and Area B are determined via two separate UC problems. The independent market clearing processes in area A and B can be converted from social welfare maximization problems into

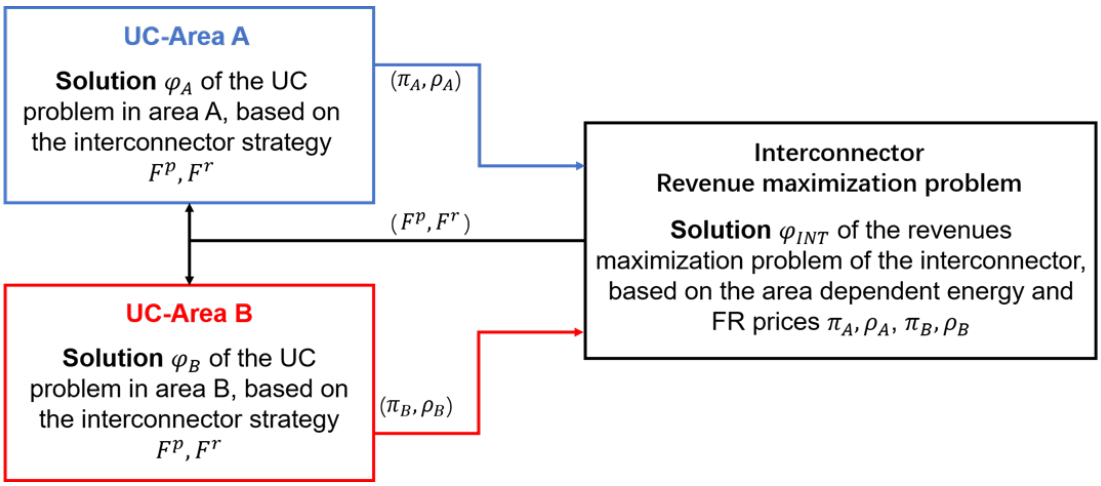


Figure 3.1: Implementation scheme of the MA.

equivalent operational cost minimizations (i.e. UC problem) under typical assumptions of perfect competition and demand inelasticity [57].

The interconnector operates as a profit-seeking entity that, on the basis of the price signals in the two areas (π_A, π_B for power and ρ_A, ρ_B for FR), allocates its capacity F^{max} to optimally profit from the congestion surplus associated to the exchange of power F^p and FR headroom F^r. In this context, it should be emphasized that, the interconnector has been modelled as a price-maker entity that optimally allocates its capacity considering the impact of its decisions on the UC solutions of Area A and B and the resulting prices. In addition, although the optimal decisions of each of the three entities are computed separately, their optimal solutions are interdependent.

As in Fig. 3.1, the optimal decisions in area A and B depend on the capacity allocation of the interconnector, which in turn is affected by the energy and FR prices associated to the UC solutions. Hence, the solution of the MA is expressed as an equilibrium: the interconnector decisions (F^{p*},F^{r*}) are optimal for certain prices (π^*,ρ^*) and, in turn, they induce those very same prices when considered in the UC problems.

3.2.1 Analytical Formulation for Area A and B

The UC formulation for the MA is slightly different than in the CA case, as it considers the generation units in each area separately. However, all the fundamental assumptions in Chapter 2.3.4 still apply. The generation scheduling decisions in area A are determined through the following optimization problem:

$$\varphi_A(F^p, F^r) = \min_{H_A, P_A, R_A} \sum_{\tau=1}^{\theta} \Delta t(\alpha_{A,\tau} H_{A,\tau} G_{A,\tau}^{max} + \beta_{A,\tau} P_{A,\tau} + \gamma_{A,\tau} P_{A,\tau}^2 \Delta t) \tag{3.1}$$

subject to constraints (2.13), (2.14), evaluated at $k = A$. Differently from the previous case, F^p and F^r are not decision variable of the problem but rather fixed quantitates which are determined separately by the interconnector, as detailed in Chapter 3.2.2. The minimized operating cost φ_A in Area A can be thus parametrized by the interconnector decisions F^p and F^r. Specifically, the price π_A and φ_A can be derived from the marginal cost and marginal saving of the system according to the unit variation of the fixed quantities F^p and F^r. Similarly, the UC problem for area B can be described by:

$$\varphi_B(F^p, F^r) = \min_{H_B, P_B, R_B} \sum_{\tau=1}^{\theta} \Delta t(\alpha_{B,\tau} H_{B,\tau} G_{B,\tau}^{max} + \beta_{B,\tau} P_{B,\tau} + \gamma_{B,\tau} P_{B,\tau}^2 \Delta t) \tag{3.2}$$

subject to constraints (2.13), (2.14) evaluated at $k = B$, and with F^p and F^r as fixed quantities. As for Area A, φ_B denotes the minimized operational cost in Area B as a function of the interconnector operational decisions F^p and F^r.

3.2.2 Analytical Formulation for Interconnector

At any time t, the interconnector determines the optimal repartition of its capacity between F^p and F^r in order to maximize the associated congestion surplus. Denoting by π_A and π_B

the prices of energy in area A and B, and by ρ_A and ρ_B the prices of FR, the interconnector problem is expressed as:

$$\varphi_{INT} = \underset{\pi_A,\pi_B,\rho_A,\rho_B,F^p,F^r}{\arg\max} (\pi_A - \pi_B)F^p + (\rho_A - \rho_B)F^r \tag{3.3}$$

subject to:

$$-F^{max} \leq F^p + F^r \leq F^{max} \tag{3.4}$$

$$\pi_A = -\frac{\partial \varphi_A(F^p, F^r)}{\partial F^p} \tag{3.5a}$$
$$\pi_B = \frac{\partial \varphi_B(F^p, F^r)}{\partial F^p} \tag{3.5b}$$
$$\rho_A = -\frac{\partial \varphi_A(F^p, F^r)}{\partial F^r} \tag{3.5c}$$
$$\rho_B = \frac{\partial \varphi_B(F^p, F^r)}{\partial F^r} \tag{3.5d}$$

The revenues of the interconnector are given by the sum of, **i).** the product of the energy price differential between two areas and the exchanged energy, **ii).** the product of the FR price differential between area A and B and the FR headroom. The revenue due to the power transfer F^p implies actual flow from one area to the other. Conversely, the revenue linked to the FR headroom F^r is related to the service availability. Here, the actual provision of the service is not required.

The constraint (3.4) limits the allocation of F^p and F^r within the maximum capacity F^{max}, whereas equation set (3.5) are introduced to model the price-making approach of the interconnector. Note in fact that the prices in at which the congestion surplus is evaluated correspond

to the shadow prices of power and FR in the two areas. In particular, π_k, corresponds to the marginal cost of providing one additional unit of power, i.e. the marginal reduction of system operational costs when an additional unit of power is provided by the interconnector. This variational cost appears with a minus sign in (3.5a) and a plus sign in (3.5b), since the positive sign of F^p is associated with energy flow from area B to area A (with a cost increase in the former and a cost reduction in the latter). Similarly, ρ_k corresponds to the marginal saving of fulfilling the frequency requirements when one additional unit of FR is provided by the interconnector. The same sign convention of the energy prices in (3.5a) and (3.5b) also apply in the present case to the FR prices in (3.5c) and (3.5c). By considering π_k and ρ_k as decision variables in problem (3.3)-(3.5) and accounting explicitly for their relationships with the UC in areas A and B, the proposed modelling framework considers a strategic behaviour of the interconnector that explicitly takes into account the impact of its operational decisions on the UC of the interconnected areas and on the resulting price signals.

It is interesting to note that the MA solution, as characterized by equations (3.1)-(3.5), actually corresponds to the Nash equilibrium of a competitive game where three self-interested agents (the two independent power systems and the HVDC) autonomously determine their operational strategies (unit commitment decisions and capacity allocation of the HVDC) in order to maximize their own objective function (equation (3.1) and (3.2) for system A and B, equation (3.3) for the interconnector). At the equilibrium of the MA solution, each of the three independent agents cannot unilaterally modify their operational strategies in order to improve its objective function.

It should be noted that the existence and uniqueness of the MA solution (or equivalently of its associated Nash equilibrium) are guaranteed in the 2-area case analysed in the present work but such result does not in general hold true when more complex cases (e.g. meshed networks or network with losses) are considered. We wish to emphasize that this is not related to the novel operational paradigm presented in Chapter 2, but it is rather an intrinsic limitation in the analysis of competitive market-based interactions between agents in meshed networks. This limitation has already been discussed in the literature: a detailed analysis on this point is presented, for a slightly different problem, in [68]. It is shown here that, under very general

assumptions and in presence of network constraints, a pure Nash equilibrium and a market solution might not exist. Other analyses on this point, considering for example the effect of nonlinearities, can be found in [69] [70] [71].

The issues on the existence of a MA solution can be overcome by introducing the notion of approximate or ϵ-Nash equilibria. This is an established mathematical concept that allows to relax the best-response condition of the individual competitive players. At this approximated solution, the potential payoff improvement of each agent, deriving from a unilateral change of its own strategy, is limited to a (small) fixed quantity ϵ. With this alternative formulation, the ϵ-Nash equilibrium and the associated MA solution are such that the improvement in the payoff of each agent, deriving from a unilateral change of its own strategy, is limited to a (small) fixed quantity ϵ.

The ϵ-Nash equilibrium is an established mathematical notion that allows to relax the best-response condition of the individual competitive players and allows to obtain an approximated Nash equilibrium in cases where a precise equilibrium might not exist.

For a formal definition [72] [73], consider the n-player game characterized by the tuple (N, K, u), where:

- N is a finite set of n players, indexed by i;
- $X = X_1 \times ... \times X_n$, where X_i is the set of strategies available to player i;

Each vector $x = (x_1, x_2, ..., x_n) \in X$ is called a strategy profile;

- $u = (u_1, ..., u_n)$ where $u_i : X \to R$ is a real-valued utility (or payoff) function for player i.

The equilibrium notion can then be formally defined as follows:

Definition 1 (ϵ-Nash equilibrium): A strategy profile $x = (x_1, x_2, ..., x_n)$ is an ϵ-Nash equilibrium for $\epsilon > 0$, if for all players i and for all strategies $x_i' \neq x_i$, $u_i(x_i, x_{(-i)}) \geq u_i(x_i', x_{(-i)}) - \epsilon$.

Under the definition of ϵ-Nash equilibrium, each player i cannot improve its payoff u_i by more than the (small) quantity ϵ if it changes its strategy from x_i to x_i'.

The existence of the ϵ-Nash equilibria is always guaranteed for some sufficiently large ϵ [72], whereas an example of its application in an electricity market context is presented in [74].

3.2.3 Model Framework and Implementation Scheme

In previous works the outcomes of competitive interactions between self-interested agents were usually determined through iterative resolution of the optimization problems of the individual entities. However, these approaches generally exhibit large computational times and convergence issues. To avoid these drawbacks and to explicitly consider the price-making strategy of the interconnector, the resolution procedure presented in this work adopts a one-shot scheme. The MA solution is directly obtained through the MATLAB *fmincon* routine for nonlinear optimization, considering explicitly the profit-maximization problem of the interconnector in equation (3.3) as the objective function and accounting implicitly for the autonomous UC decisions in areas A and B through the inclusion of equations (3.5) as nonlinear constraints, characterizing the prices as the Lagrange multipliers returned by the resolution of (3.1) and (3.2) with the MATLAB quadprog routine. A schematic representation of the resolution procedure is presented in Fig. 3.2, together with an indication of the key interactions between the decision variables. In particular, the proposed method is able to consider at once two different elements:

- Impact of capacity allocations on prices: the operational choices of the interconnector (i.e. the capacity allocation variables F^p and F^r) have a non-negligible impact on the prices of energy (π_A,π_B) and FR (ρ_A,ρ_B) in the two areas. This effect is characterized analytically through equations (3.5) expressing the prices as the marginal variations of the UC costs in area A and B.

- Impact of prices on capacity allocations: in turn, the price signals have a direct effect on the congestion revenues of the interconnector, as they modify the spreads collected for

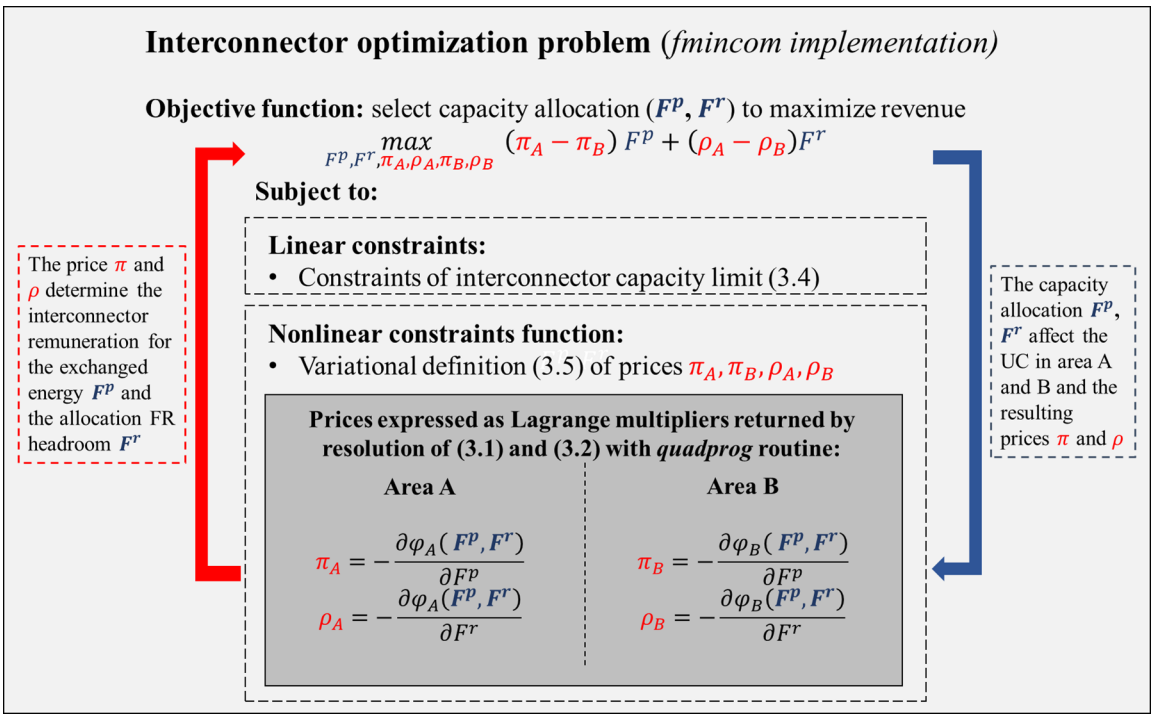


Figure 3.2: Schematic representation of the resolution procedure for the MA approach and of the key interactions between the decision variables.

energy and FR headroom. This is modelled explicitly in the objective function (3.3).

3.3 Case Studies

This chapter compares the key features and outcomes of the CA and the MA in some relevant case studies. Case setups in Chapter 2 sill apply in this case study. Table 2.1 provides the characteristics of the generation technologies in two areas, and the system parameters are D_k=1/50s, ν_k=0.5s, f_k^{roc}=0.5Hz (for both areas) σ_A=10s, σ_B=15s, Δf_A^{qss}=0.5Hz, Δf_B^{qss}=0.2Hz and ΔG_A=1.8GW and ΔG_B=1.5GW [44], [52]. Simulations have been implemented in MATLAB R2019a on Intel i7-8565U CPU, 1.80GHz processor with 64GB RAM. The computational time, in all cases, is about 1s for the CA and 127s for the MA.

Results from the CA that are assessed in the last chapter are compared with solutions from the proposed MA. Sensitivity analyses on the impact of interconnector capacity, generation costs, and maximum infeed loss, with ad hoc modifications of relevant parameters, are presented in Chapter 3.3.1 to 3.3.4.

3.3.1 Base Case - Comparisons between CA and MA

The generation and demand balance profiles in GB and France under MA are presented in Fig. 3.3. These profiles display minor differences compared to the CA profile shown in Fig. 2.4, attributable to the distinct scheduling solutions derived from the two approaches. The allocation of the interconnector capacity in the CA and MA case are compared in Fig. 3.4. The power flow F^p from France to GB remains always positive in the CA and MA case. Similarly, the FR availability F^r is always greater than zero in both cases. Hence, power flows from France to GB through the interconnector and, in case of a generation fault in GB, FR would follow the same path. It is worth emphasizing that, in the chosen framework, the security of the interconnected systems is evaluated separately and therefore the generation in France has separately allocated enough FR to secure the French system in case of frequency events there. Note that the allocation of the interconnector capacity for FR is particularly relevant when the GB net demand (i.e. total demand minus wind generation) is lower. For instance, the typically low levels of inertia overnight entail high FR requirements.

Both the CA and the MA allocate part of the HVDC capacity for FR. In the early hours, the share of capacity dedicated to FR is higher/lower than the one for energy in the MA/CA, respectively. In later hours, the net demand in GB is higher and the FR requirement are less demanding, although an increase in wind availability is reported between 12:00 and 16:00 (Fig. 3.3). The interconnector is used only to exchange energy in the CA. Conversely, in the MA, a small part of the interconnector capacity is allocated for FR when GB wind generation is higher, confirming the tendency to allocate more FR than the CA.

Fig. 3.5 displays another metric to compare the CA and the MA, i.e. the price differentials of power and FR availability exchanged over the interconnector. These are defined as:

$$\delta_P = \pi_A - \pi_B \tag{3.6a}$$

$$\delta_R = \rho_A - \rho_B \tag{3.6b}$$

In the CA (dashed lines), the condition $\delta_P{=}\delta_R$ holds when FR is allocated through the interconnector (night hours). If this were not the case, the objective function of the UC problem (2.12) could be improved simply by allocating more capacity to the quantity with higher differential. Note that, after 07:00, this balance between energy and FR allocation to ensure equal price

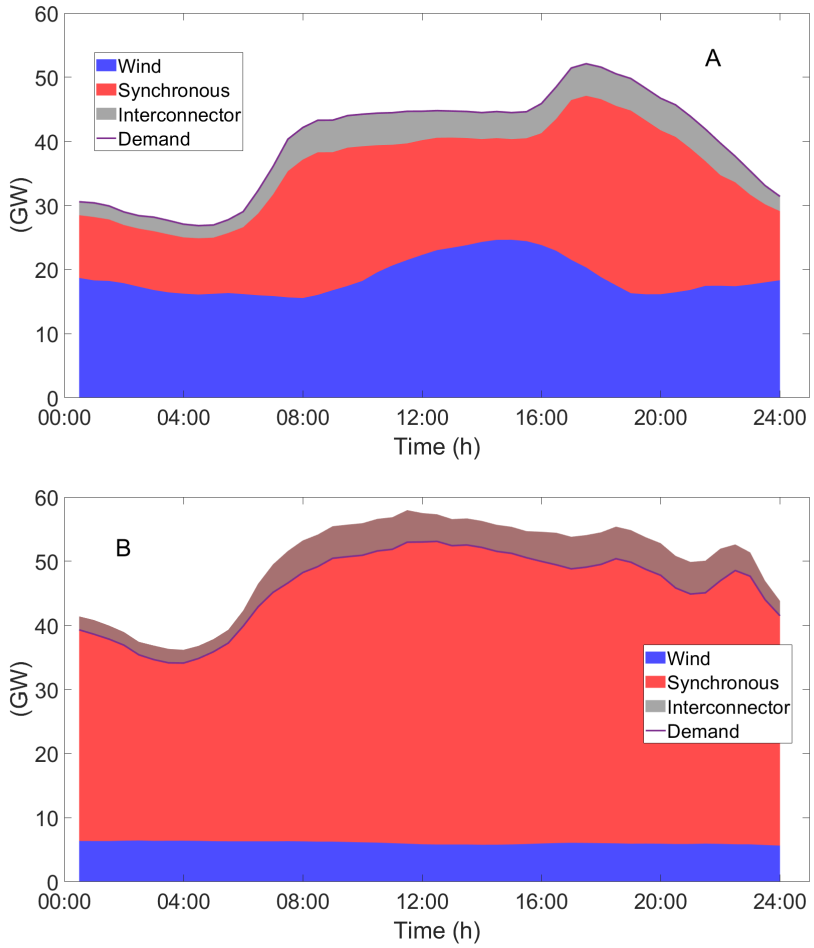


Figure 3.3: GB and France generation mix and demand profile under MA.

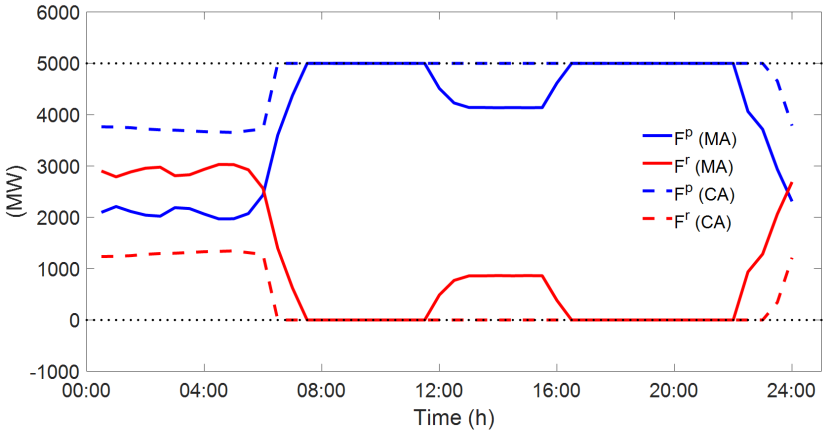


Figure 3.4: The capacity repartition of the interconnector in the CA and MA.

differentials cannot be achieved as the exchanged energy has reached F^{max}; as a result, the two price differentials diverge.

Some differences are reported under the MA, where the allocation of the HVDC link is determined in order to maximize the congestion surplus and the revenues of the interconnector. It can be seen in Fig. 3.4 that, in this case, an increasing share of interconnector capacity is allocated to FR in night hours and early afternoon. By withdrawing capacity for the exchange of energy, the interconnector is able to significantly increase the energy price differential δ_P (blue solid line in Fig. 3.5).

In the intervals 07:00 - 11:30 and 16:30 -22:00, the solutions of the two approaches are equal. In these hours, the large share of synchronous generation committed in the GB has i) increased π_A, the marginal cost of energy in GB and ii) reduced the value of FR in GB as consequence of the increased amount of system inertia. Hence, the energy price differential δ_P is significantly greater than the FR one δ_R, even without capacity withdrawing. The full HVDC capacity is allocated to energy also in the MA.

Table 3.1: Base case results

Daily system operational cost ($M£$)		Daily line revenue ($M£$)	
CA	MA	CA	MA
151.80	152.17	12.02	12.25

The total system operational cost and interconnector revenues for the two analysed scenarios are in Table 3.1. In the MA, the daily interconnector profit, i.e. the congestion rent collected

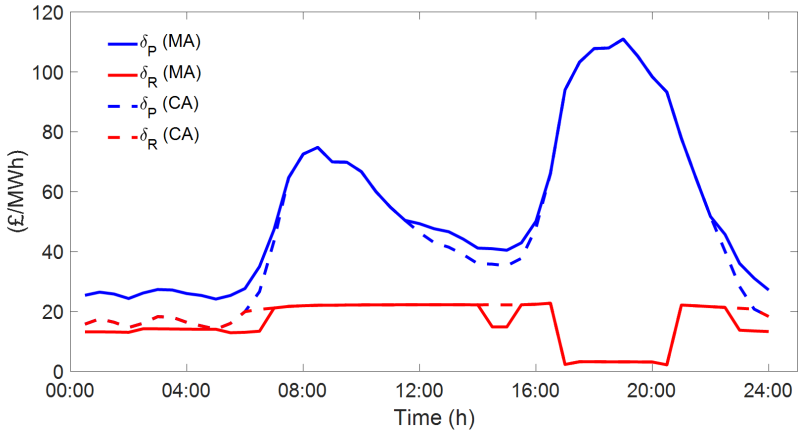


Figure 3.5: Electricity and FR price differentials in the CA and MA scenarios.

over the line for the exchange of energy and FR, reaches 12.25 M£. This is 1.91% higher than the same quantity evaluated in the CA solution. This is expected, since the MA explicitly models the interconnector as a self-interested profit-maximizing agent, whereas, in the CA, the interconnector is managed to maximize social welfare and does not receive any revenues. As a result, in the MA the capacity allocated for energy is reduced with respect to the CA case during low inertia periods in GB, in order to induce a higher energy price differential and achieve higher interconnector revenues. This is suboptimal in terms of overall social welfare: the system operational costs in the MA are 0.24% higher than in the CA.

As discussed, the proposed modelling paradigm advocates the utilization of the interconnector capacity for the joint exchange of energy and FR between connected systems. In order to assess the potential benefits of this new approach with respect to established frameworks with exclusive exchange of energy, the results of the two cases are compared in terms of system costs and line revenues/utilization in Table 3.2.

Table 3.2: Multi-service VS. energy-only exchange over the interconnector

		Energy+FR	Energy-only
System operational cost ($M£$)	CA	151.80	151.98
	MA	152.17	152.26
Line revenue ($M£$)	CA	12.02	11.18
	MA	12.25	11.91
Average line utilization for energy (%)	CA	92.88	98.38
	MA	78.98	90.76
Average line utilization for FR (%)	CA	7.12	0
	MA	21.02	0
Average line utilization (%)	CA	100	98.38
	MA	100	90.76

Note also that the proposed Energy+FR paradigm allows full utilization of the line capacity, with a +1.6% and a + 9.2% utilization rate with respect to the energy-only case in the CA and MA solutions, respectively.

3.3.2 Impact of Varying the Interconnector Capacity

Referring back to the findings from Chapter 2.4.2, the social welfare does not exhibit a consistent upward trend with unlimited expansion of the link capacity. Drawing from these results, the sensitivity of the line utilization, systems operational costs and line revenues to the interconnector capacity is assessed in Table 3.3 for four values of F^{max}, limited within 10GW.

As expected, a larger F^{max} allows a more efficient sharing of resources between the two systems and ensures lower operational costs in the CA case. With respect to the case with no line (0 GW) system operational costs are reduced by 4.20%, 9.22% and 14.65% with a line capacity of 2GW, 5GW and 10GW, respectively. The system operational cost in the MA scenario follows a similar trend, going from 167M£ in the case of no interconnection to 145M£ when the maximum line capacity of 10 GW is considered. The differences with the CA become more relevant as the line capacity increases, since there are more opportunities and incentives for the interconnector to withdraw capacity and increase congestion revenues, especially for energy exchange. This becomes particularly relevant in the case with 10 GW, where the line utilization rate for energy goes from 85% in the CA to 64% in the MA and the overall used line capacity is withdrawn by about 12% in the MA. As a result, the interconnector achieves a 21.8% increase in revenues, at the expense of a 1.2% increase in generation costs.

Table 3.3: Results of sensitivity study on interconnector capacity

Interconnector Capacity		0GW	2GW	5GW	10GW
System operational cost ($M£$)	CA	167.22	160.20	151.80	142.72
	MA	167.22	160.24	152.17	144.46
Line revenue ($M£$)	CA	0	6.42	12.02	12.64
	MA	0	6.44	12.25	15.40
Average line utilization for energy (%)	CA	-	99.87	92.88	84.98
	MA	-	93.11	78.98	63.89
Average line utilization for FR (%)	CA	-	0.13	7.12	15.01
	MA	-	6.89	21.02	24.25

3.3.3 Increasing Synchronous Generation Costs in France

Two alternative scenarios with different generation costs are constructed and compared to the Base Case (BC) results. The parameters $\alpha_{B,\tau}$, $\beta_{B,\tau}$, $\gamma_{B,\tau}$ of the production costs of synchronous generation in France vary from the values assumed in the BC (Table 2.1), to those in Case 1 ($5£/MWh$, $20£/MWh$, $2e-3£/MWh^2$, respectively) and in Case 2 ($7£/MWh$, $25£/MWh$, $2.5e-3£/MWh^2$). The resulting daily system operational costs, line revenues and line utilization are in Table 3.4. As expected, the system operational cost increases from the BC to Case 1 and Case 2 in both CA and MA as generation becomes more expensive. Interestingly, the interconnector revenue and the line capacity utilization reach their minimum values in Case 1 and then increase again in Case 2.

Table 3.4: Sensitivity to the thermal generation cost in France

		Base case	Case 1	Case 2
System operational cost ($M£$)	CA	151.80	298.61	341.81
	MA	152.17	299.45	342.42
Line revenue ($M£$)	CA	12.02	3.03	11.10
	MA	12.25	4.36	11.75
Line utilization (%)	CA	100	75.72	88.63
	MA	100	58.12	85.66

To explain this trend, it is useful to analyse the energy price differentials in Fig. 3.6. In the BC, the inequality $\delta_P = (\pi_A - \pi_B) > 0$ holds at all times, with generators with lower production cost in France providing energy support to GB through the interconnector. In Case 1, δ_P becomes negative ($\pi_B > \pi_A$), although the production cost of synchronous units is France is still lower than in GB. Note that the French demand profile is generally higher than the GB one (Fig. 3.3). Moreover, the absolute value of δ_P is relatively low; the potential support and value of the interconnector are thus reduced.

The line capacity utilization drops from 100% of the BC to 76% of Case 1 in the CA, with a 74.8% reduction in line revenues. The line utilization is further reduced in the MA case (58.12%), since the interconnector withholds capacity to increase price differentials and collect higher revenues. In Case 2, the values assumed by δ_P are remarkably lower than zero. Compared to Case 1, the higher price differential ensures increased line revenues and line utilization (e.g.

89% in the CA). This is seen in the hourly capacity allocation in Fig. 3.7. As the synchronous generation costs in France increase from the BC to Case 1 and Case 2, the direction of the power flow gradually reverses. In Case 1, the power flows from GB to France.

However, the overall amount of power flowing through the line is lower than the BC, where the entire capacity was dedicated to power flows in most hours of the day. In Case 2, with higher electricity prices in France, the capacity allocated for power exchanges from GB to France (negative values in the Fig. 3.7) is higher than in Case 1 at almost all times, leading to a higher utilization rate. Note that the allocation of FR is not significantly affected by the changes to the generation costs.

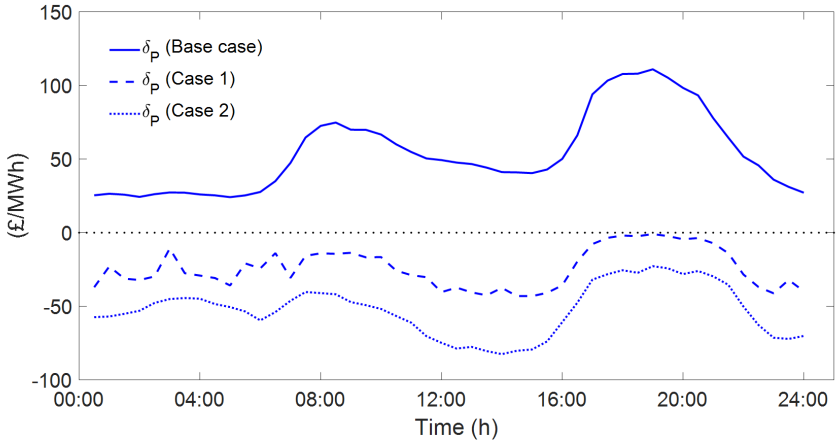


Figure 3.6: Energy price differentials for different generation cost in France (MA).

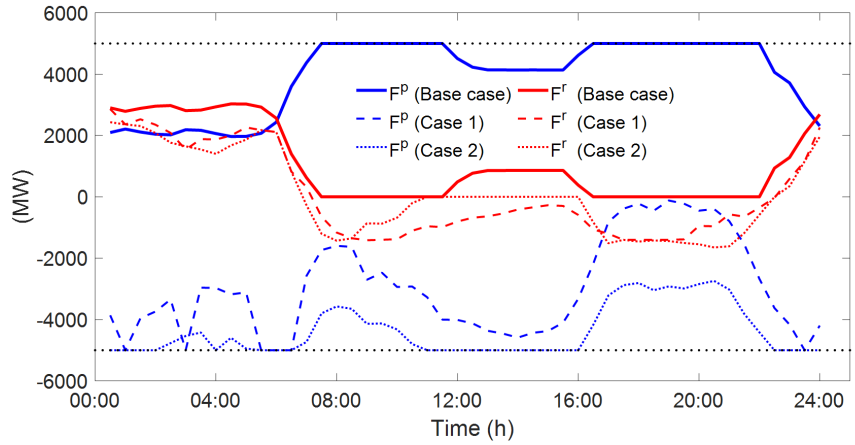


Figure 3.7: Capacity allocation of the interconnector for different cost parameters of thermal generation in France (MA).

3.3.4 Changing the Maximum Infeed Loss in GB

This section evaluates the impact of lower (1500 MW) and higher (2100 MW) infeed loss ΔG_A in GB with respect to the set value of 1800 MW in the BC. The daily system operational costs, interconnector revenues and the average capacity utilization under the CA and the MA are presented in Table 3.5.

Table 3.5: Sensitivity to the maximum infeed loss in Great Britain

Maximum infeed loss		1500MW	1800MW	2100MW
System operational cost ($M£$)	CA	150.13	151.80	153.65
	MA	150.47	152.17	154.00
Line revenue ($M£$)	CA	12.34	12.02	11.89
	MA	12.59	12.25	12.16
Average line utilization for energy (%)	CA	92.92	92.88	92.58
	MA	80.73	78.98	78.73
Average line utilization for FR (%)	CA	7.08	7.12	7.42
	MA	19.26	21.02	21.24

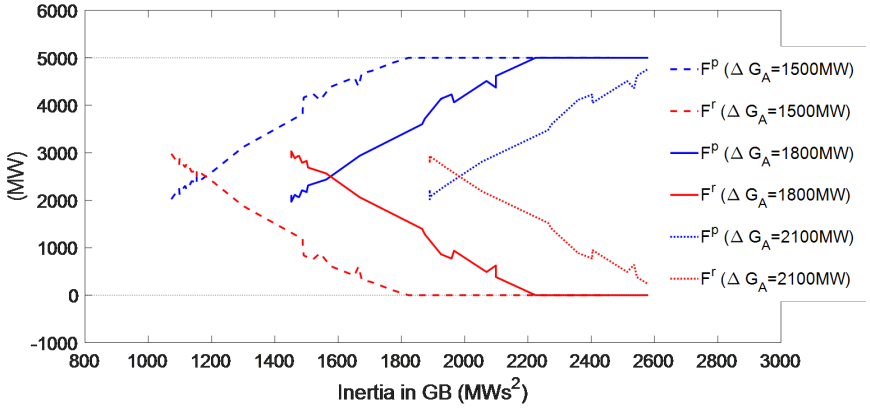


Figure 3.8: Interconnector capacity allocation in the MA case, for different values of maximum infeed loss in GB and for increasing values of system inertia.

When moving from $\Delta G_A = 2100MW$ to $\Delta G_A = 1500MW$, the system operational cost decreases by around 2.3% in the CA and MA, since lower levels of inertia are needed. At the same time, a higher infeed loss leads to lower line revenues, as a larger share of its capacity is utilized for FR, which is exchanged at a lower price differential. In the CA case, the average line utilization for FR goes from 7.08% to 7.42% as the maximum infeed loss increases. This percentage further increases in the MA, as the interconnector reduces the capacity allocated for energy in order to increase its price spread and achieve higher revenues.

The allocation of the HVDC capacity is presented in Fig. 3.8 for the different cases, to further emphasize its relationship with the frequency requirements of the interconnected systems. The results over the 24h interval have been reordered according to increasing values of GB system inertia (x-axis). As expected, lower inertia levels correspond to a higher utilization of the interconnector for exchange of FR availability (as the FR requirements in GB increase).

A similar trend occurs when the impact of the maximum infeed loss is considered: for equal values of system inertia, more capacity will be allocated for FR when ΔG_A is higher. Albeit the monotonicity trends are evident, there are some small oscillations in the values of energy and FR allocation. These are generally caused by different system conditions (e.g. inertia levels) in France, which impact the MA solution in correspondence of similar values of GB inertia. It is worth noting that capacity allocation of energy and FR does not change uniformly as GB inertia increases, and some small jumps appear in the line. For adjacent points in the plot, they have close GB inertia level. However, the corresponding system inertia levels in France for such points may vary significantly due to the specific demand and generation profile at those time, which impacts the scheduling decisions and prices. Thus, possible variations in energy and FR prices finally lead to slight difference in the capacity allocation.

3.4 Conclusion

This chapter presented a novel market-based framework to quantify the potential impact of interconnectors on the efficiency and security of interconnected systems, considering the possibility of simultaneous exchange of energy and frequency response services through the lines. Under the proposed market approach, the interconnector is modelled as a self-interested agent aiming to maximize its profit. This novel setup is proposed and validated as a potential alternative to a traditional centralized approach in Chapter 2 where the interconnector is centrally operated to minimize the total system operational costs. Results have shown how interconnectors can improve social welfare by enabling a mutual exchange of resources between systems with different characteristics and generation mixes. These benefits are marginally reduced in a

market setup where the interconnectors withdraw their capacity to achieve higher price spreads and thus increase their revenues.

The results in this work call for a revision of the current regulatory framework which acknowledges the importance of multi-service allocation of interconnection capacity in a competitive market framework. The analysis also showed that the proposed multi-service framework, if compared with the existing energy-only paradigms, can ensure lower system costs and, at the same time, higher revenues for privately-owned interconnectors.

For simplicity, in order to better highlight the main qualitative aspects of the proposed novel paradigm, the analytical formulation presented in Chapter 2 and 3 considered exclusively two-area systems. While the extension to a generic radial system is straightforward, the more complex adjustments in the modelling framework are required to account for meshed networks. Chapter 6 gives one example of the modelling extension to multi-area system with meshed topology. This will be expand in the future for a more detailed and comprehensive analysis.

3.5 Future Works

This work can also be extended for a wider spectrum of ancillary services characterizing the interconnector operation. The interplay between the inter-area flexibility provided by interconnectors and flexibility provided locally by other assets (e.g. battery storage) will be analyzed in a market-based approach. Similarly, the agent-based modeling framework can be considered to include modelling of other relevant assets in the interconnected power systems. In particular, the competitiveness of interconnectors against profit-making supply companies is subject of ongoing work.

For simplicity, in order to better highlight the main qualitative aspects of the proposed novel paradigm, the analytical formulation presented in Chapter 2 and 3 considered exclusively two-area systems. While the extension to a generic radial system is straightforward, the more complex adjustments in the modelling framework are required to account for meshed networks. This extension introduces various possibilities for participant roles, such as a distinct business

interconnector entity for all links, several profit-oriented interconnector agents, and a mix of regulated and business interconnectors. An initial evaluation that considers both regulated and business interconnectors within a meshed network topology has been proposed and examined in Chapter 6.

Other discussions regarding the transmission losses and the availability of the interconnector are considered and will be incorporated in the future steps.

3.5.1 Incorporating the Cost of Losses

Consistently with other high-level analyses on the transmission infrastructure [52], [53], the initial modelling framework presented in this work does not account for the impact of losses on social welfare and interconnector revenues. From a qualitative point of view, it is reasonable to expect that, if losses are considered, a larger share of the interconnection capacity will be dedicated to FR purposes, since this requires only the allocation of the line capacity (with the exception of the actual service provision following a frequency event) and therefore does not correspond to any power losses. Specifically, under a CA, the costs for losses are sustained by the central entity in charge of scheduling the system (e.g. the system operator). Under the MA, the owner of the HVDC link has to sustain its own cost for losses.

The current modelling framework will be extended to provide a quantitative evaluation of this aspect through the inclusion of non-linear (e.g. quadratic) constraints to account for the impact of losses. This is not a critical challenge, as the resulting non-linear optimization problem could in general be reformulated and solved as a second-order cone programming problem. An alternative option is to incorporate HVDC losses by exploiting the results presented in Section II and IV of [45], which proposes linear or piece-wise linear formulations of the losses related to the HVDC technology. As in the previous case of extension to meshed networks, it is worth noting that the novel multi-service methodology proposed in our work does not introduce additional layers of complexity towards the integration of losses.

3.5.2 Impact of Outages

The formulation presented in this work followed a deterministic approach where the availability of the relevant components (not only of the interconnector but also of the generators) is assumed to be fixed and known a priori. However, in reality, the available capacity of the interconnector might vary over time as a result for example of planned maintenance or unexpected outages. The positive effect on social welfare by employment of interconnector will be attenuated if one considers the interconnector subject to any possible unavailability since the sharing of resources between connected systems will inevitably reduce. However, it is still reasonable to assume that the key conclusions of the results still hold: the simultaneous exchange of energy and FR improves total social welfare, while the adoption of market-based framework reduces social welfare by withdrawing capacity utilization.

The modelling framework presented in this paper will be expanded in order to quantitatively analyze this issue. In particular, the UC formulation in (2.12) to (2.16) can be replaced by an alternative stochastic model where the commitment of the generation units and the allocation of the regulation resources required for system security takes explicitly into account the potential failures of the different system components and the associated uncertainties. Alternatively, the deterministic solution obtained with the current methodology in this work can be tested ex-post in a stochastic scenario, evaluating the impact of unplanned outages through Monte Carlo simulations.

Chapter 4

Assessment of the Impact of Wind and Demand Variability on the Flexible Operation of Interconnectors

This chapter delves into the impact of wind and demand variability on the short-term operation of the interconnectors. The underlying modelling approach adopts frameworks proposed in Chapter 2. The framework envisages the simultaneous cross-border exchange of power and inertia-dependent frequency response services through the interconnector. Two operational paradigms, including the centralized approach in Chapter 2 and market approach in Chapter 3 are discussed. To assess the impact of varying wind availability and demand levels on the operation of interconnectors, a sampling-based methodology is employed, focusing on analyzing the sensitivity of both operational and economic metrics. A comprehensive set of case studies is developed, specifically examining the interconnections between Great Britain and France. These studies highlight the benefits that interconnectors can provide across a diverse array of system conditions, demonstrating their critical role in enhancing grid stability and efficiency under fluctuating renewable inputs and consumer demands.

4.1 Introduction

As the penetration of RES in power systems increases significantly to reach decarbonization targets, the variability of the RES power output has become a critical issue [75]. As discussed in the previous chapters, the stability of the power system is critical for the secure and continuous operation, which is crucially related to the system inertia. RES, notably, do not contribute to the system's inertia due to their connection to the network through power electronics. Moreover, the oscillations and the uncertainties in RES generation, along with the fluctuation in the demand side pose a growing impact on power system operation, as increased balancing resources will be required to match demand and supply and regulate the system frequency.

Regarding the impact of RES variability, [76] proposed a novel technique that combines physical, statistical and economic elements in order to assess the sensitivity of the GB power system with respect to the most relevant weather-related variables, i.e. wind availability and power demand. A probabilistic approach is adopted in [77] to assess the impact of wind integration within a market framework, applying Monte Carlo simulations to model the variations in wind and demand. The research [78] examines how integrating wind power generators affects the transient stability of a power system, taking into account various system load conditions. It seeks to understand the connection between system transient stability and different levels of net-load. The paper [79] explores the influence of load variability modeling on power system transient stability by examining various Probability Distribution Functions (PDFs). It proposes guidelines for selecting the most suitable PDFs for this purpose. The impact of wind variability was assessed in [80] with regard to the Ireland-GB interconnected system.

Possible scenarios, characterised by high RES availability and low system demand are particularly challenging for system security. Reduced levels of inertia and frequency regulation resources could further hinder a cost-effective RES integration [81]. Therefore, this chapter continues to discuss the impact of the variability from power systems on the proposed operational and market model of the interconnector in the Chapter 2 and 3.

Two scheduling approaches, consistent with the model in Chapter 2 and 3, are considered:

under a centralized approach, the interconnector is operated to minimize system operational costs. Alternatively, under a competitive market approach, the interconnector is modelled instead as a profit-seeking business asset. Case studies make use of a simple but yet effective model of the GB-France interconnected power networks. Simulations have been carried out considering randomly sampled GB wind and demand profiles as inputs for the two scheduling approaches, evaluating the results on the basis of key operational and economical metrics.

The analytical formulation and modelling framework underlying this work has been presented in Chapter 2 and 3 also in the publication [82]. The contributions from this chapters include:

a. Implementation of a detailed statistical sampling method that utilizes historical data to comprehensively evaluate the performance of the interconnector across a range of system conditions. This method enables a nuanced understanding of how the interconnector functions under diverse scenarios.

b. Detailed quantitative assessment of how variations in demand and wind conditions affect the performance of the interconnector, focusing on crucial operational and economic metrics. This analysis provides insights into the interconnector's efficiency, profitability in response to fluctuating energy supply and demand under different market paradigms.

This chapter is organized as follows: Chapter 4.2 provides the description and formulation of the centralized and market approaches for interconnector operation. Chapter 4.3 shows the detailed methodology of the sensitivity analysis with respect to wind availability and demand levels. The case study of the GB-France system is presented in Chapter 4.4, while the conclusive remarks follows at the end.

4.2 Model Formulation

The model developed in this chapter is consistent with Chapter 2 and 3. It consists in two power systems as shown in Fig. 2.2, which are connected through a single interconnector. A

key feature of this model is that the interconnector not only enables the exchange of energy between the two areas, but it also allows mutual provision of FR. This framework, in its simplicity, allows to capture the fundamental relationships between the identified sensitivity factors relevant to both power systems (i.e. the variability of wind generation and demand) and the interconnector's operation.

On the basis of the modelling framework already introduced in [82], the optimal and secure operation of the interconnector is determined by means of two different methodologies, a centralized approach (CA) and a market approach (MA).

4.2.1 Centralized Approach (CA) and Market Approach (MA)

Under CA, the optimal system operation in the two areas is centrally coordinated via a single unit commitment (UC) problem. The objective of the MA is to minimize the whole system operational cost by optimally scheduling generations and allocating interconnector capacity. The UC assumptions and formulations are consistent with equation (2.12) to (2.16).

In MA, the power system and the interconnector are modelled as independent profit-seeking entities that determine their operational decisions in order to maximize their own profit. Chapter 3.2 deduced the mathematical formulation of MA, from equations (3.1) to (3.5). The outcome is then characterized as the Nash equilibrium of the competitive game, where no agent can improve its profit by changing its strategy unilaterally. The interactions among self-interested agents and numerical implementation of the MA is described in Fig. 3.1 and 3.2.

4.3 Assessment Methodology

In order to evaluate the effect of demand and renewable generation variability on the operation of the interconnector, the optimal repartition of the link capacity (utilized for both energy exchange and FR allocation) has been calculated for a wide range of system conditions over a fixed time window of 24 hours. The sensitivity analysis has been performed for both the CA

and MA, adopting the total system operational costs and the interconnector's revenues as key metrics, accordingly.

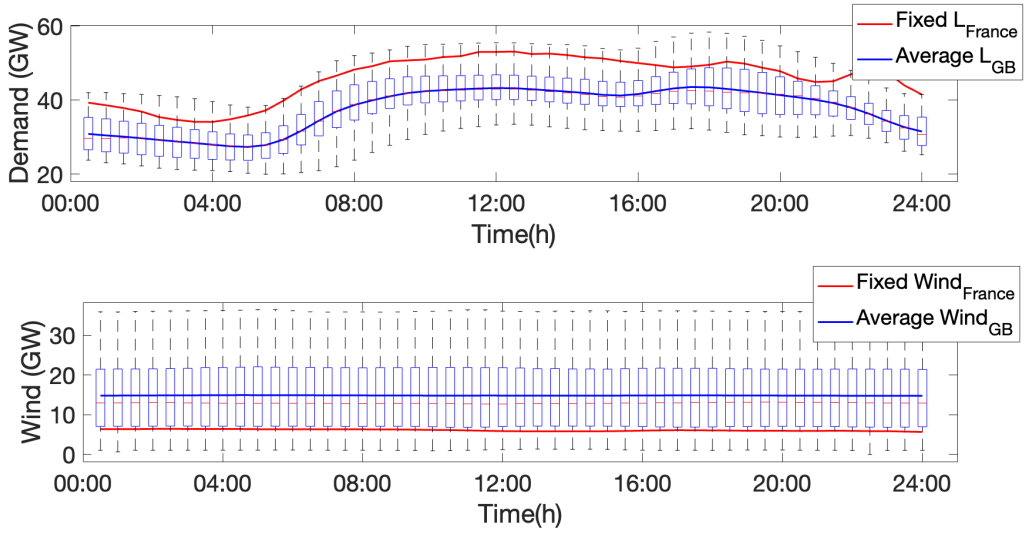


Figure 4.1: Comparison of demand levels (top) and wind half-hourly generation (bottom) between France and GB. Red and blue traces represent the half-hourly average values for France and GB, respectively. The blue boxes correspond to the 25^{th}-75^{th} percentiles of the GB profiles, whose minimum and maximum half-hourly values are indicated in black.

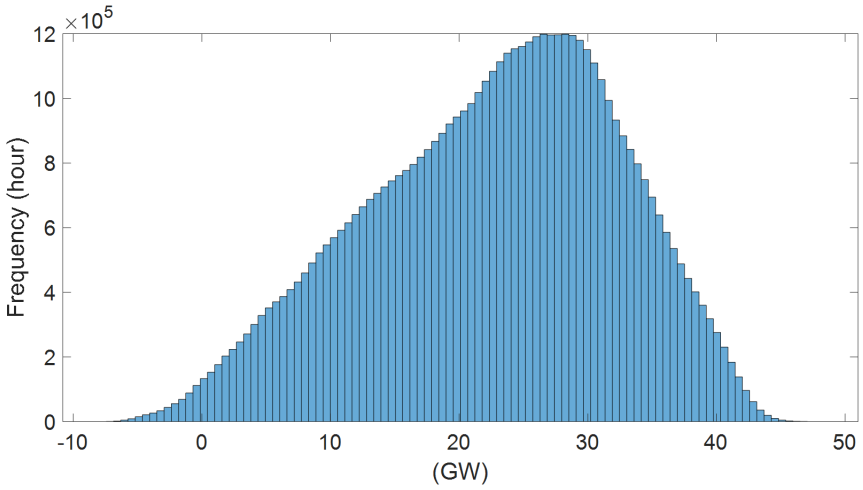


Figure 4.2: Hourly frequency plot of GB net demand (demand minus wind generation) in the considered dataset.

Areas A and B are intended to represent the GB and France power systems, linked by a single interconnector. Furthermore, the assessment of the wind and demand variability pertains only the GB system, whereas these quantities have been kept fixed in France. The GB demand and wind daily profiles have been taken from a large dataset of $n = 20$ annual scenarios (with 30 min granularity) of wind availability and demand consumption for 2030 [43]. The variability

of the GB system demand with respect to its average half-hourly values (blue solid line) is highlighted in the upper side of Fig. 4.1 by indicating the 25^{th} -75^{th} percentiles (blue boxes) and the minimum-maximum values (black dashes) of demand at each half hour. A constant load profile (red curve) is considered for France, instead. The same graphical convention is utilized in the lower side of Fig. 4.1 for wind generation in the two systems, showing a high variability of the possible wind realisations in GB at each time step.

Furthermore, the figure shows that GB is characterized by higher average wind levels and lower demand levels than France. The distribution of the GB net demand (demand minus wind available generation), evaluated on an half-hourly basis, is presented in Fig. 4.2. The net demand assume values between -7.8GW and 48.2GW, with a mean of 22.6GW and standard deviation of 9.8 GW.

In the reminder of the chapter, for simplicity, we will denote by $SD_{i,j}$ and $SW_{i,j}$ the GB demand and wind generation samples (respectively) for the i^{th} 30-minute interval of year j. The quantities SD and SW correspond therefore to matrices of dimension $n_{HH} \times 20$, where $n_{HH} = 17520$ quantifies the number of 30-minute intervals in one year. A detailed description of the sampling-based methodology adopted to perform the sensitivity analysis is summarized in Algorithm 4.1. In Phase 1), the dataset for demand and wind is divided in 4 different groups, in order to perform separate analyses in each season of the year and highlight relevant seasonal trends in the operation of the interconnector. In Phase 2), for each of the four seasonal periods (indexed by m), N different daily samples s are generated. For each of them, distinct demand and wind profiles ($SD_s^{(m)}$ and $SW_s^{(m)}$, respectively) are randomly extracted from the available dataset. The CA and MA problems presented in Chapter 2 and Chapter 3 are then solved for each sample, considering $SD_s^{(m)}$ and $SW_s^{(m)}$ as demand and available wind generation in the GB system, respectively. Finally, in Phase 3, a representative yearly dataset is built, combining N_a elements from the sampled data in each of the four seasons.

Algorithm 4.1 – Sampling-based methodology

1) Initialization

- Partition available demand datasets into four seasonal groups of equal size, with $m = 1, \ldots, 4$:
  $SD^{(m)} = \{SD_{i,j} : n_{HH} \cdot \frac{1}{4} \cdot (m-1) < i < n_{HH} \cdot \frac{1}{4} \cdot m, j \in 1, ..20\}$
- Partition wind dataset SW into seasonal groups $SW^{(m)}$, with $m = 1, \ldots, 4$, through the same procedure detailed in the previous point, replacing $SD_{i,j}$ with $SW_{i,j}$.
- Define sample size: N

2)) Sample selection and numerical simulations

for $m = 1 : 1 : 4$

for $s = 1 : 1 : N$

- Extract a random 24h demand profile $SD^{(m)}$ and wind profile $SW^{(m)}$ (with 30-minute resolution)
  $SD_s^{(m)} = \{[SD_{48 \cdot \delta + 1, j}, ..., SD_{48 \cdot (\delta+1), j}] \subset SD^{(m)}$
  $SW_s^{(m)} = \{[SW_{48 \cdot \delta + 1, j}, ..., SW_{48 \cdot (\delta+1), j}] \subset SW^{(m)}\}$
- Calculate the associated CA/MA solution $\phi_s^{(m)}/\varphi_s^{(m)}$ by solving equations (2.12)-(2.16) / (3.1)-(3.5), replacing the GB demand vector L_A with $SD_s^{(m)}$ and the GB available wind generation $G_{A,wind}^{max}$ with $SW_s^{(m)}$.

3)) Yearly aggregated results

- Build a representative yearly sampling of results, selecting N_a random samples from each seasonal group:
  $\tilde{SD} = \bigcup_{m=1}^{4} \bigcup_{l=1}^{N_a} SD_{S_l}^{(m)}$ **and** $\tilde{SW} = \bigcup_{m=1}^{4} \bigcup_{l=1}^{N_a} SW_{S_l}^{(m)}$
- Evaluate the associated yearly aggregated results for the CA and MA solutions $\phi_s^{(m)}$ and $\varphi_s^{(m)}$, respectively)

4.4 Case Studies

This Chapter presents the numerical results arising from the application of the CA and MA formulations (Chapter 2,3) and the proposed sampling-based method (Chapter 4.3) to the GB-France interconnected system. The model has been validated over a dataset of N=1000 random combinations of wind and demand samples in each season. A total of $N_a = 500$ samples has been selected in each season to build yearly profiles with 2000 samples. The main parameters of the generation technologies are kept consistent with case studies in Chapter 2 and 3, and are listed in Table 2.1.

For simplicity, only two distinct generation technologies have been considered: synchronous generation, which is, capable of providing inertial response and FR, and wind generation, which does not provide any ancillary service. Other system parameters are taken from [83], [25], with D_k=1/50s, ν_k=0.5s,f_k^{roc}=0.5Hz (for both areas) σ_A=10s, σ_B=15s, Δf_A^{qss}=0.5Hz, Δf_B^{qss}=0.2Hz and ΔG_A=1.8GW and ΔG_B=1.5GW. The rated capacity of the HVDC interconnector between GB and France is 5GW [84].

Seasonal and yearly aggregated results are presented in Chapter 4.4.1, with a particular focus on the MA. A detailed comparison of the interconnector's performance under CA and MA is provided in Chapter 4.4.2, whereas Chapter 4.4.3 assesses the correlation of wind and demand level against simulation outputs.

4.4.1 Seasonal and yearly aggregated results

Table 4.1 reports the mean μ, the standard deviation σ and the relative standard deviation μ/σ of the wind and net-demand levels in GB. In accordance with Algorithm 1, the data referring to n years are grouped in four seasons, each corresponding to three months of the year (e.g., S_1 contains the profiles from January to March). Note that the wind generation output is higher in the autumn and winter months, whereas higher (relative) variability is experienced in spring and summer. The net demands exhibit similar trends, even if the relative standard deviation is in general lower.

Table 4.1: Seasonal wind and net demand level

		Mean (GW)	Standard deviation (GW)	Relative std (%)
Wind	S_1	830.66	403.73	48.60
	S_2	575.08	356.07	61.92
	S_3	531.35	337.22	63.45
	S_4	823.45	430.68	52.28
	Yearly	690.11	403.79	58.51
Net Demand	S_1	1164.09	446.71	36.45
	S_2	1075.23	378.52	35.20
	S_3	1048.11	348.64	33.26
	S_4	1071.58	457.29	42.67
	Yearly	1108.61	401.74	36.24

The CA and MA solution has then been calculated for each of the $N = 1000$ yearly demand/wind profile contained in the input data. The relevant stochastic metrics (mean and standard deviation) of the resulting daily system operational cost and line revenue exhibit consistent trends between CA and MA between CA and MA. Due to this redundancy, only the MA solutions are detailed in Table 4.2.

Table 4.2: Operational cost and line revenue results under MA

		Mean ($M£$)	Standard deviation ($M£$)	Relative std (%)
Daily system operational cost	S_1	181.77	50.16	27.60
	S_2	164.46	38.56	23.45
	S_3	159.89	34.68	23.57
	S_4	172.66	50.31	29.14
	Yearly	170.07	44.49	26.16
Daily line revenue	S_1	17.61	9.45	53.66
	S_2	15.38	7.44	48.37
	S_3	14.59	6.75	46.26
	S_4	16.15	9.29	57.52
	Yearly	15.97	8.34	52.19

Generally speaking, the system costs follow the same trends of the net demand: when the share of total demand that needs to be supplied by synchronous generators is higher, the system costs increase accordingly. Note also that the relative standard deviation of the system costs is generally lower if compared with the same metric for the net demand, as lower generations costs associated to high wind penetration are counterbalanced by higher costs for system security (more inertia and FR needs to be allocated). In terms of daily revenues collected by the

Table 4.3: Yearly aggregated results under CA and MA

		Mean	Standard deviation	Relative std dev.(%)
Daily system operational cost (M£)	CA	169.86	44.61	26.26
	MA	170.07	44.49	26.16
Daily line revenue (M£)	CA	15.68	8.64	55.12
	MA	15.97	8.34	52.19

interconnector, these are generally higher in seasons with high net demand in GB, as larger energy price differentials can be captured.

4.4.2 Yearly-aggregated results under CA and MA

Having evaluated the general trends of the input data and their relationship with the performance metrics of the MA, the analysis has then focused on the comparison between the CA and MA solutions. The stochastic metrics of the daily system operational costs and line revenues for the two approaches are reported in Table 4.3, considering yearly-aggregated results as determined in Phase 3 of Algorithm 4.1. As expected, lower operational costs are obtained in the CA (-0.12% on average with respect to the MA) since in this case the system costs are explicitly minimized by a centralized coordinator. However, it can be seen the overall costs of the market approach are only slightly higher. Moreover, the standard deviation in the two approaches does not exhibit significant differences, suggesting that the adoption of market solutions for the operation of interconnectors does not lead to higher cost variability with respect to centralized frameworks. The comparison of the daily line revenues, reported in the bottom part of the table, has considered the value of φ_{INT} (defined in (3.3) for both CA and MA, albeit such revenue is not actually collected by the interconnector in the CA scenario. The results show that the interconnector in the MA, acting as a profit-seeking agent, can modify its capacity allocation with respect to the CA (i.e. by withdrawing capacity) in order to achieve higher revenues. At the same time, it appears that the margin for revenue improvement through these self-interested strategies remains limited (only +1.85% on average).

For a more detailed comparison of the interconnector strategies in the two approaches, the capacity allocations for energy and FR in the two scenarios are plotted as a function of net

demand in Fig. 4.3, considering that the flows F^p and F^r take positive values if the associated quantity is exchanged from area B (France) to area A (GB). Purple and blue dots shown in the scatter plots correspond to the simulation results under CA and MA respectively, based on sampled input wind and demand profiles. For each sample, average half-hourly capacity allocation decisions are considered.

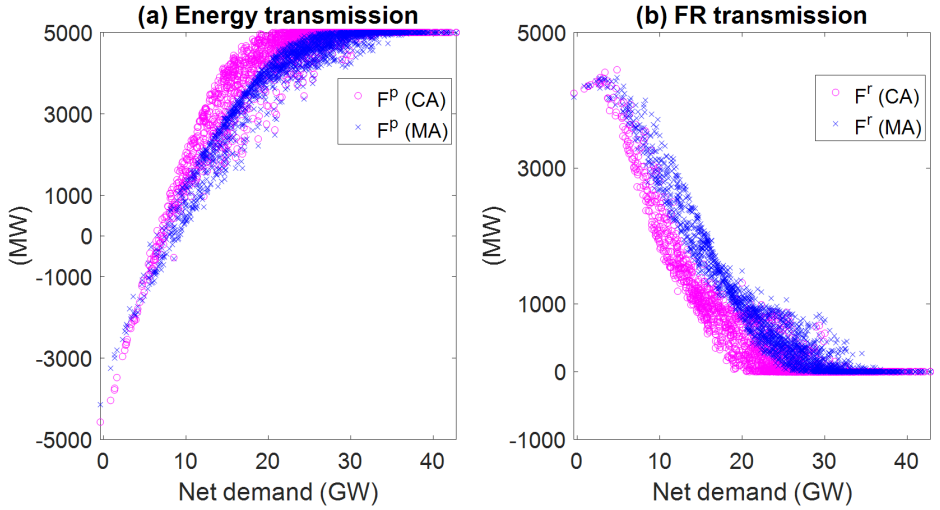


Figure 4.3: Line capacity allocation in CA, MA for different GB net demand level.

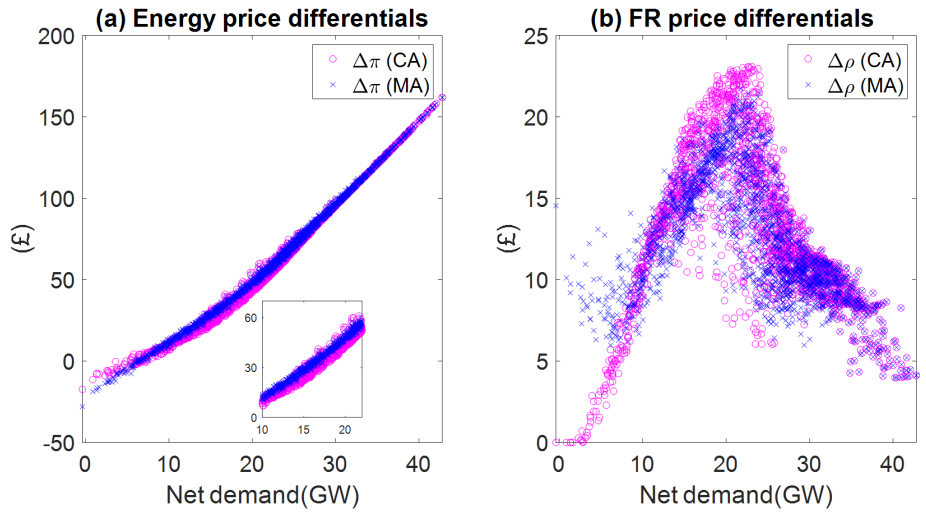


Figure 4.4: Electricity and FR price differentials between GB and France in CA and MA for different GB net demand level.

One of the most evident trends in Fig. 4.3 is that, both in the CA and MA, more capacity is allocated for energy transmission when the net demand in GB is higher. This is reasonable in the CA, since it is cheaper to fulfil the demand by transferring energy from France rather than using the more expensive GB synchronous generators. To analyse the same trends for the

MA and motivate its differences with respect to the CA, it is useful to consider the energy and FR price differentials between the two areas, which are reported in Fig. 4.4 and are defined as follows:

$$\Delta\pi = \pi_A - \pi_B \tag{4.1a}$$

$$\Delta\rho = \rho_A - \rho_B \tag{4.1b}$$

Note that, when F^p is positive (i.e. energy is exchanged from France to GB), the amount of capacity allocated by the interconnector is generally lower in the MA than in the CA. At the same time, as highlighted in the zoomed section of the left plot in Fig. 4.4, the price differential $\Delta\pi$ is slightly higher in the MA. This difference can be explained by the self-interested behaviour of the interconnector in the MA, which withdraws capacity in order to increase price differentials and therefore achieve higher revenues. The same trends occur (with opposite sign) for low values of net demand, when F^p is negative and energy is exchanged from France to GB.

Note that the interconnector's capacity is fully used for energy exchange when net demand is over 18GW in the CA, while the line is saturated for net demand values above 22GW in the MA, due to the capacity withdrawing. Once the line is saturated (net demand is above 18GW/22GW for purple and blue dots), $\Delta\pi$ keeps growing because of the increasing GB demand. Conversely, $\Delta\rho$ starts to drop as a result of lower FR prices in GB: since the line is fully utilized, more synchronous generation is brought online to accommodate the local net demand, thus reducing FR requirements.

4.4.3 Correlation Assessment

A correlation analysis has been conducted to assess if there exists a relevant linear relationship between the input data (wind generation and demand) and the key performance metrics

of the simulation (operational costs, line revenues and capacity allocations). The estimated coefficients, together with the coefficient of determination R^2, are provided in Table 4.4. The R^2 is the statistical measure that indicates the proportion of the variance for a dependent variable explained by one or more variables in a regression model. The general definition of the coefficient of determination R^2 is:

$$R^2 = 1 - \frac{\sum_i (y_i - \hat{y}_i)^2}{\sum_i (y_i - \bar{y})^2} \tag{4.2a}$$

where y_i is the observed data set, $\hat{y}_i$ is the fitted value from the regression model, and $\bar{y}$ is the mean of the observed data. These values can be computed manually based on the regression analysis, or calculated directly using the certain linear regression function, such as *fitlim* in Matlab. The most relevant correlation concerns operational costs and line revenues, for which the R^2 coefficient is equal to about 0.95 in both the CA and MA. As expected, the variation in system costs can be almost entirely explained by the associated changes in the input data. When wind is lower and demand is higher, more synchronous generation needs to be brought online, leading to higher costs (and vice versa). This explains also the strong correlation that has been obtained for the rotating inertia in GB. Note that lower values of R^2 are obtained instead for the metrics that quantify the differences between CA and MA, since in these cases more complex dynamics are at play. A more detailed analysis on this point is provided in Fig. 4.5 and Fig. 4.6, where differences in line revenues and costs are plotted as a function of energy capacity withdrawing and GB net demand, respectively.

From the left plot in Fig. 4.5, it is straightforward to note the monotone increasing relationship between the withdrawing capacity percentage and the line revenues. The more the interconnector is able to reduce its line utilization (thus inflating the price differential), the more its revenues will increase. However, it is worth emphasizing that this monotone relationship is not linear, as the increase of the energy price differential in the interconnector objective function (3.3) is accompanied by a variation in the opposite sense of the exchanged energy. Similar

Table 4.4: Correlation of wind and demand with computed metrics

		Coefficient (Wind)	Coefficient (Demand)	R^2
Operational cost (£)	CA	-104.04	125.36	0.950
	MA	-103.78	125.09	0.951
Line revenue (£)	CA	-20.864	21.962	0.961
	MA	-19.955	21.253	0.948
Inertia-GB (MWs^2)	MA	-0.054762	0.047782	0.986
Line revenue differentials (£)	MA-CA	0.90992	-0.70446	0.59
Difference in operational cost (£)	MA-CA	0.25955	-0.27064	0.39
Difference in Energy Capacity allocation (%)	$\frac{\text{MA-CA}}{\text{CA}}$	6.1531e-06	-5.7435e-06	0.603
Difference in FR capacity allocation (%)	$\frac{\text{MA-CA}}{\text{CA}}$	-5.4445e-06	5.0513e-06	0.491

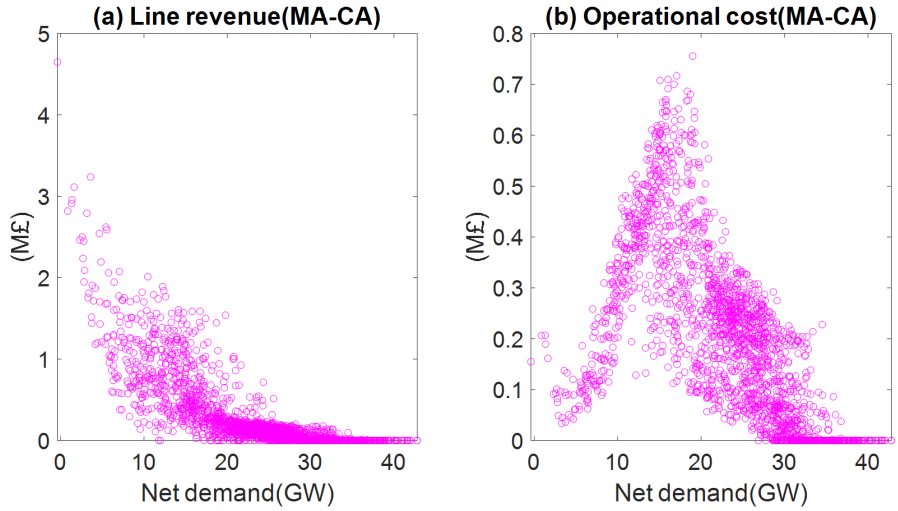


Figure 4.5: Line revenue and operational cost differentials between CA and MA for different levels of GB net demand.

considerations can be made for the operational cost, albeit a more significant linear correlation can be found in this case. From the left plot in Fig. 4.6, it can be seen that a linear correlation exists between net demand and line revenue differences when GB net demand is lower than 18 GW. At higher values, the line becomes saturated, with negligible differences between MA and CA. The line saturation also explains the change in the correlation sign between GB net demand and differences in operational costs, displayed in the right plot of Fig. 4.6.

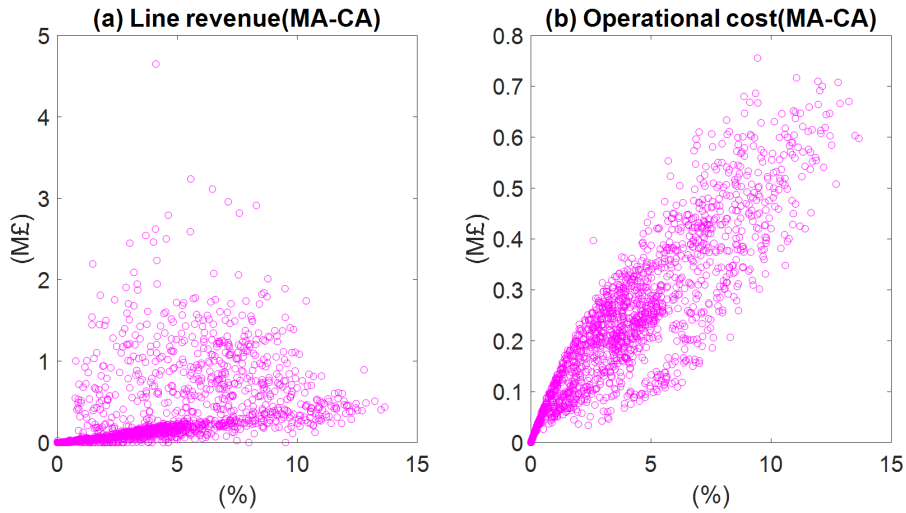


Figure 4.6: Line revenue and operational cost differentials between CA and MA for different levels of energy capacity withdraw in MA.

4.5 Conclusion

In this chapter, a sampling-based method is adopted to assess the impact of wind and demand variability on the short-term operation of interconnected power systems. A comprehensive modelling framework is used, considering simultaneous exchange of energy and FR services through the link, and comparing the outcomes of two distinct operational approaches (centralized and market-based). Simulations have been run under different combination of sampled seasonal wind and demand profiles in GB, comparing the aggregated yearly results between two approaches. The study has shown that relevant differences between CA and MA when the GB net demand level is low, since the interconnector has more incentive to withdraw capacity for energy exchange when operating independently and pursuing self-profit. As the net demand level increases, the line capacity is saturated in both cases (CA and MA), and results become identical.

4.6 Future Works

Future work will expand the model to encompass meshed networks, incorporating a broader spectrum of ancillary services. Futher effort will evaluating sensitivities with respect to addi-

tional external factors (e.g. generator or line outages).

Furthermore, it is anticipated that a stochastic scheduling model will be developed to enhance the optimization of service allocation. The model will specifically address the uncertainties associated with wind variability, fluctuating demand, and potential outages, ensuring a more robust and efficient distribution of resources.

Chapter 5

Flexible Operation of Multi-Service Interconnectors with Thermostatically Controlled Loads

This chapter introduces an additional source of flexibility from demand side Thermostatically controlled loads (TCLs) to the multi-service model in Chapter 2 and Chapter 3. The adoption of this category of flexible demands is due to their significant contribution from both residential and commercial sectors. In comparison to technologies like storage, the majority of the TCLs are already in place, positioning them as the pivotal and practical choice in case study for providing demand side response. The TCLs in this model provide the same services with the interconnector energy and ancillary services, which are energy arbitrage under regular operation, and frequency response under generation outages. However, the interconnector facilitates the cross-border service exchange, while the TCLs offer services locally. The work provides the comprehensive analysis of comparing the contributions of interconnectors and TCLs flexibility from different layers of system, under both a centralized approach and market approach. The former considers the both the interconnectors and TCLs as centrally-operated assets; the latter envisages them as profit-seeking private entities. This model is applied to the GB-France, HVDC-connected system, with the flexible TCLs only functioning in the GB.

5.1 Introduction

The transition to the low-carbon sustainable power system requires the incorporation of the Renewable Energy Resources (RES). This revolution in energy sector promises the reduction in green house gas emission, but also poses intricate challenges to the system stable and secure operation due to the intermittent nature of the RES. In this evolving landscape, the flexibility should be considered in a more holistic manner. Alongside the traditional ancillary service resources from synchronous generators, this thesis has discussed the possibility of using the transmission interconnector to provide FR service in Chapter 2 and the related market operation in Chapter 3. This chapter directs the considerable attention toward the multi-layered enhancement in the system flexibility by including demand side solutions.

Demand Side Response (DSR) can merge as a viable and innovative alternative for the grid stability. Studies [85] and [86] provided reviews of the current status and key aspects of the Demand Side Response (DSR) program, covering topics including the market, pricing schemes, regulatory frameworks, and implementation methodologies. The dynamic control of in the large-scale responsive demand is capable of replacing some of the spinning reserves, relieving pressure for part-loaded generators and contributing to the frequency stability in a more cost effective way [87]. Thermostatically Controlled Loads (TCLs), such as refrigerators, heating system, dishwashers, air conditioners, is the important class of responsive electrical loads that can be integrated in the DSR. The control of these devices through their ON-OFF states, allows the management on their energy consumption and can be adapted to provide various forms of flexibility including energy arbitrage and frequency response. Paper [88] demonstrates that the TCLs, due to their vast population and capability of being controlled simultaneously, hold great potential for providing demand response services such as fast regulation services. It further indicates that TCLs potentially offer a more cost-effective solution compared to other energy storage technologies. Therefore, this work selects the TCLs as participants in the DSR and provide short-term frequency response. Yet, the individual device capacity is not significant enough to pose influence on the power system performance. To realize the benefits from the flexible TCLs participation, the proper aggregation model is widely discussed

to evaluate effectiveness of the DSR.

The paper [89] aggregates the collection of TCLs as the stochastic battery model. The work in [90] develops the leaky storage model, exploring the potential of TCLs for short-term demand response. The optimal service portfolio for TCLs are solved by incorporating TCL dynamics into the optimization framework. The leaky storage model serves as the basic framework for the aggregated TCLs scheduling model in [91]. This work investigates the benefit of flexible TCLs by optimizing the scheduling of a diverse set of TCLs in an advanced stochastic unit commitment model, accounting the post-service energy recovery process. The TCLs in [92] are aggregated through a neural network approach considering parameters of ambient temperature, voltage and frequency, and the paper proposes a hierarchical management framework for the micro-grid operation. The paper [93] proposes using aggregated TCLs as a solution to the challenges presented by renewable energy source fluctuations in isolated microgrids, employing both a virtual battery model and frequency transient model.

The intricate control algorithms to manage the large numbers of individual demand for providing aggregated flexibility to the system is essential for realizing the DSR. The commonly adopted control strategies can be classified into centralized method and decentralized method [94]. The work [95] proposed a fuzzy-PI-based supervisory controller to centrally coordinate the demand response and secondary frequency control, mitigating the effects of communication delays in traditional centralized control approach. The aggregated control strategy is designed in [96] for the a large group of air conditioning loads, and the centralized control for the TCLs aggregators are discussed in [97]. The decentralized load control algorithm appears to be the efficient solution to release the pressure of the communication. The decentralized control methods have been derived in [98], [99]. The paper [100] introduces a novel stochastic control algorithm for accurate regulation of a large group of devices in the decentralized manner. The work in [101] discusses the potential of aggregated TCLs to arbitrage wholesale electricity market prices under the time-dependent tariff using non-disruptive load control. The less infrastructure-dependent alternative energy storage model is proposed and compared to the optimal benchmark model. The effective storage model in [89] characterising the flexibility of aggregated TCLs, is coupled with a priority-stack-based control strategy, indicating the vast potential of TCLs in providing

grid regulation services.

The above-mentioned works discussed the efficiency that the DSR brings to the system with proper modelling and control strategy. The study in [44] proposes security constrained unit commitment formulation to substantiates the advantages from incorporating the HVDC interconnectors and TCLs. However, the model in this study focuses solely on assessing synergistic flexibility through centralized coordination. It does not capture or discuss the market behavior of flexibility resources. To address this research gap, this chapter explores the synergy and interaction between interconnectors and TCLs across various market paradigms. The main contributions of this Chapter include:

a. Introduction of the comprehensive model of aggregate flexibility from the TCLs, conceptualized as a dissipative storage unit known as the leaky storage model. This model, which captures the high-level flexibility of the storage unit, is designed to facilitate integration into optimization formulations.

b. Proposal of the optimization model that incorporates interactions between flexibility resources across different system layers, specifically between TCLs and interconnectors. Building on the multi-service model discussed in previous chapters, all flexibility resources are designed to simultaneously provide energy services and primary frequency response.

c. Evaluation of the techno-economic benefits and competition between flexibility resources under the comprehensive market-based model. It develops detailed business models that position demand-side and transmission-side flexibility as profit-seeking entities and quantify their value across different market designs.

This chapter outlines the model and control of TCLs configured as the aggregated leaky storage model, which is integrated into the power system scheduling model with the interconnector serving as a flexibility provider. It then introduces and examines the market interactions between demand-side and transmission-side flexibility, treating them as business agents within a market-based framework. To maintain consistency and enable comparisons with discussions in previous chapters of the thesis, the model is evaluated using the same GB-France case study.

This assessment illustrates the impact of business demand-side agents on the independent interconnector.

5.2 Modelling and Control of the Aggregated Thermostatically Controlled Loads

This chapter investigates two principal DSR services within the framework of TCLs modelling: the energy arbitrage and the frequency response (FR). Energy arbitrage focuses on the strategical management of demand-side responsive appliances, shifting power consumption from periods of peak demand to off-peak demand hours, thereby facilitating a redistribution of the demand profile. On the other hand, the FR service involves a prompt reduction in the aggregated power usage in response to a sudden shift in grid frequency, thereby restoring the balance between power generation and demand, and effectively preventing the system frequency from dropping beyond tolerable boundaries. This allows responsive demand, such as TCLs, is able to dynamically respond to the real time pricing and balancing the supply and demand. Giving rise to these abilities, the responsive demand is considered as the cost-effective, and dynamic sources of flexibility than conventional static demand management methods and frequency response sources.

Based on works [90], [91], this chapter summarizes key features in the TCLs modelling and how to embed them in the optimization model.

5.2.1 Aggregated TCL Modelling

The typical TCL operates in two states, an *on* state where the appliance's motor is consuming power, and an off state where the power usage is minimal. The control of the TCLs is implemented around the set point value with deadband threshold. If the temperature exceeds the upper deadband limit, the system initiates cooling by activating the cooling mechanism.

Conversely, if the temperature drops below the lower deadband limit, the system switches to a heating mode.

The temperature evolution of the thermostatically controlled appliance x is typically described by the first-order temperature model:

$$\frac{\mathrm{d}T^x(t)}{\mathrm{d}t} = -\frac{1}{\eta^x}[T^x(t) - T^x_{off} + s^x(t) \cdot (T^x_{off} - T^x_{on})] \tag{5.1}$$

where η^x the device thermal time constant, and s^x is the binary variable showing the state of the device, with 1 for *on* and 0 for off. The term $T^x_{off} - T^x_{on}$ incorporate the physical model of heat exchange, where T^x_{on} are asymptotic cooling or heating temperature, and T^x_{off} are ambient temperature. Following the linearity of the dynamic thermal model, the aggregated model, accounting for the dynamics of the average temperature of the population under the assumption of identical characteristic of devices (including T_{on}, T_{off}, η), can be expressed as (5.2).

$$\frac{1}{N}\sum_x \frac{\mathrm{d}T^x(t)}{\mathrm{d}t} = -\frac{1}{N}\sum_x \frac{1}{\eta}[T^x(t) - T_{off} + s^x(t) \cdot (T_{off} - T_{on})] \tag{5.2}$$

$$\frac{\mathrm{d}\bar{T}(t)}{\mathrm{d}t} = -\frac{1}{\eta}[\bar{T}(t) - T_{off} + \theta(t) \cdot (T_{off} - T_{on})] \tag{5.3}$$

Considering the assumption of identical parameters among devices, the superscript x can be dropped in the aggregated model (5.3). The hypothetical aggregated model generalizes the population state as the fraction of devices in *on* state, as $\theta(t) = \frac{1}{N}\sum_x S^x(t) \in [0, 1]$. The average temperature of the aggregated devices group ($\bar{T}(t)$) can be essentially approximated as the temperature of a single, large appliance with a fluctuating cooling rate.

The work [90] shows that different capabilities of heterogeneous TCLs can be combined to form a single envelop model. To provide a more instructive understanding of the TCLs flexibility for system level applications, the aggregated thermal model is effectively expressed as an energy

storage unit in the power system context. The average temperature $\bar{T}(t)$ is reinterpreted with the aggregated energy level $S(t)$, and the energy level and the evolution of energy unit is then described as:

$$\frac{\mathrm{d}S(t)}{\mathrm{d}t} = -\frac{1}{\hat{\eta}}S(t) + P(t) \tag{5.4}$$

The selection of the effective envelop thermal time constant $\hat{\eta}$ for the aggregated model are illustrated in [90] by identifying and choosing the most restrictive effective time constant among all appliance. The unit dissipates its stored energy at an inherent rate of $\hat{\eta}$, which is then replenished by the power consumption $P(t)$. The $P(t)$ is defined by the aggregated consumed power $\sum_x P^x(t)$.

Unlike the battery unit, the TCLs model cannot physically discharge electricity. Instead, it can only increase/decrease the energy consumption compared to the steady-state value. This work follows the control strategy proposed in [100] where the action of TCLs are coordinated by the TCLs controller in a decentralized manner. To ensure the function of the TCLs units, the physical limit for the aggregated model is bounded by the individual devices [90].

$$\hat{S}_{min} = \max_x S^x_{min} \leq S(t) \leq \hat{S}_{max} = \min_x S^x_{max} \tag{5.5}$$

$$\hat{P}_{min} = \max_x P^x_{min} \leq P(t) \leq \hat{P}_{max} = \min_x P^x_{max} \tag{5.6}$$

The implementation of the demand response for either the energy arbitrage or other ancillary services should not interfere with the primary cooling or heating capabilities of appliances. Setting only temperature limits for energy and power consumption is inadequate for achieving this goal, as appliances may simply operate continuously at these temperature boundaries, thereby undermining their temperature regulation capabilities. Hence, it is essential to regulate temperature fluctuations of appliances average out to zero over a defined time window w,

aligning demand response efforts with the preservation of TCLs' operational efficiency. Given the linearly related population-average temperature and stored energy level, this can be equally expressed as (5.7). The in-depth explanation can be found in [90].

$$\frac{1}{w}\int_{w} S(t)\,dt \;= S_0 \tag{5.7}$$

5.2.2 Demand Side Response Formulation of TCLs

In line with the formulation in Chapter 2 and 3, the coordinated optimal scheduling of energy and FR from adaptive TCLs are incorporated in the system scheduling problem with the interconnector. Similar to the service provision from the interconnector, two distinct services are considered in the scheduling model, energy arbitrage during regular operation and frequency services under contingencies. This work considers TCLs enabling the allocation of the primary frequency response (for up to 30s) in support for the maximum infeed loss following the criteria discussion in Chapter 2.2.1. The real-time balancing service and other medium-term services are not included in this analysis.

The TCLs controller tracks the reference power profile that makes the devices to deliver its energy arbitrage and FR simultaneously while meet its normal cooling service constraints of appliances [90]. The energy arbitrage saves money from the actual power variation over the time window, while the FR is the reserved capacity that is not called under the contingency. The availability fees is paid to the TCLs' FR regardless of whether the service is delivered or not. Based the the fundamental characteristics of aggregated TCLs, this section includes the TCLs response model that mathematically consists of a set of linear constraints on the energy/power consumption as well as the provision of FR.

Given a generic time window w consisting of T steps within the time interval Δt, the discrete energy level $\mathcal{S} = \{S_t\}_{t=1}^{T}$ is formulated in the problem as decision variables. The S_t and S_{t+1} represent the energy level at the beginning and end of interval t, where the corresponding P_t

implies the constant power consumption in each single time interval t. The reinterpretation of the TCLs model by 5.4 as the leakage storage unit allows the straightforward integration in the optimization model. The storage unit depletes the energy in the rate of $\hat{\eta}^{-1}$, and is restored through power consumption $P(t)$. This captures the dynamic process of energy dissipation and replenishment within the storage unit. The energy evolution equation in discrete form is derived from (5.4) by assuming the constant power consumption level in each time instant:

$$S_{t+1} = S_t \cdot e^{-\frac{\Delta t}{\hat{\eta}}} + \hat{\eta} \cdot P_t \cdot (1 - e^{-\frac{\Delta t}{\hat{\eta}}}) \tag{5.8}$$

The energy arbitrage commitment leads to the actual energy profile changing over the defined time window, while the secure operation requires the device to maintain sufficient margin of energy and power at all times for the deliverability of frequency services. The power consumption over time interval t can be derived by inverting (5.8) with energy levels S_t and S_{t+1}.

The mathematical constraints (5.9) are implemented for the DSR and also ensures the primary cooling function.

$$\hat{P}_{min} \leq P_t \leq \hat{P}_{max} \tag{5.9a}$$

$$\hat{S}_{min} \leq S_t \leq \hat{S}_{max} \tag{5.9b}$$

$$0 \leq R_t \leq P_t - \hat{P}_{min} \tag{5.9c}$$

$$\frac{1}{T}[a_1 S_1 + \sum_{t=2}^{T-1} S_t + a_2 S_T] = \bar{S}_0 \tag{5.9d}$$

The optimization should meet the TCLs temperature boundary explained in the previous section. The regulation operation cannot exceed the energy and power limit (5.9a) and (5.9b). With regard to the FR service, the provision is enforced by (5.9c) to ensure adequate reserve for FR and power for operation. For the normal function of the TCLs demand, the temperature

fluctuation over the time window T can be revert from (5.7) to discrete expression (5.9d) by integrating (5.4). The value of parameters a_1, a_2 can be derived: $a_1 = (\frac{1}{\Delta t} - \frac{\gamma}{\beta})\hat{\eta}$, $a_2 = (\frac{1}{\beta} - \frac{1}{\Delta t})\hat{\eta}$ by adopting $\gamma = e^{-\frac{\Delta t}{\hat{\eta}}}$ and $\beta = \hat{\eta} \cdot (1 - e^{-\frac{\Delta t}{\hat{\eta}}})$. It worth pointing out that $a_1 + a_2 = 1$. The detailed mathematical derivation is illustrated in [91].

5.3 Optimal Scheduling of Multi-Service Interconnector and TCLs

The interconnected power system bears the same framework in Chapter 2 and Chapter 3, where the interconnector operates as both a regulated assets that aims at enhancing the total system benefit, and a merchant asset that targets profit maximisation from the congestion surplus. Beyond the interconnector and traditional generations, the two-area model framework in this Chapter is summarized in Fig. 5.1, and showcases the inclusion of TCLs. The capacity of the interconnector will be optimally allocated between the power flow and FR, while the flexible TCLs are capable of offering flexibility in peak load shaving and FR. Each power system is modelled as the single bus bar system and neglects the internal transmission networks. To analytically assess the quantitative benefits that the DSR could bring synthetically with the multi-service interconnector, this work include the flexible TCLs in the Area A. The Area B still embraces only the inflexible loads with both synchronous generators and RES.

Two scheduling approaches are discussed in the following sections. First, the Centralized Approach (CA) is derived as one Unit Commitment problem to optimize multiple aspects, including the generation commitment and dispatch, TCLs operation and the interconnector capacity allocation. This conventional CA provides the lower bound on the total system operational cost. Alternative Market Approach (MA) is also adopted by viewing the aggregated TCLs as profit-seeking business assets and coordinates the DSR from the payment-maximization/cost-minimization business perspective.

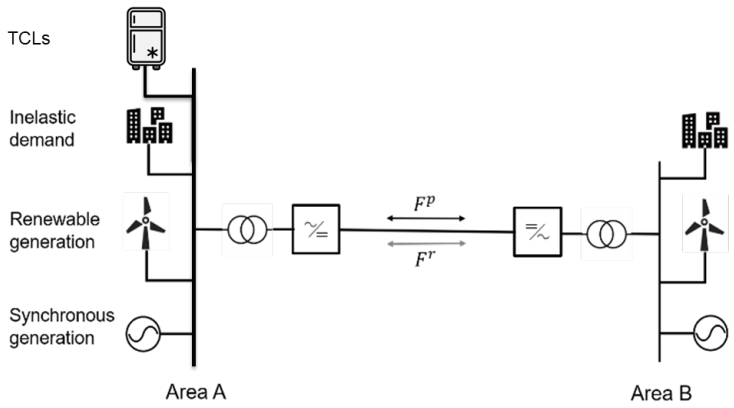


Figure 5.1: Schematics of the two-area interconnected power system with DSR.

5.3.1 Centralized Approach (CA) Formulation

Following Chapter 2.3, the UC problem is formulated as a deterministic, linear programming (LP) model by including the continuous variable $H_\tau \in [0, 1]$ to represent the percentage commitment level of the generation fleet. The LP model enables the efficient calculation of the corresponding power and FR prices by adopting the Lagrange multiplier of the associated constraints.

The CA formulation is adapted from Chapter 2.3.5 and are listed in equations (5.10) to (5.14) by introducing new decision variables S_A^{TCL}, R_A^{TCL} for the TCLs energy level and reserved FR headroom by the TCL unit. The set for decision variables in the UC problem ξ_t now is redefined as: $\xi_t = \{H_{k,\tau}, P_{k,\tau}, R_{k,\tau}, F^p, F^r, S_A^{TCL}, R_A^{TCL}\}$. The demand side aggregated TCLs are modelled as the price-taking battery like storage unit, which makes the payment for the electricity consumption. The flexibility provision from TCLs are mapped as constraints in the UC model, based on the essential features in Chapter 5.2.

The optimization problem is considered on a generic day, with time interval of Δt=30 mins with $T = 48$ time steps, covering 24-h horizon. The objective function of the UC is to minimize the total system generation cost:

$$\min_{\xi_t} \sum_{t=1}^{T} \{ \sum_{k\in\{A,B\}} \sum_{\tau=1}^{\theta} \Delta t(\alpha_{k,\tau} H_{k,\tau} G_{k,\tau}^{max} + \beta_{k,\tau} P_{k,\tau} + \gamma_{k,\tau} P_{k,\tau}^2 \Delta t) \}_t \tag{5.10}$$

subject to the power system operation and security limits(5.11), (5.12), TCLs operation boundaries (5.13), and interconnector constraint (5.14). It is worth noting that, the original UC formulation proposed in Chapter 2 does not include the inter-temporal constraints, which allows the drop of the time dependence notations (subscript t) from the decision variables. While, in the battery-like storage model, the constant power consumption $P_{A,t}^{TCL}$ for a given time interval t is computed by (5.8). This equation introduces the inter-temporal relationships between the energy level S at the beginning and end of time interval (S_t, S_{t+1}). In the following equation set (5.13), the decision variables is denoted with the time-dependent subscript t, where $t \in T$. However, the time-dependent variables $S_{A,t}^{TCL}, R_{A,t}^{TCL}$ do not introduce impacts on the remaining of the formulation. To enhance the clarity, other constraints including equations (5.11), (5.12) and (5.14), for the specific time step t, still omit the notation t.

With the inclusion of new flexible demand TCLs in area A, the optimization not only needs to meet the TCLs operation limits, but requires consider the impact on the system scheduling. Considering the two functions that the TCLs perform, energy arbitrage and FR services, the modifications on the formulation are embodied on the demand balance constraint (5.11a) by including the flexible demand P_A^{TCL}, and the frequency service constraints (5.15). The aggregated system frequency response $\hat{R}_A$ has three separate sources, from traditional generators $\sum_{\tau=1}^{\theta} R_{A,\tau}$, from the interconnector exchange F^r and from aggregated TCLs R_A^{TCL}.

$$\sum_{\tau=1}^{\theta} P_{A,\tau} + F^p - L_A - P_A^{TCL} = 0 \tag{5.11a}$$

$$\sum_{\tau=1}^{\theta} P_{B,\tau} - F^p - L_B = 0 \tag{5.11b}$$

$$0 \leq H_{k,\tau} \leq 1 \tag{5.11c}$$

$$P_{k,\tau} + R_{k,\tau} \leq H_{k,\tau} G_{k,\tau}^{max} \tag{5.11d}$$

$$R_{k,\tau} \leq r_{k,\tau} H_{k,\tau} G_{k,\tau}^{max} \tag{5.11e}$$

$$R_{k,\tau} \leq s_{k,\tau} (H_{k,\tau} G_{k,\tau}^{max} - P_{k,\tau}) \tag{5.11f}$$

$$\mu_k r_{k,\tau} H_{k\tau} G_{k,\tau}^{max} \leq P_{k,\tau} \tag{5.11g}$$

$$\hat{R}_A \geq \Delta G_A - D_A[L_A + P_A^{TCL} - R_A^{TCL}]\Delta f_A^{qss} \tag{5.12a}$$

$$\hat{R}_B \geq \Delta G_B - D_B L_B \Delta f_B^{qss} \tag{5.12b}$$

$$2\Delta G_k \nu_k \sigma_k - {\nu_k}^2 \hat{R}_k - 4\Delta f_k^{roc} \sigma_k \hat{H}_k \leq 0 \tag{5.12c}$$

$$q_k - \hat{H}_k \hat{R}_k \leq 0 \tag{5.12d}$$

$$\hat{P}_{A,min}^{TCL} \leq P_{A,t}^{TCL} \leq \hat{P}_{A,max}^{TCL} \tag{5.13a}$$

$$\hat{S}_{A,min}^{TCL} \leq S_{A,t}^{TCL} \leq \hat{S}_{A,max}^{TCL} \tag{5.13b}$$

$$0 \leq R_{A,t}^{TCL} \leq P_{A,t}^{TCL} - \hat{P}_{A,min}^{TCL} \tag{5.13c}$$

$$\frac{1}{T}[a_1 S_{A,1}^{TCL} + \sum_{t=2}^{T-1} S_{A,t}^{TCL} + a_2 S_{A,T}^{TCL}] = S_{A,0}^{TCL} \tag{5.13d}$$

$$P_{A,t}^{TCL} = \frac{1}{\hat{\eta}(1 - e^{-\frac{\Delta t}{\hat{\eta}}})} \cdot S_{A,t+1} - \frac{e^{-\frac{\Delta t}{\hat{\eta}}}}{\hat{\eta}(1 - e^{-\frac{\Delta t}{\hat{\eta}}})} \cdot S_{A,t} \tag{5.13e}$$

$$-F^{max} \leq F^p + F^r \leq F^{max} \tag{5.14}$$

$$\hat{R}_A = \sum_{\tau=1}^{\theta} R_{A,\tau} + F^r + R_A^{TCL} \tag{5.15a}$$

$$\hat{R}_B = \sum_{\tau=1}^{\theta} R_{B,\tau} - F^r \tag{5.15b}$$

$$\hat{H}_k = \frac{1}{f_0}(\sum_{\tau=1}^{\theta} h_{k,\tau} H_{k,\tau} G_{k,\tau}^{max} - h_k \Delta G_k) \tag{5.15c}$$

The constraint set (5.11) bounds the power system dispatch from the power system level.

(5.11a) and (5.11b) defined the local power system supply/balance constraints. Equations (5.11c) to (5.11g) constrain the upper and lower bound of dispatch level of each technologies and limit the combined power and FR provision within the generators' technical limits, including the generator maximum capacity (5.11d), FR provision headroom (5.11e) and slope (5.11f). (5.11g) is to constrain the power dispatch level μ times higher than the generator headroom, in order to avoid invalid dispatch results .

The power system post-fault frequency security should be guaranteed by constraints (5.12) which are set based on SQSS standards for quasi-steady-state frequency deviation, RoCoF, and frequency deviation at nadir. The allocation of the frequency services from synchronous generators, interconnector, and TCLs are defined in (5.15) which should be optimized under the sudden maximum loss of generation.

The service allocation limits referring to the aggregated TCLs and the interconnector, are listed in the constraint set (5.13) and (5.14). The implementation of energy arbitrage and FR under generation loss should not exceed the operation limits (5.13a)-(5.13c), and also ensure the normal cooling function without affecting the customers' comfort level (5.13d). The rated interconnector capacity limit is reflected in (5.14).

5.3.2 Market Approach (MA) Formulation

Considering the independent business characteristics of the interconnector and TCLs, the proposed MA in Chapter 3 is extended to taking the aggregated flexible demand TCLs as another market player instead of just the price-taking inelastic loads. In this configuration, the model treats independent power systems (designated as area A and B), the interconnector, and the flexible demand of TCLs in area A, as depicted in Figure 5.1, as separate profit-seeking agents.

To emphasize the value of the business flexible demand in providing DSR, the market framework includes the aggregated, price-responsive TCLs model that optimizes the power consumption profile and reserve FR capacities according to the timely prices. The TCLs aggregator exchanges the information of S_A^{TCL}, R_A^{TCL} with the interconnected market-based power system model in

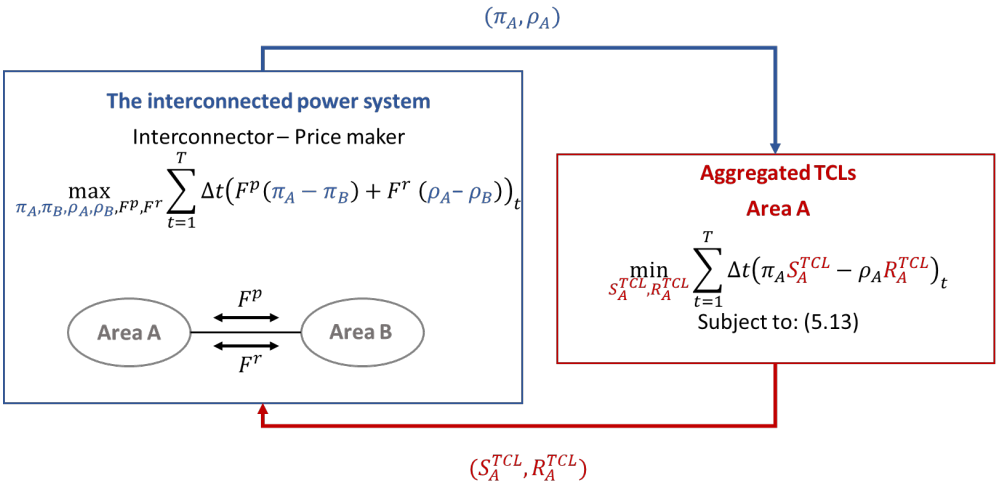


Figure 5.2: Interactions among market participants in MA

Chapter 3, in which the interconnector and the linked power systems determine the optimal solutions for their own benefits and the outcome is characterized as the market equilibrium. The interactions among the self-interested demand side TCLs, the interconnetor and the involved power systems are summarized in Fig. 5.2. For the clarity in discussion, the MA model developed in Chapter 3 will be referred as the interconnected market model in the following paragraphs.

In the whole model, the aggregated TCLs operate as the independent business asset that optimize the energy consumption (S_A^{TCL}) and FR service (R_A^{TCL}) over the time window depending on the relevant market electricity and FR availability prices (π_A, ρ_A) from the interconnected market model. On the basis of the (S_A^{TCL}, R_A^{TCL}), the interconnected market model proceeds the market clearing to find the optimal solution following the implementation procedure described in Fig. 3.1.

In the interconnected market model, the quantities of energy level S_A^{TCL} and FR R_A^{TCL} are the fixed quantities for the power system A. The independent power system A and B optimize the dispatch decisions based on the fixed profile of S_A^{TCL} and R_A^{TCL}, and and offer the local electricity and FR prices considering the link capacity allocation results (F^p, F^r) which are in turn affected by the price signals from power systems.

The final market equilibrium can be found by the iterative interactions between the independent TCLs and the interconnected market model.

A. Analytical formulation for aggregated TCLs

The cost function of the flexible TCLs at time interval t is defined by the sum of two terms, 1) the electricity cost, which is calculated by the product of amount of consumed power and the electricity prices, and 2) the availability fee from offering FR, which is calculated by the product of the amount of reserved capacity for FR and the associated FR prices. The objective function of the self-interested TCLs is to minimize the cost function φ_{TCL} across the time window T, and can be formulated as:

$$\varphi_{TCL}(\pi_A, \rho_A) = \min_{S_A^{TCL}, R_A^{TCL}} \sum_{t=1}^{T} \Delta t \{\pi_A P_A^{TCL} - \rho_A R_A^{TCL}\}_t \tag{5.16}$$

The local TCLs optimization should be subjected to the the operation feasibility constraints (5.13).

B. Analytical formulation for the interconnected market model

1) Interconnector

As the independent merchant asset, the formulation of interconnector in Chapter 3.2.2 is recalled as following. The interconnector optimizes its capacity repartition between F^p, F^r to maximize the congestion surplus:

$$\varphi_{INT} = \arg\max_{\pi_A, \pi_B, \rho_A, \rho_B, F^p, F^r} \sum_{t=1}^{T} \Delta t \{(\pi_A - \pi_B)F^p + (\rho_A - \rho_B)F^r\}_t \tag{5.17}$$

The congestion surplus is summed by the 1) the revenue from the energy exchange; 2) the revenue related to providing FR service availability. The optimization problem (5.17) is defined as the price-making process, where the interconnector formulation optimizes the decision variable set $(\pi_A, \pi_A, \rho_B, \rho_B, F^p, F^r)$, subject to the link capacity limit (5.14), and the power system marginal prices π_k, ρ_k.

2) Area A

Differently from the CA where the interconnector and TCLs operation are optimized

centrally, the independent power system A carries out the self-scheduling based on the fixed quantities of interconnector strategy F^p, F^r, and fixed power consumption and FR profiles P_A^{TCL}, R_A^{TCL} from the independent TCLs aggregators. The UC optimizes the generation dispatch (H_A, P_A, R_A) through the optimization problem φ_A which is parameterized by the independent decisions $(F^p, F^r, S_A^{TCL}, R_A^{TCL})$.

$$\varphi_A(F^p, F^r, S_A^{TCL}, R_A^{TCL}) = \min_{H_A, P_A, R_A} \sum_{t=1}^{T} \sum_{\tau=1}^{\theta} \Delta t \{\alpha_{A,\tau} H_{A,\tau} G_{A,\tau}^{max} + \beta_{A,\tau} P_{A,\tau} + \gamma_{A,\tau} P_{A,\tau}^2 \Delta t\}_t \quad (5.18)$$

The operation is subject to local generator and FR constraints (5.11) to (5.12), evaluated at $k = A$.

3) Area B

The same derivation of UC formulation in power system B, keeps consistent with the model for area A, but only takes the interconnector strategy F^p, F^r as fixed quantities. The constraints are evaluated at $k = B$ in (5.11) to (5.12).

$$\varphi_B(F^p, F^r) = \min_{H_B, P_B, R_B} \sum_{\tau=1}^{\theta} \Delta t \{\alpha_{B,\tau} H_{B,\tau} G_{B,\tau}^{max} + \beta_{B,\tau} P_{B,\tau} + \gamma_{B,\tau} P_{B,\tau}^2 \Delta t\}_t \quad (5.19)$$

5.4 The Implementation of the MA

To find the equilibrium in the competitive market, the numerical resolution of the coordination between the price-responsive TCLs and the interconnected power system, is performed with the iterative approach. The direct implementation of the iterative interactions in Fig. 5.1 introduces the computational difficulties and convergence issues. This section presents details

in the iterative process to find the market equilibrium .

The iterative procedures for the MA implementation is illustrated in Algorithm 5.1. To avoid the lumpy updates on the variables over the iteration process, which brings the high possibility in the convergence failure, two methods to solve the challenges are adopted in the numerical implementations. First, the updated variables over the iteration are reprocessed by the conservative convex combination between the new computed solutions $(\pi_k, \rho_k, S_A^{TCL}, R_A^{TCL})$ and the input values $\tilde{\pi}_k, \tilde{\rho}_k, \tilde{S}_A^{TCL}, \tilde{R}_A^{TCL}$. This step efficiently constrains the update step in each iteration round not varying significantly and moving in the optimized direction, in order to reach the final convergence. The combination are formulated as, $\forall y \in [0, 1]$:

$$\tilde{\pi}_A = y \cdot \pi_A + (1 - y) \cdot \tilde{\pi}_A, \tag{5.20}$$

$$\tilde{\rho}_A = y \cdot \rho_A + (1 - y) \cdot \tilde{\rho}_A, \tag{5.21}$$

$$\tilde{S}_A^{TCL} = y \cdot S_A^{TCL} + (1 - y) \cdot \tilde{S}_A^{TCL}, \tag{5.22}$$

$$\tilde{R}_A^{TCL} = y \cdot R_A^{TCL} + (1 - y) \cdot \tilde{R}_A^{TCL}, \tag{5.23}$$

To ensure a stable iterative update of the TCLs profile and avoid unrealistic power profile, the quadratic term $\lambda(P_A^{TCL} - P_0^{TCL})^2$ that penalizing the power deviation from the steady-state value is introduced in the objective function (5.16). This term penalizes the power derivation and prevents power consumption profile from excessive fluctuation. The objective function can be formulated as (5.24). To facilitate a quantitative comparison of the two approaches, the same penalty term has been integrated into the objective function for the CA approach (5.10) within the case study. This integration allows for a detailed quantitative analysis in subsequent case studies. It is important to note that the penalty term does not exist in the scheduling process, particularly under the CA. Instead, this term is included solely to facilitate numerical convergence and to provide a basis for quantitative comparison in the case study.

$$\varphi_{TCL}(\pi_A, \rho_A) = \min_{S_A^{TCL}, R_A^{TCL}} \sum_{t=1}^{T} \Delta t \{\pi_A P_A^{TCL} - \rho_A R_A^{TCL} + \lambda (P_A^{TCL} - P_0^{TCl})^2\}_t \tag{5.24}$$

Algorithm 5.1 – Iteration steps in Market approach

1) Initialization

- Define the input quantities for independent agents with the tilde sign as $\tilde{\pi}_k, \tilde{\rho}_k, \tilde{S}_A^{TCL}, \tilde{R}_A^{TCL}, \forall t \in T$
- Assign initial state value of the profit-seeking TCLs: $\tilde{S}_{A,0}^{TCL} = 0, \tilde{R}_{A,0}^{TCL} = 0, \forall t \in T$

2) Iteration procedures

- Calculate the prices π_A, ρ_A by solving the optimization problem (5.17), (based on the implementation scheme explained in Fig. 3.2), with the defined initial input quantities $S_A^{TCL} = \tilde{S}_A^{TCL}, R_A^{TCL} = \tilde{R}_A^{TCL}$.
- Calculate the convex combination of the price signal $(\tilde{\pi}_A, \tilde{\rho}_A)$ by (5.20) and (5.21).
- Compute the resulting TCLs profile S_A^{TCL}, R_A^{TCL} from (5.24) based on $\tilde{\pi}_A$ and $\tilde{\rho}_A$.

3) Check the convergence

IF
$e_s = \left| S_A^{TCL} - \tilde{S}_A^{TCL} \right| < \epsilon$ and $e_r = \left| R_A^{TCL} - \tilde{S}_A^{TCL} \right| < \epsilon$, for $\forall t \in T$,
Return the equilibrium solutions:
$S_A^{TCL*} = \tilde{S}_A^{TCL}, \quad R_A^{TCL*} = \tilde{R}_A^{TCL}$

ELSE
Repeat the Step 2) with the updated $\tilde{S}_A^{TCL}, \tilde{R}_A^{TCL}$ values according to (5.22) and (5.23).

5.5 Case Studies

The GB-France HVDC-connected power system model is adopted as case study in this Chapter. The area A and area B, represent GB and France aggregated system respectively with the deterministic demand profiles selected from a typical weekday. Relevant technology parameters considering the typical 2030 low carbon scenarios are kept consistent with previous chapters and summarised in Table 2.1, and the system parameters are D_k=1/50s, ν_k=0.5s, f_k^{roc}=0.5Hz (for both areas) σ_A=10s, σ_B=15s, Δf_A^{qss}=0.5Hz, Δf_B^{qss}=0.2Hz and ΔG_A=1.8GW and ΔG_B=1.5GW [44], [52]. The capacity of the cross-border interconnector is assumed consis-

tently in this work with 5GW. The parameters related to the price-responsive flexible demand TCLs are summarized in Table 5.1 from the data in [90]. Through a trial-and-error process, the parameters for implementing the iteration are chosen to be ϵ =0.5, λ=0.05.

The generic 24 hours optimization horizon with time step Δt=30mins is chosen for the simulation. Both CA and MA are running and compared according to the simulation setup in the following section 5.5.1. Another case study that discussed the value of introducing DSR from TCLs are presented in Chapter 5.5.2.

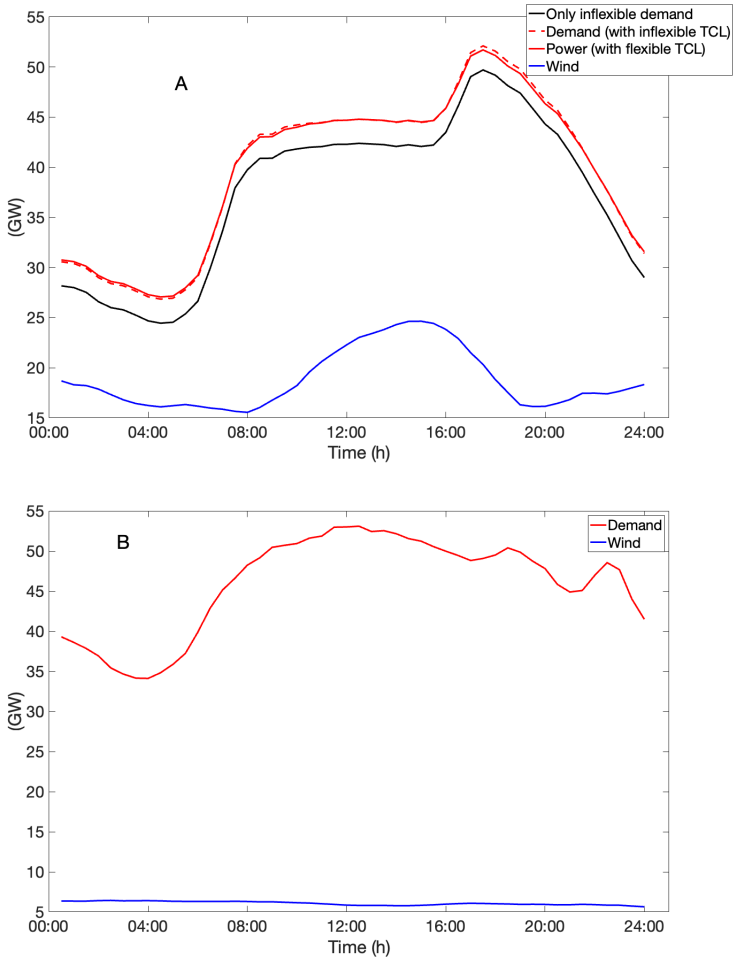


Figure 5.3: Wind and Demand Profiles in GB (A) and France (B).

Table 5.1: TCL parameters

$\hat{S}^{TCL}_{A,max}$ (GWh)	$\hat{S}^{TCL}_{A,min}$ (GWh)	$S^{TCL}_{A,0}$ (GWh)	$\hat{P}^{TCL}_{A,max}$ (GW)	$\hat{P}^{TCL}_{A,min}$ (GW)	$P^{TCL}_{A,0}$ (GW)	$\hat{\eta}$ (h)	a_1	a_2
12.9	10.7	11.8	6.4	1.3	2.4	5	0.4917	0.5083

5.5.1 Base Case

The case study starts from comparing the base case results from the CA and MA. To analyse the time-variant performance, the GB and France demand and wind profile are provided in Fig.5.3. The traditional CA solves the system scheduling to minimize the total short-term operational cost, while the MA finds the market equilibrium through the market interaction among independent players. The interconnector behaviour is firstly compared in Fig. 5.4. During the low net demand hours according to Fig.5.3(22:00-07:00, and 12:00-16:00), the merchant interconnector allocates more capacity to the FR by withdrawing the capacity for power exchange in order to maximize the congestion surplus. The conclusion for the market-operation of independent interconnectors in Chapter 3 still hold after introducing the flexible demand TCLs in area A.

The following part focuses on the TCLs operation features and the differences between the CA and MA. Fig. 5.5 gives the power profile and FR services allocation of aggregated TCLs, in which the blue line is the power level, and the red line refers the reserved capacity for FR. It is worth noting that the power consumption of TCLs generally responds to the local price signals in area A, which is given by Fig. 5.6. During the hours 8:00-12:00, and 16:00-22:00, the aggregated TCLs decrease its electricity consumption due to the increasing electricity prices during the peak demand hours (Fig.5.3). The allowed capacity for FR is allocated accordingly without violating the TCLs P_{min}^{TCL} limit, and is driven by the less demanding FR requirements. Concordantly, the interconnector allocates full capacity to the power import from the France to GB over these time slots. Accordingly, in the low inertia hours (22:00-08:00, 12:00-16:00), which is characterized by the lower net demands, the relative lower electricity prices presented in Fig.5.6 drive the TCLs to consume power for recovering temperature in order to maintain the average energy level and satisfy the demand side comfort requirement. In these hours, the relative higher FR prices in area A, along with more power capacity margin remained for TCLs to adjust their consumption, motivate both the interconnector and the TCLs to increase the capacity allocation for FR.

It worth noting that, the resulting market operation of the TCLs and interconnector, leads to

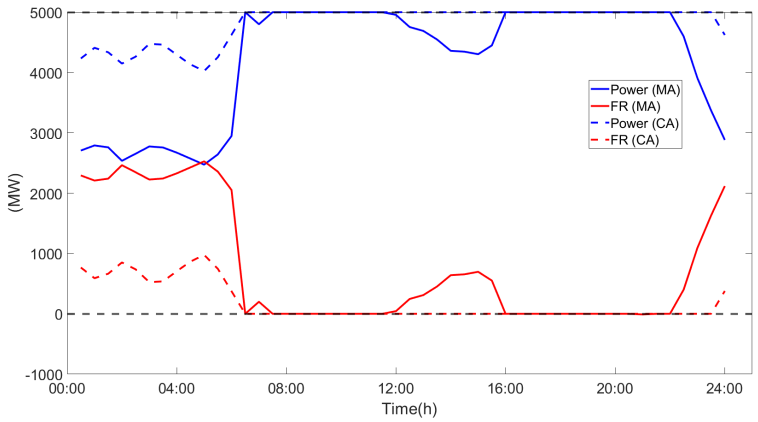


Figure 5.4: The capacity repartition of the interconnector in the CA and MA.

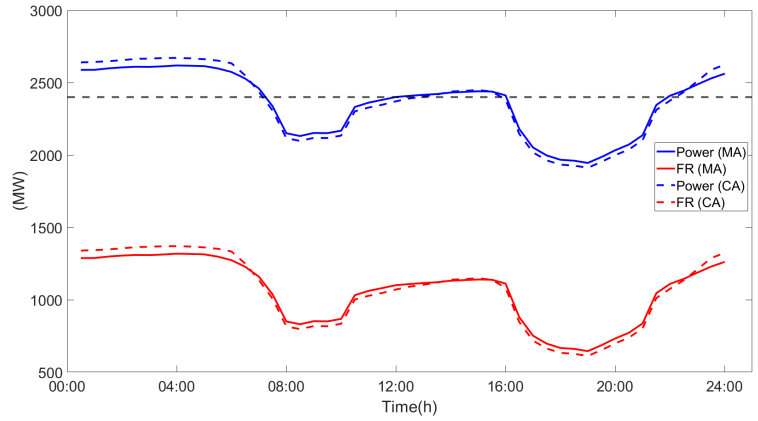


Figure 5.5: Power and FR services allocation profile of TCLs.

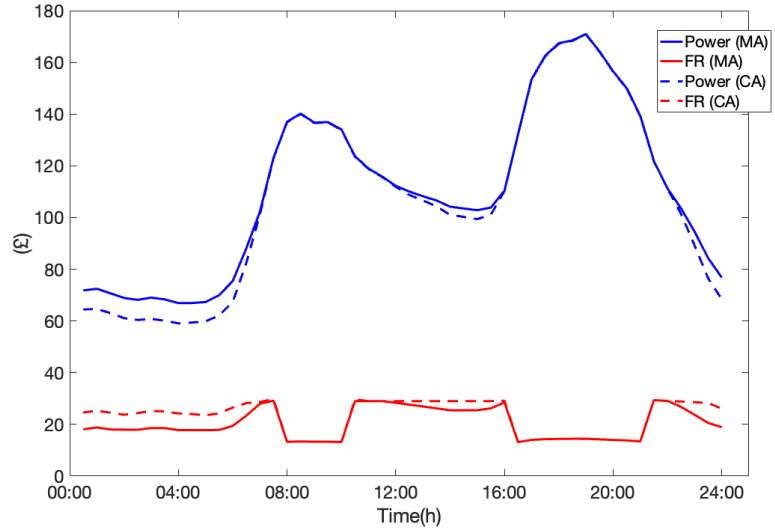


Figure 5.6: The power and FR prices in GB under CA and MA.

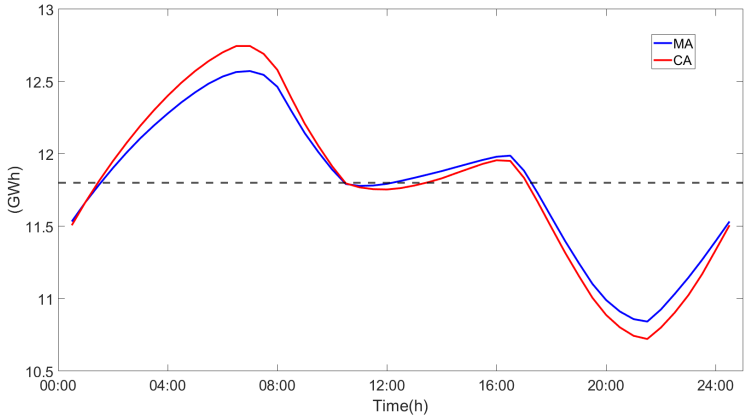


Figure 5.7: The energy profile of TCLs

a higher electricity prices, and lower FR prices during the low net demand hours (22:00-07:00, and 12:00-16:00) in Fig. 5.6. The resulting power, FR and energy profiles in Fig. 5.5 and Fig. 5.7 show that, under the MA, independent self-interested TCLs reduce the variation of power profile. The self-adaption behaviour of TCLs minimizes its payment to the power system. In the final results, the daily operational cost of the independent aggregated TCLs is $11.46M£$ over 24h, saving $1.26M£$ in total than that in the CA.

5.5.2 Comparison Between Models with/without Flexible TCLs

The following results described the impact of employing the flexible TCLs on the interconnected power system, by comparing the results between models shown in Fig. 2.2 and Fig. 5.1.

The numerical daily results from the system level are given in Table 5.2. From the power system operation perspective, with participation of the flexible demand TCLs, the total operational cost can be further reduced in both CA and MA by around 0.5%. However, the self-interested behaviour of the interconnector and DSR from TCLs make the total interconnected system sustain losses in social welfare (higher operational cost than CA). Regarding the interconnector operation, the congestion surplus of the link from the electricity and FR trading is reduced due to the TCLs' flexibility in FR provision and the energy arbitrage. In Table 5.2, the interconnector's revenue is shrunk by 2.3% and 1.3% under CA and MA. Compared the inefficiency of line utilization rate in the energy-only model, the line utilization rate in the multi-service

framework all reach 100% with/without including the flexible operation of the TCLs. In addition, the capacity of the link used for reserving headroom for FR is reduced significantly after introducing flexible TCLs, which means that the FR support from the adjacent area less demanding because of the efficient and cheap option of local sources.

Table 5.2: Model with/without TCLs

		TCL+Interconnector	Interconnector only	
		Energy+FR	Energy+FR	Energy-only
System operational cost ($M£$)	CA	150.84	151.80	151.98
	MA	151.51	152.17	152.26
Line revenue ($M£$)	CA	11.74	12.02	11.18
	MA	12.09	12.25	11.91
Average line utilization for energy (%)	CA	96.8	92.88	98.38
	MA	84.2	78.98	90.76
Average line utilization for FR (%)	CA	3.2	7.12	0
	MA	15.8	21.02	0
Average line utilization (%)	CA	100	100	98.38
	MA	100	100	90.76

To better understand how the inclusion of profit-seeking TCLs in a multi-service market impacts the interconnector, the capacity repartition results under MA are compared between the model with/without TCLs, as shown in Fig. 5.8. It can be noticed that during the low demand periods (from 22:00 to 7:00 and also between 12:00 to 16:00), the merchant interconnector augments its energy import from France to GB while simultaneously reducing the capacity allocated for FR. This is due to the presence of TCLs in the MA, which drives up the GB local electricity price and depresses the FR price. This motivates the independent interconnector prioritize the

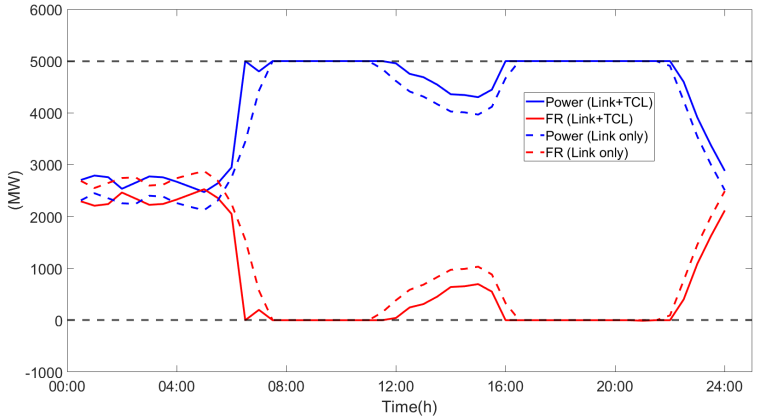


Figure 5.8: The capacity repartition of the interconnector in the model with/without TCLs.

services for F^p to maximize the congestion surplus.

5.6 Conclusions

This chapter is built upon the multi-service model discussed in Chapter 2 and Chapter 3 that treated the interconnector as the solution for the flexibility provision. In this chapter, the work extends the model by integrating a new dimension of flexibility - demand side resources. The aggregated TCLs are picked as the representative example that is able to participate in the energy arbitrage activities under the regular operation and also FR under the case of the infeed loss. The comprehensive conceptualized leaky storage unit model is discussed as the high-level presentation of the large group TCLs, facilitating the integration into the proposed optimization model for both CA and MA. Comparative case studies are presented against the works in Chapter 2 and 3, offering a deeper understanding of the of the flexibility provision from different dimensions and the their mutual interactions.

In the CA, instead of treating all loads as inflexible demand, the TCLs in area A are allowed to provide flexibilities. Results substantiate the contribution of the coordination of the interconnector and flexible demand to enhance overall social welfare. This chapter also investigates the value of flexible TCL from the market perspective, thereby complementing the analysis provided in Chapter 3 by introducing another market player from the demand side. Enabled to participate in the market clearing process, the TCLs model is motivated to accrue the total benefit from gaining availability fee from providing FR, and reducing electricity costs from energy arbitrage over the defined time window. With the ability of leveraging the demand profile and supporting frequency service, the TCLs positively affect the local electricity and FR prices. Meanwhile, the price differentials between regions are the driving force for the merchant interconnector, reaping benefit from the congestion surplus. The additional local business flexibility provider TCLs exerts downward pressure on the revenue margin remained for the interconnector. The link therefore adapts the strategy accordingly to maximize its profit, effectively responds to the dynamics from the generation side and demand side.

Taking a comprehensive view of the interplay between transmission side and the demand-side, this study highlights the future pathways for the interconnector development, especially for the merchant interconnector. The planning and operation decisions of the link cannot only follow the conventional market indicators, but should require a broader understanding of the interactions among different stakeholders.

5.7 Future Works

In the next step, the work could broaden the scope of frequency services from primary frequency response to encompass a wider range, including secondary responses facilitating the frequency recovery to quasi-steady-state, and high frequency responses to positive frequency deviations from both the interconnector and demand side responsive loads.

Additionally, the new ancillary services - enhance frequency response, already implemented in Great Britain, are expected to be included in the research. Demand side response, interconnectors, and battery storage systems are all capable of providing these services. The provision of multi-speed frequency response services among various resource stakeholders and their interactions will be evaluated across different market frameworks.

Chapter 6

Market-Based Operation of Interconnectors in a Multi-Area Power Network with Meshed Topology

The chapter assesses the techno-economic benefits of interconnectors that operate in a multi-area power network and whose capacity can be utilized for simultaneous exchange of power and fast-frequency services. The optimal repartition of the interconnection capacity is initially computed with a traditional centralized approach proposed in Chapter 2, where the interconnectors are modelled as network assets contributing to the minimization of aggregate system operational costs. The centralized approach is then used as benchmark against an alternative market-based paradigm in Chapter 3 where interconnectors can act as profit-seeking agents that maximize their collected congestion surplus. This novel methodology is applied to a model of an interconnected Great Britain-France-Ireland multi-area system, quantifying the potential benefits on system efficiency of multi-service interconnectors and assessing the impact of their self-interested scheduling on the system operational costs.

6.1 Introduction

This chapter extended the works in Chapter 2 and Chapter 3, considers a modelling setup of multi-area systems with a meshed topology connected through interconnectors. The study is inspired by the ongoing research trend of applying the multi-service operation model to increasingly intricate network structures. This would open up to the modelling of multi-service interconnectors operating in a multi-area network characterized by a meshed topology. The development of a modelling framework to test the operation of multi-service interconnectors within meshed networks represents the basis to explore the effectiveness of future network development plans. In fact, the revised Regulation on Trans-European Energy Networks of the European Union (EU) [102], which entered into force in June 2022, operationalizes the ambitions set in the EU offshore strategy [103]. It includes new infrastructure categories for hybrid offshore grids and radial lines, as well as permitting provisions to accelerate the scale-up of meshed offshore grids. Another fundamental motivation for the proposed work involves the assessment of the potential benefits for interconnectors that operate under a market-driven, profit-seeking framework rather than following the traditional top-down paradigm which envisages a centralized coordination of the network asset.

The research gaps in the flexible operation of the interconnector and also their market paradigms are summarized and discussed in the Chapter 2 and 3. Such as the authors in [39] investigate a flexible operation of the interconnector between GB and France in order to integrate RES whilst reducing system operational costs and carbon emissions. The methodology developed in [33] characterizes the techno-economic operation of interconnected transmission systems and coordinates power transfers through HVDC links. The work in [45] presents a framework for including both Alternating Current (AC) and HVDC losses in a zonal or nodal market pricing mechanism. The study [104] investigated the influence of electricity prices in one country on those in neighboring countries, selecting Switzerland as the case study because of its considerable capacity for cross-border trading. However, the references above neglect the possibility of allocating interconnector capacity to ancillary services. Another research stream investigates the simultaneous scheduling of power and reserves via interconnectors under a centralized, cost-

based approach. The authors in [43] introduce a methodology for evaluating potential economic benefits of utilizing the emergency power control functionality of HVDC links for the provision of fast frequency containment reserves. However, the assessment of inertial and frequency response requirements is not directly incorporated in a power system scheduling model. A cost-based and centralized scheduling model to compute the value of multi-service operation of interconnectors in multi-area power systems is investigated in [44]. Under the same centralized approach, the methodology in [105] assesses the optimal value for the allocation of inter-area power flows and frequency response of HVDC and AC interconnectors in a two-area system.

The economic value stemming from the decentralized operation of a multi-area system is analyzed in [106] and [83]. These works adopt a Lagrangian relaxation approach to solve the multi-area economic dispatch problem in a decentralized manner. The simultaneous power-reserve trading considering wind uncertainty in an interconnected multi-area system is presented in [107]. Although implementing a market-based decentralized scheduling formulation, the interconnectors in the above-mentioned papers are still treated as network assets. In practice, they do not explicitly determine the inter-area power flow exchanges. This represents a clear limitation affecting business opportunities and relevant industry actors. In fact, system operators are actually requested to put in place solutions which acknowledge the flexibility of interconnectors in competitive markets [25]. This would not be limited to inter-area power exchanges but it would also include balancing services. An initial attempt to model and quantify the market value for interconnectors is presented by the authors in [82]. Their proposed methodology is applied to a two-area system, analyzing the self-interested operation of the tie-line. This simultaneously allocates its capacity for power exchanges and frequency response (FR) provision in order to maximize its collected congestion revenues. The nonlinear interplays between the decision variables, which represent an intrinsic feature of market-based clearing formulations, can be handled in [82] thanks to the simple topology of the network under exam. The extension of this formulation to more complex and realistic [103] meshed topologies is not straightforward. Particularly, the existence of a unique market equilibrium, which holds in the two-area model presented in Chapter 3, is not guaranteed in a more complex meshed multi-area model where the operational decisions of one interconnector affect indirectly the power

flow and therefore the congestion surplus on other lines. Moreover, the numerical calculation methodology adopted in Chapter 3 for the two-area case is in general unable to deal with this increased complexity and alternative resolution approaches need to be implemented.

In summary, the literature review highlights an important research gap. In fact, none of the references above addresses the three following modeling features, simultaneously: i) a multi-service (power and FR) operational paradigm to allocate the interconnector capacity, ii) a market-based formulation that allows the interconnectors to operate independently to maximize their revenues and iii) the methodology to account for complex inter-area synergies, typical of power systems with a meshed network topology. This work is focused on developing a comprehensive model framework that considers both operational and market advancements within a multi-area system. Such setup can accommodate several realistic cases such as the Great Britain (GB) - France -Ireland system or the potential development of a large multi-area HVDC network in the North Sea and the Baltic Sea [108].

The main contribution of this Chapter are summarized as follows:

a. Extension of the novel modelling framework capable of accommodating the multi-service (power and FR) operational paradigm for profit-seeking interconnectors in multi-area power systems with a meshed network topology. The proposed Market Approach (MA) methodology, which characterizes interconnectors as revenue-maximizing independent agents, is compared with a traditional Centralized Approach (CA) where the interconnectors are network regulated assets.

b. An effective enumeration method to numerically solve the Market Approach (MA) problem and determine the market equilibrium solution. This methodology allows to account for all the nonlinear interplays between the relevant decision variables (in particular between prices and capacity allocation decisions) in a meshed network topology. The upper bound on the approximation error of the proposed approach is expressed as a function of the selected discretization step, allowing to achieve the desired trade-off between solution accuracy and computational complexity.

c. Simulative implementation of the proposed methodology on a representative model of the multi-area GB-France-Ireland system. A comprehensive set of case studies is developed to compare the Market Approach (MA) solution with the Centralized Approach (CA) in terms of social welfare and of the potential system inefficiencies introduced by the self-interested operation of the interconnector in the MA. The benefits of a multi-service framework with respect to a power-trading-only approach are also estimated. Results concerning the operation of the link between France-Ireland, currently under construction, may serve as reference solution for its future operation.

The Chapter is organized as follows: Chapter 6.2 illustrates the main modelling features of the meshed multi-area power system. Chapter 6.3 presents the mathematical formulation of the CA and MA. The details of the proposed enumeration method for the MA resolution are in Chapter 6.4. Numerical assumptions and relevant results are illustrated in Chapter 6.5. Finally, Chapter 6.7 provides conclusive remarks and discusses ongoing and future work.

6.2 Modelling and Assumptions

The optimal multi-service operation of interconnectors is assessed considering an insightful three-area power system characterized by a meshed topology. The schematic of the network model is represented in Fig. 6.1, which is extended from Chapter 2. The topology configuration is basic but highly representative, with meshed connections linking every area to its adjacent counterparts. This model serves as the underlying framework for the in-depth investigation and allows for a comprehensive examination of the interconnector dynamics and system performance within the meshed network topology. Each area is modelled as an equivalent single-bus bar network characterized by synchronous generation, renewable generation and inflexible demand. All connections between areas are via HVDC interconnectors and no AC link is considered. It follows that all areas remain asynchronous, i.e., the frequency dynamics in each area are all decoupled. Moreover, a single-equivalent interconnector may account for all the links between each pair of areas.

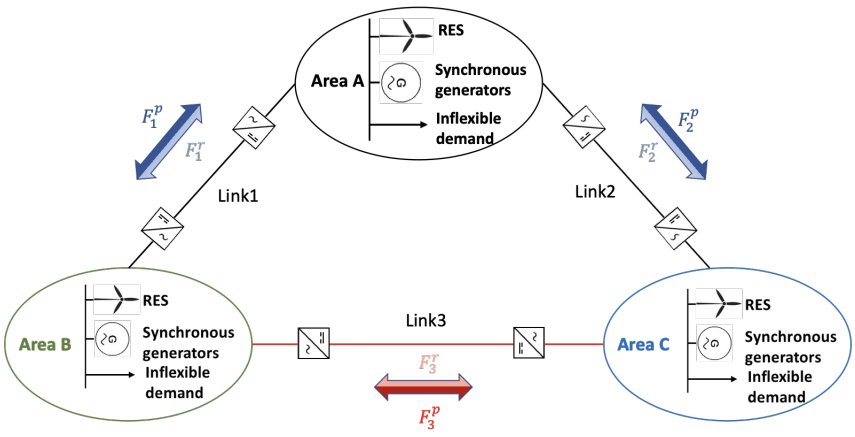


Figure 6.1: Schematics of the multi-area power system with a mesh topology.

The multi-service paradigm keeps consistent with Chapter 2, and is adopted for managing the interconnectors envisages the possibility to allocate the lines' capacity to a twofold purpose. It is assumed that the capacity of each link can be used for power exchange F^p and for the provision of primary FR, denoted by F^r, between connected areas. The former quantity F^p refers to actual inter-area power flows occurring during regular operation of the power system. The latter term F^r pertains to FR exchanges which only occur in presence of a fault e.g. an infrequent, large infeed generation loss in one area. As a result, an important consideration for frequency services is that interconnectors maintain sufficient power margins at all times to ensure the deliverability of the FR they have committed to. It is worth emphasizing that the inter-area provision of FR via interconnectors would let the assets in a certain area contribute to the local frequency regulation in the other areas, with no impact on the local frequency dynamics. The delivery of FR support via interconnectors is designed to ensure that assistance in frequency regulation is provided where it is needed without disrupting the local area's frequency equilibrium. Considering each area in Fig. 6.1 separately, it is reasonable to assume that the points of connection of the two relevant interconnectors might actually be placed at different geographical locations. Hence, this setup envisages the use of individual converters and associated control systems. It follows that the directions of the power flows in each link can be set independently. Furthermore, the direction of any power flow through the interconnectors is driven by the price differential between the two areas; in general, power will flow from the area characterized by a lower price towards the one with higher price. Given the strong interplay between the price for electricity and the price for FR, both depending on the actual

commitment and dispatch of the system, it is relevant to simultaneously optimize the allocation of F^p and F^r of each link.

To this end, the impact of network topology on power flows is assessed by means of the associated incidence matrix $\boldsymbol{A}$. The number of rows of $\boldsymbol{A}$ equals the number of areas N, which are indexed by $i \in \mathcal{N}$ with $\mathcal{N} = \{A, B, C\}$. The number of columns of $\mathcal{M}$ equals the number of links M which are indexed by $m \in \mathcal{M}$ with $\mathcal{M} = \{1, 2, 3\}$. The generic element $A_{i,m}$ in the i^{th} and m^{th} column of $\boldsymbol{A}$ specifies whether the link m and the area i are connected, and can be expressed by:

$$\boldsymbol{A_{i,m}} = \begin{cases} 1 & \text{if area } i \text{ is the sending end of link } m \\ -1 & \text{if area } i \text{ is the receiving end of link } m \\ 0 & \text{otherwise} \end{cases} \tag{6.1}$$

By this convention, the incidence matrix for the network topology in Fig. 6.1 can be expressed by the matrix $\boldsymbol{A}$. The power exchange has a positive sign when occurring from area A to B (Link1), from B to C (Link2) and from A to C (Link3).

$$\boldsymbol{A} = \begin{bmatrix} 1 & 1 & 0 \\ -1 & 0 & 1 \\ 0 & -1 & -1 \end{bmatrix} \tag{6.2}$$

The operation of the interconnectors is investigated under two different setups, the centralized approach (CA) and the market approach (MA).

6.3 Formulation

The CA is formulated to obtain a benchmark solution of the optimal operation of the interconnected system in Fig. 6.1. Under the CA, all interconnectors are operated as regulated assets. The generation commitment and dispatch decisions in Area A, B and C and the capacity repartition of Link1, Link2, Link3 are scheduled simultaneously by solving a centralized security-constrained UC problem to minimize the total system operational costs.

In this thesis, the Unit Commitment (UC) is consistently presented as a deterministic, linear programming optimization problem. To achieve this result, binary variables for typical on/off commitment of generators are relaxed and formulated as continuous variables. In fact, the commitment decisions of the generic technology $x \in \mathcal{X}$ in area i can be expressed with $H_{i,x} \in [0, 1]$ which indicates the fraction of total generation capacity which is brought online. The proposed UC is evaluated over the discrete time interval T, considering a time step Δt. However, the formulation does not include inter-temporal constraints and it can therefore be solved independently at each time step. On this basis, the time index is dropped in the rest of this chapter for improved readability of the notation.

Furthermore, the UC considers the allocation of ancillary services to be deployed in response to an infrequent, large infeed generation loss. The mutual allocation of IR and FR at each area ensures that the local Rate of Change of Frequency (RoCoF), frequency nadir and the quasi steady-state frequency deviation remain above specified thresholds, respectively. Synchronous generators are the sole providers of IR. Since the areas are asynchronously interconnected, it is not possible to exchange IR between areas. Hence, in case of a frequency event in one area, there will be no support from the IR from other areas. Moreover, FR in one area can be provided by the local synchronous generators and by the interconnectors connected to that area. These assets are able to rapidly modify the actual inter-area power flow to provide FR and alleviate the underfrequency condition. Other types of ancillary services, such as the second-to-second frequency regulation in normal operation or other long-term contingency reserves are not considered in this work.

6.3.1 Centralized Approach (CA)

The decision variables of the UC problem correspond to the following set:

$$\Psi_{CA} = \bigcup_{i \in \mathcal{N}, x \in \ X, \forall m \in \mathcal{M}} \{H_{i,x}, P_{i,x}, R_{i,x}, F^p_m, F^r_m\} \tag{6.3}$$

where $\mathcal{N}, \mathcal{X}, \mathcal{M}$ denote the set of areas, generation technologies and interconnectors, respectively. For each area $i \in \mathcal{N}$ and generation technology $x \in \mathcal{X}$, $H_{i,x}$is the share of generation committed capacity, $P_{i,x}$ the dispatch level and $R_{i,x}$ is the allocated FR headroom. Moreover, for each link $m \in \mathcal{M}$, F^p_m is the capacity allocated for cross-border power exchange, whereas F^r_m is the capacity allocated for cross-border FR exchange.

The objective function $\mathcal{F}(\Psi_{CA})$ of the CA formulation is defined in the right-hand side of (6.4) as the total system operation costs over a single time period. This corresponds to the sum of two distinct components, multiplied by the considered time interval Δt: (i) the no-load generation cost expressed as the product of $c'_{i,x}[£/MWh]$ and the on-line generation capacity $H_{i,x}\ \bar{G}_{i,x}$, and (ii) the generation production cost, where $c''_{i,x}[£/MWh]$ and $c'''_{i,x}[£/(MW)^2h]$ multiply the dispatch level and its square value, respectively. Note that no explicit cost term is included in the objective function for the provision of FR. In the case, for example, of generation technologies, these costs are implicitly accounted for as the financial loss for increasing the on-line capacity to maintain a certain power headroom for FR.

The UC problem under the CA is therefore characterized by the following optimization problem (6.4)-(6.8):

$$\min_{\Psi_{CA}} \mathcal{F}(\Psi_{CA}) = \min_{\Psi_{CA}} \Delta t \sum_{i \in \mathcal{N}} \sum_{x \in \mathcal{X}} (c'_{i,x} \cdot H_{i,x} \cdot \bar{G}_{i,x} + c''_{i,x} \cdot P_{i,x} + c'''_{i,x} \cdot P^2_{i,x}) \tag{6.4}$$

subject to:

$$\sum_{x\in\mathcal{X}} P_{i,x} - \sum_{m\in\mathcal{M}} A_{i,m}\cdot F^p_m = L_i \qquad \forall i\in\mathcal{N} \tag{6.5a}$$

$$0 \le H_{i,x} \le 1 \qquad \forall i\in\mathcal{N}\,\forall x\in\mathcal{X} \tag{6.5b}$$

$$P_{i,x} + R_{i,x} \le H_{i,x}\cdot\bar{G}_{i,x} \qquad \forall i\in\mathcal{N}\,\forall x\in\mathcal{X} \tag{6.5c}$$

$$R_{i,x} \le r_{i,x}\cdot H_{i,x}\cdot\bar{G}_{i,x} \qquad \forall i\in\mathcal{N}\,\forall x\in\mathcal{X} \tag{6.5d}$$

$$R_{i,x} \le s_{i,x}\cdot(H_{i,x}\cdot\bar{G}_{i,x} - P_{i,x}) \qquad \forall i\in\mathcal{N}\,\forall x\in\mathcal{X} \tag{6.5e}$$

$$\mu_i\cdot r_{i,x}\cdot H_{i,x}\cdot\bar{G}_{i,x} \le P_{i,x} \qquad \forall i\in\mathcal{N}\,\forall x\in\mathcal{X} \tag{6.5f}$$

$$\hat{R}_i \ge \Delta G_i - D_i\cdot L_i\cdot\Delta f^{qss}_i \qquad \forall i\in\mathcal{N} \tag{6.6a}$$

$$2\Delta G_i\cdot\nu_i\cdot\sigma_i - {\nu_i}^2\cdot\hat{R}_i - 4\Delta f^{roc}_i\cdot\sigma_i\cdot\hat{H}_i \le 0 \qquad \forall i\in\mathcal{N} \tag{6.6b}$$

$$q_i - \hat{H}_i\cdot\hat{R}_i \le 0 \qquad \forall i\in\mathcal{N} \tag{6.6c}$$

$$\hat{R}_i = \sum_{x\in\mathcal{M}} R_{i,x} - \sum_{m\in\mathcal{M}} A_{i,m}\cdot F^r_m \qquad \forall i\in\mathcal{N} \tag{6.7a}$$

$$\hat{H}_i = \frac{1}{f_0}\Big(\sum_{x\in\mathcal{X}} h_{i,x}\cdot H_{i,x}\cdot\bar{G}_{i,x} - h_i\Delta G_i\Big) \qquad \forall i\in\mathcal{N} \tag{6.7b}$$

$$-\hat{F}_m \le F^p_m + F^r_m \le \hat{F}_m \qquad \forall m\in\mathcal{M} \tag{6.8}$$

Constraint (6.5a) enforces the supply/load balance in each area $i \in N$. The synchronous and renewable generation at each area can be higher/lower than the local demand L_i, thus accounting for the power exchanges over the interconnectors. Constraints (6.5b)-(6.5f) refer to

technical capabilities of generators. For each area $i \in N$, (6.5b) follows from the definition of $H_{i,x}$ as the fraction of online generation capacity with respect to the total installed capacity of technology x. The dispatch level and FR headroom are limited in (6.5c) by the maximum on-line power capacity $H_{i,x} \cdot \bar{G}_{i,x}$. The FR allocation $R_{i,x}$ is bounded by (6.5d), which considers the maximum percentage headroom for FR, parametrized by $r_{i,x}$, and by (6.5e), which links $R_{i,x}$ to the dispatch level by means of the slope $s_{i,x}$. Constraint (6.5f) aims at preventing trivial solutions with large FR and zero generation output by imposing that $P_{i,x}$ is μ_i times larger than the maximum available FR.

The frequency-related constraints (6.6) ensure sufficient allocation of IR and FR to maintain, in case of a generation fault in any area i, quasi-steady-state frequency (6.6a), RoCoF (6.6b) and frequency nadir (6.6c) above specified thresholds. The mathematical formulation of these constraints is presented in [82]. The equality (6.7a) provides a compact expression of the system level FR required at area i, while (6.7b) denotes the allocated post-fault system inertia at area i. Finally, (6.8) ensures that the capacity limits of the different lines are not violated.

6.3.2 Market Approach (MA)

Under the MA, a generic interconnector $m \in \mathcal{M}$ is operated as an independent, profit-seeking asset. It autonomously determines its capacity allocation in order to maximize the collected congestion revenues Θ_m. Such revenues are defined as the sum of two terms in (6.9). Denoting by π_i the electricity price in area i, the first term is the product between the power flow F^p_m and the electricity price differential between the areas connected by the link m. The second term extends this structure to the FR allocation F^r_m and the corresponding differential of the prices ρ_i between the interconnected areas:

$$\Theta_m = \Delta t \left(F^p_m \sum_{i \in \mathcal{N}} -A_{i,m} \cdot \pi_i + F^r_m \sum_{i \in \mathcal{N}} -A_{i,m} \cdot \rho_i \right) \tag{6.9}$$

Given the meshed topology of the network in Fig. 6.1, the self-interested operation of a profit-seeking interconnector may influence the formation of both the electricity and FR prices in all system areas.

To accommodate the realistic scenario where cross-border interconnectors are typically regulated transmission assets, the MA assumes that only one of the $\mathcal{M}$ interconnectors in Fig. 6.1 operates as a profit-seeking merchant asset, representing a potential future participant in the market. This choice allows the investigation of the new proposed MA paradigm for a single link $m \in \mathcal{M}$, focusing on the effect of its profit-seeking operation on the scheduling and economics of the rest of the interconnected system. The rest of the assets forming the multi-area system in Fig. 6.1 is thus managed in a centralized coordinated manner.

A. Integrated system operation under the MA

In order to compute the centralized optimal operation of the system while taking into account the market-based operation of the interconnector $\bar{m}$ the UC methodology and the associated optimization problem (6.4)-(6.8) in Chapter 6.3.1 are modified as follows. The set of decision variables Ψ_{CA} is replaced by:

$$\Psi_{MA} = \bigcup_{i \in \mathcal{N}, x \in \mathcal{X}, \forall m \in \bar{\mathcal{M}}} \{H_{i,x}, P_{i,x}, R_{i,x}, F^p_m, F^r_m\} \tag{6.10}$$

The former decision variables $F^p_{\bar{m}}$ and $F^r_{\bar{m}}$ of problem (6.4)-(6.8) are replaced by fixed exogenous quantities $\bar{F}^p$ and $\bar{F}^r$. Constraint (6.8) is only evaluated for all $m \in \bar{\mathcal{M}}$, where $\bar{\mathcal{M}} = \mathcal{M} \backslash \{\bar{m}\}$. As a result of these changes, it is possible to characterize the solution of the UC and the associated electricity prices π_i and FR prices ρ_i as functions of the external parameters $\bar{F}^p$ and $\bar{F}^r$, i.e. the operational decisions of the profit-seeking interconnector $\bar{m}$. In the subsequent analysis, the electricity price and FR are indicated as $\Pi(\bar{F}^p, \bar{F}^r)$ and $\Gamma(\bar{F}^p, \bar{F}^r)$, respectively.

B. Maximization of the Congestion Revenues

In the considered MA framework, the independent profit-seeking link $\bar{m}$ determines in-

dependently its capacity allocation on the basis of the price signals of the interconnected areas in order to maximize the congestion revenues $\Theta_{\bar{m}}$. In other words, if $\bar{F}^p$ and $\bar{F}^r$ are fixed exogenous quantities for the modified UC problem, these are indeed the decision variables in the revenue-maximization problem (6.11)-(6.12) solved by link $\bar{m}$:

$$\max \Theta_{\bar{m}} = \max_{\bar{F}^p, \bar{F}^r} \Delta t \left(F^p_{\bar{m}} \sum_{i \in \mathcal{N}} -A_{i,\bar{m}} \cdot \pi_i + F^r_{\bar{m}} \sum_{i \in \mathcal{N}} -A_{i,\bar{m}} \cdot \rho_i \right) \tag{6.11}$$

subject to:

$$-\hat{F}_{\bar{m}} \leq F^p + F^r \leq \hat{F}_{\bar{m}} \tag{6.12}$$

Constraint (6.12) accounts for the capacity limits of the link $\bar{m}$. As in the previous case, it is possible to characterize the optimal solution of (6.11)-(6.12) as a function of the considered prices π and ρ, denoting the capacity allocation for power exchange and FR provision as $\gamma_p(\pi, \rho)$ and $\gamma_r(\pi, \rho)$, respectively. Note that $\gamma_p(\pi, \rho)$ and $\gamma_r(\pi, \rho)$ are expressed as general functions of the system prices for compactness and simplicity of notation. However, in practice, they only depend on the price signals of the areas j connected by the self-interested link, i.e., such that $A_{j,\bar{m}} \neq 0$.

C. Characterizing the MA solution as a market equilibrium

On the basis of the analytical framework presented in the previous subsections, the solution of the MA can now be defined as the set of quantities ($\bar{F}^{p*}$,$\bar{F}^{r*}$,π^*,ρ^*) that fulfill the following equations:

$$\bar{F}^{p*} = \gamma_p(\pi^*, \rho^*) \tag{6.13a}$$

$$\bar{F}^{r*} = \gamma_r(\pi^*, \rho^*) \tag{6.13b}$$

$$\pi^* = \Pi(\bar{F}^{p*}, \bar{F}^{r*}) \tag{6.13c}$$

$$\rho^* = \Gamma(\bar{F}^{p*}, \bar{F}^{r*}) \tag{6.13d}$$

From (6.13a) and (6.13b), in the MA solution the capacity allocations of the self-interested link are optimal for the price signals π^* and ρ^*. In turn, conditions (6.13c) and (6.13d) indicate that such prices are the ones associated to the solution of the UC problem when the capacity allocations $\bar{F}^{p*}$ and $\bar{F}^{r*}$ are considered for the independent link $\bar{m}$. In other words, the MA solution corresponds to a competitive market equilibrium where each player (i.e., the profit-seeking link and the rest of the system) cannot unilaterally change its operational strategy in order to obtain a better payoff. An example of the interactions arising between the different agents in the specific case of $\bar{m} = 3$ is presented in Fig 6.2.

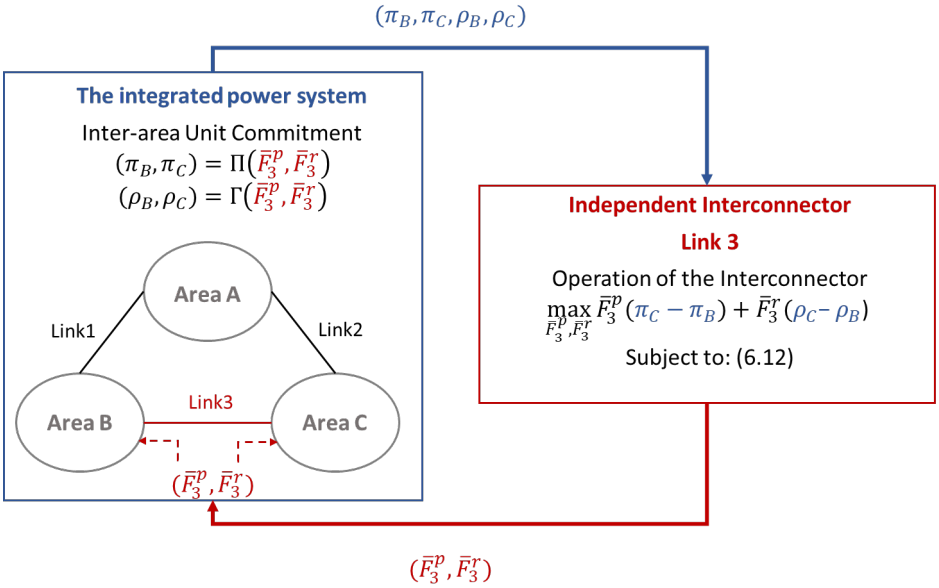


Figure 6.2: Interactions between the integrated power system and the independent merchant interconnector (taking Link3 as example) under the MA.

6.4 Numerical Solution

Market interaction problems like the one formulated in Chapter 6.3.2 exhibit relevant nonlinear interplays between the decision variables involved. For example, the congestion revenues of the profit-seeking interconnector in (6.11) are expressed as the product of its capacity allocations and the price differentials for electricity and FR between two different areas. These

prices depend in non-trivial ways from the optimal UC solution which, in turn, under the realistic hypothesis of *price-making* interconnectors, is affected by their allocation choices. The methodology in [82] proposed a direct resolution for this type of problems, characterizing the price formation as a nonlinear constraint of the interconnector profit optimization, utilizing the MATLAB Nonlinear Programming (NP) solver fmincon to calculate the desired solution.

The extension of this approach to the current more complex problem, which considers multi-area systems with a meshed topology, is not straightforward. Depending on the chosen numerical tolerances and problem parameters, the solver might not be able to provide a solution or return solutions that vary sensibly with respect to the chosen initial conditions. This strongly hints that, within the considered analytical framework, existence and uniqueness of the optimum solution might not be guaranteed.

An alternative enumeration method has been adopted in order to numerically estimate the market equilibrium solution. A grid of discretized values G is defined for the set of feasible interconnector strategies. For a fixed discretization step ΔF, the grid G can be defined as follows:

$$\begin{aligned} G := \{(\bar{F}^p, \bar{F}^r) : \ & \exists n_p \in \mathbb{N} : \bar{F}^p = -\hat{F} + n_p \Delta F \\ & \exists n_r \in \mathbb{N} : \bar{F}^r = -\hat{F} + n_r \Delta F \\ & -\hat{F} \leq \bar{F}^p + \bar{F}^r \leq \hat{F}\}. \end{aligned} \tag{6.14}$$

$$(\bar{F}^{p*}, \bar{F}^{r*}) = \arg \max_{(\bar{F}^p, \bar{F}^r) \in G} \Delta t \left(F^p_m \sum_{i \in \mathcal{N}} -A_{i,\bar{m}} \cdot \pi_i + F^r_m \sum_{i \in \mathcal{N}} -A_{i,\bar{m}} \cdot \rho_i \right) \tag{6.15}$$

subject to:

$$\begin{aligned} -\hat{F}_{\bar{m}} \leq F^p + F^r \leq \hat{F}_{\bar{m}} \\ \pi = \Pi(\bar{F}^p, \bar{F}^r) \\ \rho = \Gamma(\bar{F}^p, \bar{F}^r) \end{aligned} \tag{6.16}$$

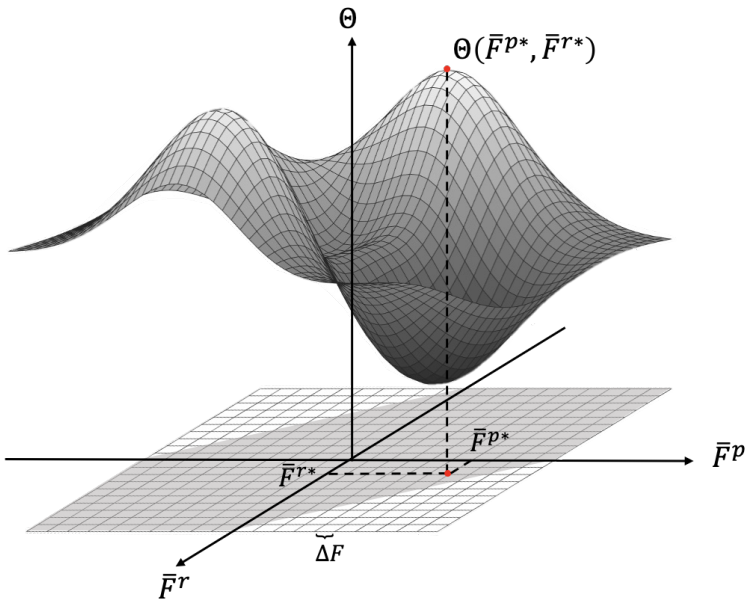


Figure 6.3: Graphical representation of the proposed enumeration approach for the calculation of the approximate market solution.

A graphical representation of the proposed method is in Fig. 6.3, where the candidate solutions in the discretized domain G are represented as the projections of the discretized grid points onto the continuous curve of the congestion surplus θ. Note that $(\bar{F}^{p*}, \bar{F}^{r*})$ in (6.15) can be calculated with a simple enumeration approach, evaluating the objective function for each pair $(\bar{F}^{p}, \bar{F}^{r}) \in G$, with a computation complexity of $\mathcal{O}(1/\Delta F^2)$. Under the assumption of the objective function in (6.15) being Lipschitz continuous with Lipschitz constant Λ, it is also possible to provide an upper bound on the approximation error of the proposed approach:

$$\Theta^* - \Theta(\bar{F}^{p*}, \bar{F}^{r*}) \leq \frac{\sqrt{2}}{2}\Lambda, \tag{6.17}$$

where Θ^* is the theoretical solution of the MA and $\Theta(\bar{F}^{p*}, \bar{F}^{r*})$ denotes the objective function in (6.15) when evaluated at the approximate discretized solution $(\bar{F}^{p*}, \bar{F}^{r*})$. The practical implementation follows steps in Algorithm 6.1.

Algorithm 6.1 – Enumeration method

1) Iterative evaluation:

- Enumeration counter:

  $k = 0$

for $(\bar{F}^p, \bar{F}^r) \in G$

- $k \leftarrow k + 1$
- $(\bar{F}^p_k, \bar{F}^r_k) \leftarrow (\bar{F}^p, \bar{F}^r)$
- Solve the UC formulated in Chapter 6.3.2 with ($\bar{F}^p_k$ and $\bar{F}^r_k$) as fixed input quantities and evaluate the associated prices $\pi_k = \Pi(\bar{F}^p_k, \bar{F}^r_k)$, $\rho_k = \Gamma(\bar{F}^p_k, \bar{F}^r_k)$.
- Calculate the congestion surplus Θ according to the expression in the right-hand side of (6.11):

  $\Theta(\bar{F}^p_k, \bar{F}^r_k) = \Delta t \left(\bar{F}^p_k \sum_{i \in \mathcal{N}} -A_{i,m} \cdot \pi_{i,k} + \bar{F}^r_k \sum_{i \in \mathcal{N}} -A_{i,m} \cdot \rho_{i,k} \right)$

end

end

2) Evaluation of optimal solution

- Find the index k^* and associated solution $(\bar{F}^{p*}, \bar{F}^{r*}) = (\bar{F}^p_{k^*}, \bar{F}^r_{k^*})$ that maximizes the collected congestion surplus Θ: $\Theta(\bar{F}^{p*}, \bar{F}^{r*}) \geq \Theta(\bar{F}^p_k, \bar{F}^r_k), \quad \forall (\bar{F}^p_k, \bar{F}^r_k) \in G$
- Return the approximated solution $(\bar{F}^{p*}, \bar{F}^{r*})$

6.5 Case Studies

The methodology proposed in Chapter 6.3.1 (i.e. the CA) and the novel formulation in Chapter 6.3.2 (i.e. the MA) have been successfully tested considering the GB-France-Ireland interconnections. The characterization of the three power systems and interconnectors refers to possible 2030 low-carbon scenarios. The interconnectors between GB and France and between GB and Ireland are currently in operation, while a first interconnector between Ireland and France is under construction [109]. The selected GB-France-Ireland system is shown in Fig. 6.4. In reference to Fig. 6.1, the three meshed areas A, B and C mimic the GB, French and Irish system, respectively. The rated capacity of the three links $\hat{F}_1 = 5GW$, $\hat{F}_2 = 1GW$, $\hat{F}_3 = 0.7GW$ is in accordance with existing and planned infrastructure in 2026 [109], [110]. Two general types of generation technologies are considered in the simulation:

a. Gas and nuclear generators are merged into a single synchronous technology, providing IR and FR, considering a weighted average of their relevant technical parameters that accounts for the relative penetration level of the two technologies in each power system.

b. Converter-interfaced wind generators in standard configuration, which are unable to provide IR and FR.

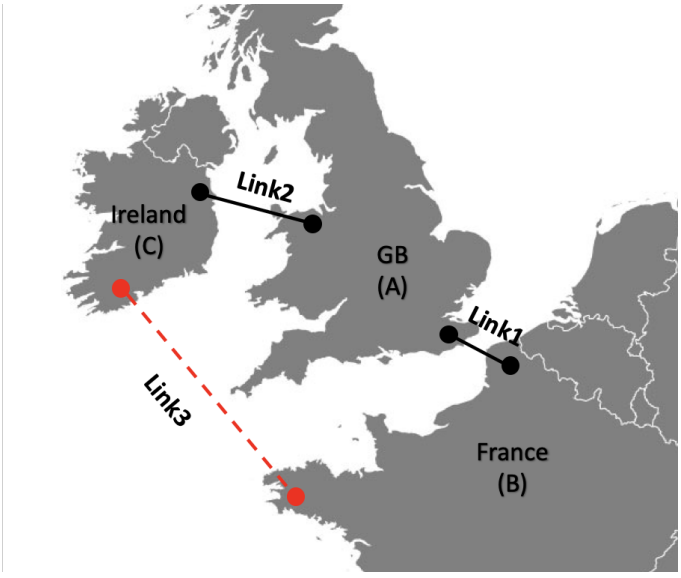


Figure 6.4: Graphical representation of the considered GB-Ireland-France case study.

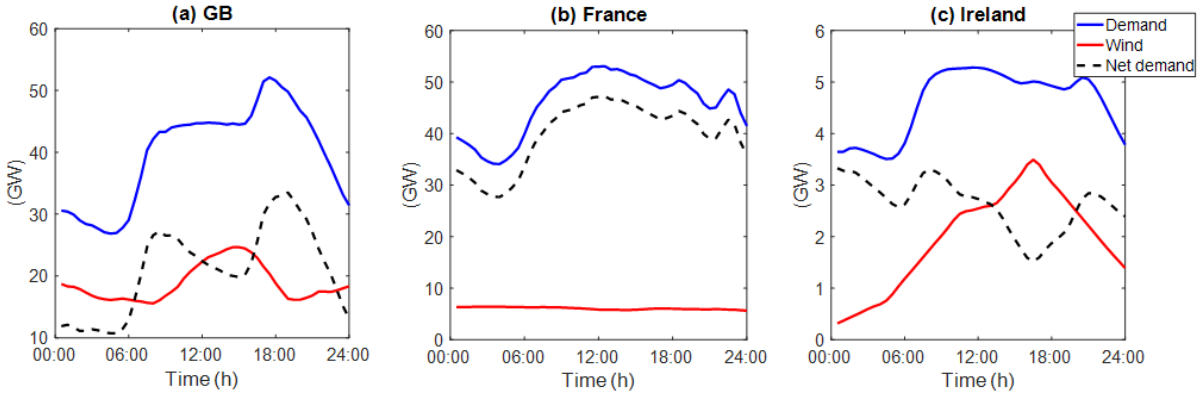


Figure 6.5: Wind and demand profiles in areas (a) GB (b) France (c) Ireland.

Table 6.1: Characteristics of synchronous and wind generation

	Synchronous			Wind		
	GB(A)	France(B)	Ireland(C)	GB (A)	France(B)	Ireland(C)
Installed Capacity $\bar{G}_{k,\tau}$ [GW]	65	85	8	40	15	4
FR headroom r_x	0.1	0.1	0.1	-	-	-
FR slope s_x	0.4	0.3	0.4	-	-	-
Constant of inertia $h_{k,x}$ [s]	4	6	4	-	-	-
No load cost,$c'_{k,x}$ [£/MWh]	7	3.5	7	1	1	1
Cost,$c''_{k,x}$ [£/MWh]	50	20	50	2	2	2
Cost,$c'''_{k,x}$ [£/(MWh)^2]	2.5e-3	5e-3	2.5e-3	1e-3	1e-3	1e-3

Characteristics and parameters of generation technologies are listed in Table 6.1 [82], [44]. It is worth emphasizing that the size of Irish system is significantly smaller than the other two.

The main primary source for synchronous generation in GB and Ireland is gas, whereas France generation mix mainly consists of nuclear synchronous power plants. Thus, the generation cost of synchronous units in France is lower than in GB. Overall, the ratio between wind and synchronous installed capacity is lower in France than in GB and Ireland. The flow through the interconnector is significantly affected by the mix of energy generation sources, loads and RES level. Consequently, for this case study, we selected typical deterministic profiles for wind and demand in each area to serve as reference results. These profiles are selected from [44] and plotted in Fig.6.5.

The parameters of the frequency security constraints considered in the case study are selected according to the national practice and frequency standard defined by the grid operators in GB, France and Ireland. Based on [10], [111], [112], [113], the chosen numerical values are the following:

- Load-damping rate: D_i=1/50s.
- Time window to assess the RoCoF: ν_i=0.5s.
- Allowed frequency deviation within ν_i: f_i^{roc}=0.5Hz
- FR frequency time: σ_A=10s, σ_B=15s, σ_C=5s.
- Maximum allowed frequency deviation at QSS: Δf_A^{qss}=0.5Hz, Δf_B^{qss}=0.2Hz, Δf_C^{qss}=0.5Hz.
- Maximum generation loss: ΔG_A=1.8GW, ΔG_B=1.5GW and ΔG_C=0.5GW.

Simulations are carried out in MATLAB 2020b with an Intel(R) i7-7820X CPU, 3.6GHz processer and 64 GB RAM. The numerical calculation of the solution for a single time period requires about 0.35 seconds and 64.97 minutes for the CA and MA problems, respectively.

6.5.1 Focus on the France-Ireland Link - Base Case

The base case evaluates the operational choices of Link3 connecting France and Ireland under the CA and MA paradigms. The focus on Link3 is interesting since this interconnector is still under construction and the comparison between CA and MA may actually provide relevant insights for the future development and management of the France-Ireland link.

The aggregate daily system operational cost and the congestion surplus associated to each interconnector under the two approaches are compared in Table 6.2 and Fig. 6.6. In particular, from the left to the right side, the bars in Fig. 6.6 illustrate the variation, in absolute terms, between the MA and CA solutions referring to the overall system operational cost and the lines' revenues. The numbers over each column express these variations in relative terms.

Results indicate only a minor increment (0.02%) in the system operational cost when implementing the MA (blue bar). However, the switching to a MA allows the Link 3 to significantly increase its revenue (+89% - grey bar) compared to the same result under the CA.

Table 6.2: Daily system results

Daily operational cost (M£)		Daily link congestion surplus revenue (M£)		
CA	MA		CA	MA
		Link1	11.142	11.117
154.41	154.44	Link2	2.567	2.759
		Link3	0.273	0.516

The operational choices of Link3 under MA have a small impact on the revenues of the other two links, with a 0.22% reduction and a 7.4% increase in the revenues of Link1 and Link2 with respect to the CA (red and black bars, respectively).

Fig. 6.7 compares the repartition of the interconnector capacity between power flow F^p and FR F^r in the CA and MA solutions. By convention, a positive sign refers to power flows from GB to France (Link1), from GB to Ireland (Link2) and from France to Ireland (Link3). In the case of Link1 and Link2, F^p and F^r are generally negative quantities both in the CA and MA solutions, implying that GB would often import power and procure FR from France and Ireland. Especially during high demand periods in GB (e.g., from 6am to midnight - see Fig.6.5), both links are almost fully used to support the demand in GB.

In the case of Link3 in Fig. 6.7(c), although relevant differences in operational strategies can be noticed, the direction of flows is generally concordant in the MA and CA, implying that the operation of the interconnector is highly driven by the system operational requirements. The power flow F_3^p changes its direction during the day. During the night (from 00:00 to 05:00), the

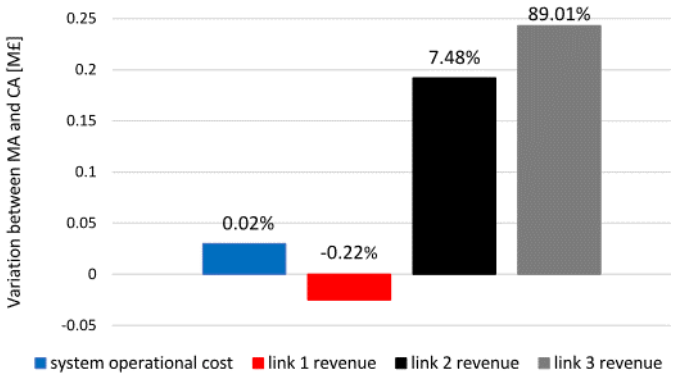


Figure 6.6: Daily variations in system operational cost (blue), link 1 revenue (red), link 2 revenue (black) and link 3 revenue (grey) between MA and CA. The numbers represent percent variations.

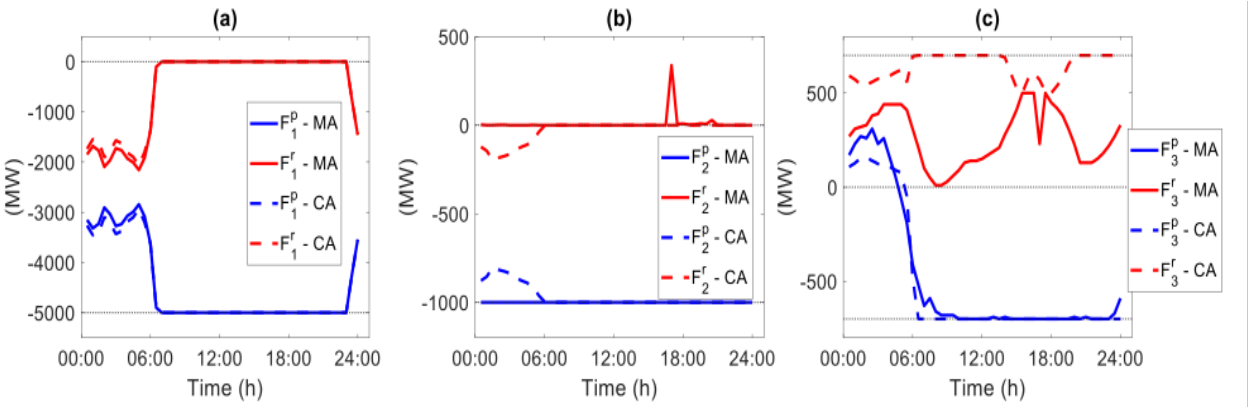


Figure 6.7: Interconnector capacity allocation for (a) Link1 (b) Link2 (c) Link3.

wind availability in Ireland significantly decreases (Fig. 6.5 (c)), and Ireland imports power from France (positive F_3^p). After 06:00, both demand and wind availability in Ireland increase, the resulting cheaper local electricity prices reverse the power flow direction, and Ireland starts to export power to France. However, the low demand level and relatively high wind power availability in Ireland requires higher allocation of FR, locally. The exchange of FR availability on Link3 remains always from France to Ireland. In this case, where the flows F_3^p and F_3^r have opposite directions, the fulfillment of post-fault FR should be firstly met by the reduction of negative F_3^p from area Ireland to France, and then use the reserved the headroom (positive F_3^r) from France to Ireland.

To better explain the different performance of the interconnectors in Fig. 6.7, the price differentials between linked areas are introduced in Fig. 6.8. Note in Fig. 6.7 (c) how the capacity

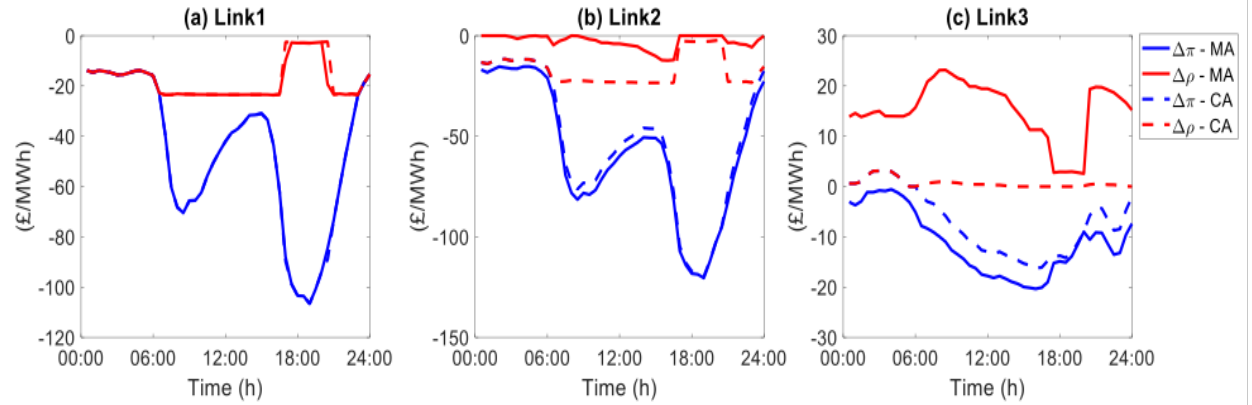


Figure 6.8: Electricity and FR availability price differentials between linked areas (a) Link1 (France-GB) (b) Link2 (Ireland-GB) (c) Link3 (Ireland-France).

withdrawing (particularly in terms of FR allocation F_3^r) performed by Link 3 in the MA leads to a significant increase of the price differential between France and Ireland in Fig. 6.8 (c). The different operational strategy of Link3 under the MA also impacts the interconnected network operation on Link1 and Link2. The increase in power and the reduction in FR exchange from France to Ireland at night (before 6 am) implies more power and less FR support from GB to Ireland (Fig.6.7 (b)). The variation of capacity allocations of Link2 and Link3 affects the scheduling of both the GB and France system, as well as the power flows between them. Hence, a slight reduction in power flow F_1^p and an increase in FR F_1^r from France to GB during the early hours of the day can be noticed in Fig. 6.7 (a). After 6 am, both Link1 and Link2 are fully used for power transmission as the price differentials of power in Fig. 6.8 (a), (b) between these areas are significantly larger than those of FR, becoming the dominant factor in determining the capacity allocation.

6.5.2 Operation of Link1 and Link2 under MA

This section performs the analysis and comparison between CA and MA, already presented in the base case of Section 6.5.1, for two alternative scenarios. In Case 1, the Link1 is selected as the single interconnector operating independently in the MA solution (i.e.,$\bar{m} = 1$). Similarly, in Case 2, is assumed that Link2 operates independently under the MA ($\bar{m} = 2$). As in the initial analysis presented in Section 6.5.1, each new case assumes that the rest of the power system (with the exception of the independent link) is operated in a centralized manner through the resolution of a single UC problem. The daily operational costs and revenues of the cases under exam are shown in Table 6.3.

Table 6.3: Market-based operation on different lines

	MA			CA
	Case 1	Case 2	Base case	
Independent link	Link1	Link2	Link3	-
Operational Cost (M£)	154.72	154.42	154.44	154.41
Link1 revenue (M£)	11.321	11.150	11.117	11.142
Link2 revenue (M£)	2.692	2.570	2.759	2.567
Link3 revenue (M£)	0.266	0.313	0.516	0.273

The conclusion highlighted in Chapter 6.5.1 are still valid for the other two cases considered here. Compared to the CA solution, it is possible to increase the congestion surplus of the independent link by withdrawing part of its capacity at the expense of a higher operational cost. The largest system operational cost occurs in Case 1 ($+0.3M£$ with respect to the base case), i.e. when Link1 is the line operating independently under the MA paradigm. This is due to the fact that Link1 is the line with the largest capacity and therefore has more margins to withdraw power and FR provision in order to induce higher price differentials and increase its line revenues when operating independently. As a result of this capacity withdrawing, price differentials between GB and France will be larger.

In Case 2, Link2 (between GB and Ireland) is the line operating independently under the MA paradigm. This interconnector improves its revenues only by 0.1% when compared with the CA case, with a resulting increase in total operational cost smaller than 0.01%. In this case, the price spreads between GB and Ireland are marginally affected by the change in operational strategies of Link2. Link1 and Link3, which are coordinated by the centralized optimizer together with the UC of the interconnected areas, are optimized to minimize power and FR price differentials between GB-France, and Ireland-France. Hence, simply changing Link2 capacity allocation strategy cannot significantly maximize the link profits. Note that the Link2 revenue in Case 2 is even smaller than in the base case and in Case 1, since the price differentials between GB and Ireland may be impacted more significantly by adjusting the operation of the other two links. The solution from MA in Case 2 is very close to the CA optimum, and the independent Link2 only has a very small incentive to change its strategies.

6.5.3 The Value of Providing Inter-Area FR

This section analyses two additional case studies to assess the impact and additional value of the envisaged multi-service paradigm for interconnectors that exchange both power and FR availability. The current traditional operational approach, which only envisages power exchanges in normal operation of the interconnector (Case A), is compared to an alternative multi-service operational paradigm (Case B). In this latter case, the two interconnectors that already exist

in practice (Link1 and Link2) maintain a business-as-usual approach (power exchange only), while Link3 allows simultaneous exchange of power and FR. Cases A and B are also compared to the base case results analyzed in Chapter 6.5.1, where all the three links provide both power and FR. Relevant results are presented in Table 6.4.

Table 6.4: System results in Case A and Case B relative to base case

Case Study		Operational Cost (%)	Link1 revenue (%)	Link2 revenue (%)	Link3 revenue (%)
Case A	CA	+0.40	-8.06	+0.48	+36.23
	MA	+0.38	-5.30	-5.96	-26.75
Case B	CA	+0.23	-8.08	-6.14	-2.24
	MA	+0.23	-7.90	-5.32	+9.84

The Case A, where FR can only be allocated locally in each area and not exchanged over the interconnectors, exhibits the highest system operational cost, with around 0.4% increase with respect to the base case, both in the CA and MA. The revenues obtained by operating Link3 under the MA are reduced by 26.75% with respect to the base case. This demonstrates that the simultaneous exchange of power and FR availability not only allows a more efficient system operation but can also represent a significant source of additional revenues for privately-operated lines. It should be emphasized, however, that the FR revenues in the MA depend on the topology of the grid and the characteristics of the interconnected areas. For example, in the considered setup, the revenues collected by Link1 and Link2 are reduced only by about 5% when exchange of FR availability is not considered.

These considerations are further supported by Case B, which envisages a multi-service operation only for Link3 and represents an intermediate scenario between the business-as-usual operation of Case A and the novel paradigm analyzed in the base case. In the Case B scenario, the increased flexibility in the operation of Link3 reduces the system costs with respect to Case A. However, these remain 0.23% higher than in the base case where full operational flexibility of all the lines is considered. Operating Link3 under MA, in this case, produces the highest revenue among all three scenarios, since Link3 can exploit the competitive advantage of being the only line capable of providing FR to its interconnected areas.

6.6 Discussions

Under the realistic GB-France-Ireland cross-border interconnected power system, the assumption is made that the connection points of different links in the same system may have different geographic locations. Therefore, they are equipped with different control systems and no co-operation is required. This configuration is suitable for the system linked by the independent merchant interconnectors, where one's control and operation are independently of one another.

Another modelling framework considering meshed topology is commonly adopted as the HVDC network, in which the two or more links are sharing the same connection node. In this scenario, the controlling methodology might change. For example in [114] in the context of long-term transmission planning, it is necessary to explicitly include the HVDC nodal voltages as decision variables to properly express and univocally define HVDC power flows in a meshed network. In fact, the HVDC power flow between two generic nodes may depend on the difference between the squared values of the corresponding nodal voltages. Hence, the introduction of voltages as decision variables may require the inclusion of quadratic constraints in the optimization problem. A wide range of approximation and linearization techniques (e.g. linearly approximated power flows in [114]) is available to facilitate the extension to meshed networks and different computational methods and solvers can be utilized to obtain a solution in these more complex scenarios.

6.7 Conclusions

This Chapter presents a novel methodology to assess the optimal operation of interconnectors in multi-area power systems with a meshed topology. In the considered framework, each link can simultaneously allocate its available capacity for power flow exchanges between the connected areas and provision of FR. This approach promotes a more efficient inter-area utilization of the low carbon resources (e.g. wind generation) whilst guaranteeing secure post-fault frequency dynamics in each area under low inertia scenarios.

The operation of the interconnectors is studied under two paradigms. The first traditional approach, proposed as benchmark solution, envisages interconnectors that are centrally operated to minimize the total multi-area system operational costs. The second market approach models instead the interconnectors as profit-seeking agents that autonomously determine their operation in order to maximize their congestion revenues. By strategically withdrawing capacity, interconnectors under the market approach induce higher price differentials between the linked areas and thus increase their collected line revenues. The numerical complexities associated to the evaluation of the market solution in meshed networks have been overcome by means of a simple but yet effective enumeration method which provides an approximated numerical solution.

The novel methodology has been applied to the realistic case study of a three-area meshed network which mimics the power systems of GB, France and Ireland. Results have shown that the profit-seeking behavior of a merchant interconnector tends to maximize its revenues by withdrawing capacity and increasing price spreads between the interconnected areas, leading to relevant increments in the collected revenues. Nonetheless, this mechanism is responsible only of a minor reduction of the total social welfare. For this reason, the proposed merchant approach can indeed represent a valid alternative to traditional centralized paradigms. The implementation of a market-oriented framework may realistically enable better scalability, higher robustness and improved efficiency with partial information.

Two elements stem from the considerations above. First, the game-oriented formulation of the MA ensures that no single interconnector can improve its revenues by further increasing its capacity withdrawing. In other words, barring collusions between players, the negative impact of market interactions on the overall social welfare will not exceed the one in the presented assessment. Second, the considered scenarios already refer to merchant interconnectors with a significant market power; no other line in fact operates between the interconnected areas and they have a significant amount of available capacity to be allocated for power exchange and FR. At first glance, under the considered assumptions, it is reasonable to infer that, in future realistic scenarios, the market power exercised by the interconnector will be comparable to the one considered in the present assessment and the same will hold for the impact of

merchant operation on the overall social welfare. However, this result calls for a detailed investigation in future works, possibly considering in an explicit manner also the competition between interconnectors and other flexible assets.

Moreover, if one considers single interconnector switching from a centralized to a market paradigm, the magnitude of the associated line revenue increment is significantly impacted not only by the rated capacity of the considered link, but also by the sizes and generation features of each area. Due to the meshed network topology, the self-interested operation of a merchant link may not only increase its revenue but also boost the congestion surplus associated to other centrally-coordinated links.

Overall, the assessment of the methodology and the results presented in this work suggest a relatively small impact of merchant paradigms on the actual social welfare. This metric can represent a useful indication in the development of new and ad-hoc policy and regulation measures regarding the most suitable schemes and frameworks for the realization of interconnector assets.

Finally, the comprehensive case studies quantified the additional value of operating interconnectors in order to provide inter-area FR, compared to traditional paradigms based on the sole exchange of power during regular operation. The insights of this paper provide strong evidence for a review of the current techno-economic operational paradigms of interconnectors, opening up to a multi-service allocation of interconnection capacity in a competitive market framework.

6.8 Future Works

The proposed modelling framework is being extended to accommodate more complex scenarios, considering larger networks and an increased number of interconnectors. To this end, the efforts will focus on enhancing the scalability and performance of the proposed methodology, improving the current enumeration approach or implementing alternative numerical techniques to ensure a timely and efficient computation of the solutions.

Future work will also quantify the impact of the market power of profit-seeking interconnectors on system efficiency under a wider range of conditions. This will be achieved by analyzing the competitive interactions between multiple merchant interconnectors. Similarly, the proposed approach represents the basis for quantifying the competitiveness of other flexible technologies, such as demand side response, storage and synchronous compensators, with respect to merchant interconnectors. Moreover, the deterministic formulation in this work could be extended with stochastic features and take into account different types of uncertainties, associated for example to the RES output or to the availability of interconnectors and generators. The optimal repartition of the interconnection capacity will also consider additional ancillary services, such as operational reserves or capacity market outcomes.

A more comprehensive model will consider the costs associated to network losses in the optimal scheduling process. Furthermore, the current model considers inertia provision only from conventional synchronous generators. Future work will assess the possibility by wind turbines of contributing to system security by providing synthetic inertia. Finally, aside from the considered short-term operation, the long-term interconnector planning and investment problem will also be analyzed from both system and market perspectives.

Chapter 7

Conclusions and Future Works

7.1 Conclusions

This thesis focuses on the evaluation of the value of the flexible operation of the cross-border interconnector in the low-carbon modern power systems, especially in the context of increasing demanding for FR services. To this end, the research directions includes, 1) coupling the inertia-dependent FR service into the interconnector energy exchange operation, 2) proposing and quantifying the market-based operation of the merchant interconnector in the competitive market, 3) analysing the impact of variability from the demand and intermittent RES generations on the multi-service operation of interconnector under different market frameworks, 4) integrating the flexibility from the demand side and exploring the synergies and interaction between the TCLs and the interconnector in offering different levels of flexibility, 5) extending and assessing the multi-service paradigm and market operation under more complex, realistic meshed networks. The conclusions from each technical chapter are summarized as follows:

I. Operational frameworks

One of the pioneering contribution in this work is the development of the multi-service framework for the interconnector which is not only operated for the conventional energy trading, but facilitates the exchange of frequency services as well. This innovative step

recognizes that the interconnector can function more than just the transmission asset to transfer the power to leverage diverse-located generation. They can also serve as the flexibility assets that contribute to both efficiency and security of the power system. Chapter 2 deduces the analytical centralized formulation as the Centralized Approach (CA), with the inertia-dependent frequency constraints to guarantee the post-fault frequency deviation level within the secure criteria. Case studies quantify the value of the multi-service interconnector in reducing total system operational cost, reducing wind curtailment and improving facility's efficiency. These contributions are amplified in the future low-carbon landscape with high-RES penetrations, and more interconnectors integration.

II. Market perspective and competition

The thesis further progresses by proposing the novel market-based operation paradigm of the interconnector. In this new mechanism, the interconnectors actively participate in the market clearing as the profit-seeking entities that autonomously determine their operation in order to maximize their congestion revenues, instead of being treated as the passive transmission component which is managed centrally for the purpose of the whole interconnected power system. The principle of the market-approach is more aligned with the operation mechanism in the liberalized power market. As demonstrated in Chapter 3, the independent merchant interconnector modelled as the *price-maker* as the Market Approach (MA), and the performance is compared to the benchmark CA solution presented in Chapter 2. It has been demonstrated that, by strategically withdrawing capacity, interconnectors under the market approach induce higher price differentials between the linked areas and thus increase their collected line revenues.

III. Impact of variability

By adopting the sampling-based method, the significant aspect in the low carbon system, the net demand level, has been further explored for its influences on the interconnected system. The thesis compares the impact of wind and demand variability on the short-term behaviour of the interconnector operation between the centralized an market-based operation framework. Compelling case studies in Chapter 4, under different combination of sampled seasonal wind and demand profiles in GB, provide substantial indications

of how the variability in renewable energy and demand level affect the interconnector strategies and related revenues when it operates as the regulated asset and the merchant asset. The findings indicate a strong correlation between the behavior of the merchant interconnector and the net demand level in Great Britain. In scenarios characterized by high wind availability and low demand, the merchant interconnector, which is capable of offering multiple services, tends to reduce its capacity for energy exchange in favor of pursuing self-profit.

IV. Interaction among flexibility across multiple dimensions

This thesis further builds the model integrating flexibility from different dimensions, including the generation side, the transmission side, and also the demand side. The demand side aggregated TCLs, capable of energy arbitrage and providing FR, has been equivalent to the leaky storage model to be embedded in the optimization formulation. Comparative case studies in Chapter 5 offer the deep understanding of the synergy and competition between the interconnector operation and the demand side response under CA and MA.

Simulations quantitatively demonstrate the mutual contribution of flexible operation of TCLs and interconnector in improving the system benefits and efficiency. Beyond investigating the value of the interconnector and TCLs as regulated assets, the thesis further ventures into the market dynamics when the two types of assets join the market clearing as independent profit-seeking agents in the competitive market. The inclusion of the market-based, flexible TCLs impacts the local electricity and FR prices, restricting the capability of the business interconnectors to optimize their strategies for maximizing the revenue. The symbiosis between the interconnector and the demand side response, pave the pathway for the future development of the merchant interconnectors with understanding interplays among multi-layer stakeholders from power systems.

V. Extension to the multi-area model under meshed network

Finally, the last research topic is the extension of the model from a single-link, two-area power system, to the multi-area power system connected in the meshed topology. The tapestry of interconnectivity among power systems allows the sharing of resources

over a wider geographic scale and amplifies the benefit that the interconnectors could bring. However, the meshed network model also introduces another layer of complexities, especially in considering their market interactions and in finding the market equilibrium. The interdependence among the interconnectors in the meshed network, requires the independent merchant interconnector to hold a more holistic view of the system dynamics.

This chapter adopts the three-area, meshed connected Europe power systems as case study, offering valuable insight into the applicability of the multi-service interconnector under both centralized and market approach. In Chapter 6, the simple but yet effective enumeration method helps capture the nonlinear interplay between relevant decision variables in the meshed network and avoid the numerical complexities in evaluating the market solution. Results have shown that the profit-seeking merchant interconnector tends to maximize its revenue by withdrawing capacity. The analysis reveals that under a game-oriented market allocation, no individual interconnector can increase profits by further reducing its capacity, thus limiting negative impacts on social welfare. The scenarios studied involve powerful merchant interconnectors with no competition in their operating areas, suggesting the significant market power and impact on social welfare. Moreover, the business behaviour and the line revenue of the interconnector is not merely affected by its own capacity rate. The size and characteristics of the linked power systems and their scheduling status, have significant impact on the magnitude and increment of the link profit. In turn, the self-interested behaviour of the merchant interconnector has the potential to boost the congestion surplus collected by the other regulated links.

In conclusion, the proposed multi-service framework for the interconnectors plays a significant role in facilitating the transition to the more cost-efficient low-carbon power system. The interconnectors enhance social welfare by enabling a mutual exchange of resources between systems with different characteristics and generation portfolios. These benefits can be maximized in the CA, providing the most economical solution for the system operation. However, these benefits are marginally reduced in the MA where the interconnectors operates as the self-interested profit-seeking entities.

With the ongoing competitiveness in the electricity market, the MA is expected to be more common in the future. In the MA, the interconnectors operate as merchant entities and can optimally profit from the congestion surplus. When compared to the CA solution, the MA might in principle correspond to slightly lower social welfare, caused by their decision to withdraw capacity for higher revenues. However, the drawbacks of MA are compensated by advantages, such as better scalability, improved efficiency with partial information and greater robustness. In addition, the existing scenarios account for a merchant interconnector possessing a substantial amount of capacity and market power. The evaluation of the methodology and findings in this study indicates a relatively minor effect of merchant paradigms on actual social welfare. It is reasonable to infer that the market power exerted by the merchant interconnector and the impact on the overall social welfare will be comparable to the present assessment. Notably, in the cross-border trading, the CA bears more limitations in aggregating details of generation portfolios from different counties, providing efficient large-scale calculations.

The incentives for the transition from the centralized to market-based operation are influenced by various factors, as evidenced by the findings in Chapter 4 to Chapter 6. These chapters highlight the impacts from the RES variability, the interplay between additional market flexibility provider, and the complexities introduced by the meshed network topology. The market-based merchant interconnector has more incentives to improve the line revenue, in the condition of low net demand (high RES), and less competitions. When the interconnector is involved in the multi-area system connected in the meshed topology, the magnitude of the associated line revenue increment is impacted not only by the rated capacity of the considered link, but also by the sizes and generation attributes of each connected area. The meshed topology potentially allows the self-interested behaviour of a merchant link to simultaneously increasing the congestion surplus both of their own and of other centrally-coordinated links. Comprehensive case studies in this research can serve as a valuable guide in creating new and specific policy and regulatory measures concerning the most appropriate schemes and frameworks for the development of interconnector assets.

7.2 Future works

This thesis lays a strong foundation for the further expansions in multiple directions. Main possible extensions are summarized as following:

I. From the flexibility perspective:

Firstly, the role of the interconnector can be enhanced to provide extensive ancillary services, which are crucial for maintaining system stability and reliability. These services include such as reserve capacities and dynamic frequency regulation, positioning the interconnector as a highly flexible asset within the grid. To meet the multi-service interconnector target, substantial advancements are necessary in several key areas of the power system infrastructure, including sophisticated control systems, communication networks to meet the evolving service requirements.

The Multi-Purpose Interconnector (MPI) is emerging as the next-generation solution in interconnector technology, enhancing operational efficiencies far beyond traditional models. Unlike conventional interconnectors that solely facilitate electricity sharing between countries, MPIs allow clusters of wind farms to directly connect to the interconnector itself. This integration significantly boosts operational efficiency. The benefits of MPIs, including their enhanced flexibility, have been widely recognized and will be further explored in the next step.

II. From the modelling perspective:

With the prevalence of the renewable resources, accompanying by increasing uncertainties, and the availability of the existing assets, the stochastic model will offer higher value to the efficient and accurate scheduling. More comprehensive stochastic models can explicitly account for the random nature of RES, as well as potential failure rates of system infrastructures. By simulating various possible outcomes, based on the specific scenarios and available information, the optimization can further consider the proper methods including robust optimization, Monte Carlo Simulation, chance-constrained optimization, scenario-based optimization.

III. From the planning perspective:

In addition, this thesis focuses on the short-term operation of the interconnector, highlighting the operational functionality and efficiency. While the planning and investment are significant aspects for the future development of the interconnector grid. Specifically, the market-based model for the investment and planning offers substantial values for the privately constructed merchant interconnectors. The future work will be extended to the long-term investment problem, balancing the incentives and risks associated with the both the regulated and private investment.

IV. From the market perspective:

The liberalized modern power system, encourages the competitive interactions among different stakeholders in the power system and achieving higher market efficiency. The agent-based model in this work looks into the interaction between the business behaviour of the interconnector. Future works can be extend to the discussion on the interconnector under one or different stakeholders. Another research direction is expected to consider the competitiveness of the interconnector against a wide range of demand side response, and also the profit-seeking generator companies from the supply side.

V. From the methodology perspective:

The market interactions among players in the competitive power system, are captured using the agent-based modelling, which is characterized by the difficulties in capturing the complex, nonlinear interactions. Along with the increased complexity in power system structure and active market players, the agent-based model faces challenges in increasing problem complexity and computational complexity. The advancement in the analytical model and methodologies are required. With the significant progress in the field of machine learning, the data-driven approach appears to be the alternative efficient method to solve the multi-agent problem under the competitive environment.

VI. From the low-carbon perspective:

The future work is expected to include a wider range of low carbon scenarios. The contribution and benefit of the flexible interconnector will be explored in greater depth,

especially in the context of linking the multiple low-carbon power systems characterized with diverse RES, such as wind, solar photovoltaic, hydropower, etc,. These technologies leverage the clean energy from different geographical, meteorological, environmental advantages. The advantages of multi-service interconnector is anticipated to amplified and bring higher values in transition towards future low-carbon power systems.

Bibliography

[1] "Global warming of 1.5°c an ipcc special report on the impacts of global warming of 1.5°c above pre-industrial levels and related global greenhouse gas emission pathways, in the context of strengthening the global response to the threat of climate change, sustainable development, and efforts to eradicate poverty," accessed: 2022-01-30. [Online]. Available: https://www.ipcc.ch/site/assets/uploads/sites/2/2022/06/SR15_Full_Report_LR.pdf

[2] "Eu 2050 long-term strategy," accessed: 2022-01-30. [Online]. Available: https://ec.europa.eu/clima/eu-action/climate-strategies-targets/2050-long-term-strategy_en

[3] "Net zero strategy:build back greener," accessed: 2022-06-30. [Online]. Available: https://assets.publishing.service.gov.uk/government/uploads/system/uploads/attachmentdata/file/1033990/net-zero-strategy-beis.pdf

[4] "Cop26 presidency outcomes," accessed: 2023-04-29. [Online]. Available: https://ukcop26.org/wp-content/uploads/2022/11/COP26-Presidency-Outcomes.pdf

[5] "Final uk greenhouse gas emissions national statistics: 1990 to 2021," accessed: 2023-05-01. [Online]. Available: https://www.gov.uk/government/statistics/final-uk-greenhouse-gas-emissions-national-statistics-1990-to-2021

[6] "Building back better – raising the uk's climate ambitions for 2035 will put net zero within reach and change the uk for the better," accessed: 2023-02-08. [Online]. Available: https://www.theccc.org.uk/2020/12/09/building-back-better-raising-the-uks-climate-ambitions-for-2035-will-put-net-zero-within-reach-and

[7] T. K. Chau, S. S. Yu, T. L. Fernando, H. H.-C. Iu, and M. Small, "A novel control strategy of dfig wind turbines in complex power systems for enhancement of primary frequency response and lfod," *IEEE Transactions on Power Systems*, vol. 33, no. 2, pp. 1811–1823, 2017.

[8] "Markets roadmap," accessed: 2023-04-29. [Online]. Available: https://www.nationalgrideso.com/research-and-publications/markets-roadmap

[9] B. Hartmann, I. Vokony, and I. Táczi, "Effects of decreasing synchronous inertia on power system dynamics—overview of recent experiences and marketisation of services," *International Transactions on Electrical Energy Systems*, vol. 29, no. 12, p. e12128, 2019.

[10] F. Teng, V. Trovato, and G. Strbac, "Stochastic scheduling with inertia-dependent fast frequency response requirements," *IEEE Transactions on Power Systems*, vol. 31, no. 2, pp. 1557–1566, 2015.

[11] "Frequency response services," accessed: 2023-1-15. [Online]. Available: https://www.nationalgrideso.com/industry-information/balancing-services/frequency-response-services

[12] K. Guerra, P. Haro, R. E. Gutiérrez, and A. Gómez-Barea, "Facing the high share of variable renewable energy in the power system: Flexibility and stability requirements," *Applied Energy*, vol. 310, p. 118561, 2022. [Online]. Available: https://www.sciencedirect.com/science/article/pii/S0306261922000460

[13] M. Huber, D. Dimkova, and T. Hamacher, "Integration of wind and solar power in Europe: Assessment of flexibility requirements," *Energy*, vol. 69, pp. 236–246, 2014. [Online]. Available: https://www.sciencedirect.com/science/article/pii/S0360544214002680

[14] P. Tielens and D. V. Hertem, "The relevance of inertia in power systems," *Renewable and Sustainable Energy Reviews*, vol. 55, pp. 999–1009, 2016. [Online]. Available: https://www.sciencedirect.com/science/article/pii/S136403211501268X

[15] F. Teng, M. Aunedi, G. Strbac, V. Trovato, and A. Dallagi, "Provision of ancillary services in future low-carbon uk electricity system," in *2017 IEEE PES Innovative Smart Grid Technologies Conference Europe (ISGT-Europe)*. IEEE, 2017, pp. 1–6.

[16] E. COMMISSION, "Electricity interconnections with neighbouring countries - second report of the commission expert group on electricity interconnection targets," 2019. [Online]. Available: https://ec.europa.eu/energy/sites/ener/files/documents/2nd_report_ic_with_neighbouring_countries_b5.pdf

[17] Ofgem, "Interconnectors," 2021. [Online]. Available: https://www.ofgem.gov.uk/energy-policy-and-regulation/policy-and-regulatory-programmes/interconnectors

[18] "Why interconnectors play an essential role in our net zero future," accessed: 2023-05-01. [Online]. Available: https://www.nationalgrid.com/stories/engineering-innovation-stories/why-interconnectors-play-essential-role-our-net-zero-future

[19] R. Nepal and T. Jamasb, "Interconnections and market integration in the irish single electricity market," *Energy Policy*, vol. 51, pp. 425–434, 2012.

[20] E. Denny, A. Tuohy, P. Meibom, A. Keane, D. Flynn, A. Mullane, and M. O'malley, "The impact of increased interconnection on electricity systems with large penetrations of wind generation: A case study of ireland and great britain," *Energy Policy*, vol. 38, no. 11, pp. 6946–6954, 2010.

[21] E. V. Mc Garrigle, J. P. Deane, and P. G. Leahy, "How much wind energy will be curtailed on the 2020 irish power system?" *Renewable Energy*, vol. 55, pp. 544–553, 2013.

[22] ENTSO-E, "Vision on market design and system operation towards 2030, institution =entso-e," Tech. Rep., 2019.

[23] C. MacIver, K. R. W. Bell, G. P. Adam, and L. Xu, "Electrical interconnectors: Market opportunities, regulatory issues, technology considerations and implications for the GB energy sector," *Energy Strategy Reviews*, vol. 38, p. 100721, 2021. [Online]. Available: https://www.sciencedirect.com/science/article/pii/S2211467X21001073

[24] Getlinkgroup, "The eleclink project," 2019. [Online]. Available: https://www.getlinkgroup.com/content/uploads/2019/12/191212-eleclink-project-november-2019.pdf

[25] Legislation.gov.uk, "Regulation (eu) 2019/943 of the european parliament and of the council of 5 june 2019 on the internal market for electricity (recast) (text with eea relevance)," 2019. [Online]. Available: https://www.legislation.gov.uk/eur/2019/943/contents

[26] Ofgem, "Decarbonisation action plan," 2020. [Online]. Available: https://www.ofgem.gov.uk/publications-and-updates/ofgem-s-decarbonisation-action-plan

[27] E. Commission, "Clean energy for all europeans package," 2019, accessed: 2022-01-30. [Online]. Available: https://ec.europa.eu/energy/topics/energy-strategy/clean-energy-all-europeans_en

[28] D. Newbery, G. C. Gissey, B. Guo, and P. E. Dodds, "The private and social value of british electrical interconnectors," *Energy Policy*, vol. 133, p. 110896, 2019.

[29] ENTSO-E, "Continental europe synchronous area separation on 8 january 2021 interim report," 2021. [Online]. Available: https://eepublicdownloads.azureedge.net/clean-documents/Publications/Position\%20papers\%20and\%20reports/entso-e_CESysSep_interim_report_210225.pdf

[30] S. Delikaraoglou and P. Pinson, "Optimal allocation of HVDC interconnections for exchange of energy and reserve capacity services," *Energy Systems*, vol. 10, no. 3, pp. 635–675, Aug. 2019. [Online]. Available: https://doi.org/10.1007/s12667-018-0288-6

[31] I. M. Sanz, P. D. Judge, C. E. Spallarossa, B. Chaudhuri, and T. C. Green, "Dynamic overload capability of vsc hvdc interconnections for frequency support," *IEEE Transactions on Energy Conversion*, vol. 32, no. 4, pp. 1544–1553, 2017.

[32] J. E. de Haan, C. E. Concha, M. Gibescu, J. van Putten, G. L. Doorman, and W. L. Kling, "Stabilising system frequency using hvdc between the continental european, nordic, and great britain systems," *Sustainable Energy, Grids and Networks*, vol. 5, pp. 125–134, 2016.

[33] A. Lotfjou, M. Shahidehpour, Y. Fu, and Z. Li, "Security-constrained unit commitment with ac/dc transmission systems," *IEEE Transactions on power systems*, vol. 25, no. 1, pp. 531–542, 2009.

[34] D. Van Hertem and M. Ghandhari, "Multi-terminal vsc hvdc for the european supergrid: Obstacles," *Renewable and sustainable energy reviews*, vol. 14, no. 9, pp. 3156–3163, 2010.

[35] D. Chattopadhyay, P. Chitkara, I. D. Curiel, and G. Draugelis, "Cross-border interconnectors in south asia: Market-oriented dispatch and planning," *IEEE Access*, vol. 8, pp. 120 361–120 374, 2020.

[36] T. Otsuki, A. B. M. Isa, and R. D. Samuelson, "Electric power grid interconnections in Northeast Asia: A quantitative analysis of opportunities and challenges," *Energy Policy*, vol. 89, pp. 311–329, 2016. [Online]. Available: https://www.sciencedirect.com/science/article/pii/S0301421515301993

[37] A. Rafiee, "Assessing the impact of electricity interconnectors on the Great Britain's power supply in 2030," *Journal of Cleaner Production*, vol. 273, p. 122699, 2020. [Online]. Available: https://www.sciencedirect.com/science/article/pii/S0959652620327463

[38] J. E. Bistline, "Economic and technical challenges of flexible operations under large-scale variable renewable deployment," *Energy Economics*, vol. 64, pp. 363–372, 2017. [Online]. Available: https://www.sciencedirect.com/science/article/pii/S0140988317301196

[39] E. Pean, M. Pirouti, and M. Qadrdan, "Role of the gb-france electricity interconnectors in integration of variable renewable generation," *Renewable energy*, vol. 99, pp. 307–314, 2016.

[40] E. Lobato, L. Sigrist, and L. Rouco, "Value of electric interconnection links in remote island power systems: The spanish canary and balearic archipelago cases," *International Journal of Electrical Power & Energy Systems*, vol. 91, pp. 192–200, 2017.

[41] B. Cleary, A. Duffy, B. Bach, A. Vitina, A. O'Connor, and M. Conlon, "Estimating the electricity prices, generation costs and co2 emissions of large scale wind energy exports from ireland to great britain," *Energy Policy*, vol. 91, pp. 38–48, 2016.

[42] E. Lobato, L. Sigrist, and L. Rouco, "Value of electric interconnection links in remote island power systems: The Spanish Canary and Balearic archipelago cases," *International Journal of Electrical Power & Energy Systems*, vol. 91, pp. 192–200, 2017. [Online]. Available: https://www.sciencedirect.com/science/article/pii/S0142061516326084

[43] A. Tosatto, M. Dijokas, T. Weckesser, S. Chatzivasileiadis, and R. Eriksson, "Sharing reserves through hvdc: Potential cost savings in the nordic countries," *IET Generation, Transmission & Distribution*, vol. 15, no. 3, pp. 480–494, 2021.

[44] V. Trovato, A. Mazza, and G. Chicco, "Flexible operation of low-inertia power systems connected via high voltage direct current interconnectors," *Electric Power Systems Research*, vol. 192, p. 106911, 2021.

[45] A. Tosatto, T. Weckesser, and S. Chatzivasileiadis, "Market integration of hvdc lines: Internalizing hvdc losses in market clearing," *IEEE Transactions on Power Systems*, vol. 35, no. 1, pp. 451–461, 2019.

[46] V. Trovato, A. Bialecki, and A. Dallagi, "Unit commitment with inertia-dependent and multispeed allocation of frequency response services," *IEEE Transactions on Power Systems*, vol. 34, no. 2, pp. 1537–1548, 2018.

[47] O. E. Oni, I. E. Davidson, and K. N. Mbangula, "A review of lcc-hvdc and vsc-hvdc technologies and applications," in *2016 IEEE 16th International Conference on Environment and Electrical Engineering (EEEIC)*. IEEE, 2016, pp. 1–7.

[48] D. Jovcic and K. Ahmed, "Vsc hvdc applications and topologies, performance and cost comparison with lcc hvdc," *High voltage direct current transmission: Converters, systems and DC grids,*, pp. 137–163, 2019.

[49] M. Yu, A. Dyśko, C. D. Booth, A. J. Roscoe, and J. Zhu, "A review of control methods for providing frequency response in vsc-hvdc transmission systems," in *2014 49th International Universities Power Engineering Conference (UPEC)*. IEEE, 2014, pp. 1–6.

[50] J. Fradley, R. Preece, and M. Barnes, "Vsc-hvdc for frequency support (a review)," in *13th IET International conference on AC and DC power transmission (ACDC 2017)*. IET, 2017, pp. 1–6.

[51] J. Beerten, S. Cole, and R. Belmans, "Generalized steady-state vsc mtdc model for sequential ac/dc power flow algorithms," *IEEE Transactions on Power Systems*, vol. 27, no. 2, pp. 821–829, 2012.

[52] P. Joskow and J. Tirole, "Merchant transmission investment," *The Journal of industrial economics*, vol. 53, no. 2, pp. 233–264, 2005.

[53] W. Hogan, J. Rosellón, and I. Vogelsang, "Toward a combined merchant-regulatory mechanism for electricity transmission expansion," *Journal of regulatory Economics*, vol. 38, pp. 113–143, 2010.

[54] Y. G. Rebours, D. S. Kirschen, M. Trotignon, and S. Rossignol, "A survey of frequency and voltage control ancillary services—part i: Technical features," *IEEE Transactions on power systems*, vol. 22, no. 1, pp. 350–357, 2007.

[55] H. Chvez, R. Baldick, and J. Matevosyan, "The joint adequacy of agc and primary frequency response in single balancing authority systems," *IEEE Transactions on Sustainable Energy*, vol. 6, no. 3, pp. 959–966, 2015.

[56] L. Zhang, T. Capuder, and P. Mancarella, "Unified unit commitment formulation and fast multi-service lp model for flexibility evaluation in sustainable power systems," *IEEE Transactions on Sustainable Energy*, vol. 7, no. 2, pp. 658–671, 2015.

[57] A. De Paola, V. Trovato, D. Angeli, and G. Strbac, "A mean field game approach for distributed control of thermostatic loads acting in simultaneous energy-frequency response markets," *IEEE Transactions on Smart Grid*, vol. 10, no. 6, pp. 5987–5999, 2019.

[58] Rte-france.com, "Electricity consumption in france," 2020. [Online]. Available: https://www.rte-france.com/en/eco2mix/electricity-consumption-france

[59] "A survey comparing centralized and decentralized electricity markets," vol. 40, p. 100812, 2022.

[60] E. Parliament, "Regulation (ec) no 714/2009 of the european parliament and of the council of 13 july 2009 on conditions for access to the network for cross-border exchanges in electricity and repealing regulation (ec) no 1228/2003," Tech. Rep., 2009.

[61] A. Gautier, *Merchant interconnectors in Europe – Merits and value drivers.* European University Institute, 2020.

[62] W. W. Hogan, "Market-based transmission investments and competitive electricity markets," *Electric choices: deregulation and the future of electric power*, pp. 135–162, 1999.

[63] S. Littlechild, "Merchant and regulated transmission: theory, evidence and policy," *Journal of Regulatory Economics*, vol. 42, no. 3, pp. 308–335, Dec. 2012. [Online]. Available: https://doi.org/10.1007/s11149-012-9189-0

[64] M. Karimi, M. Kheradmandi, and A. Pirayesh, "Merchant transmission investment by generation companies," *IET Generation, Transmission & Distribution*, vol. 14, no. 21, pp. 4728–4737, 2020, _eprint: https://ietresearch.onlinelibrary.wiley.com/doi/pdf/10.1049/iet-gtd.2020.0185. [Online]. Available: https://ietresearch.onlinelibrary.wiley.com/doi/abs/10.1049/iet-gtd.2020.0185

[65] H. Chao and R. Wilson, "Coordination of electricity transmission and generation investments," *Energy Economics*, vol. 86, p. 104623, 2020. [Online]. Available: https://www.sciencedirect.com/science/article/pii/S0140988319304207

[66] I. C. Gonzalez Romero, S. Wogrin, and T. Gómez, "Review on generation and transmission expansion co-planning models under a market environment," *IET Generation, Transmission & Distribution*, vol. 14, no. 6, pp. 931–944, 2020, _eprint: https://ietresearch.onlinelibrary.wiley.com/doi/pdf/10.1049/iet-gtd.2019.0123. [Online]. Available: https://ietresearch.onlinelibrary.wiley.com/doi/abs/10.1049/iet-gtd.2019.0123

[67] V. Ahlqvist, P. Holmberg, and T. Tangerås, "A survey comparing centralized and decentralized electricity markets," *Energy Strategy Reviews*, vol. 40, p. 100812, 2022. [Online]. Available: https://www.sciencedirect.com/science/article/pii/S2211467X22000128

[68] Y. Liu and F. F. Wu, "Impacts of network constraints on electricity market equilibrium," *IEEE Transactions on Power Systems*, vol. 22, no. 1, pp. 126–135, 2007.

[69] J. Lavaei and S. Sojoudi, "Competitive equilibria in electricity markets with nonlinearities," in *2012 American Control Conference (ACC)*. IEEE, 2012, pp. 3081–3088.

[70] D. Aussel, P. Bendotti, and M. Pištěk, "Nash equilibrium in a pay-as-bid electricity market: Part 1–existence and characterization," *Optimization*, vol. 66, no. 6, pp. 1013–1025, 2017.

[71] J. D. Weber and T. J. Overbye, "An individual welfare maximization algorithm for electricity markets," *IEEE Transactions on Power Systems*, vol. 17, no. 3, pp. 590–596, 2002.

[72] Y. Shoham and K. Leyton-Brown, "Introduction to noncooperative game theory: Games in normal form," in *Multiagent Systems: Algorithmic, Game-Theoretic, and Logical Foundations*. Cambridge Univ. Press Cambridge, UK, 2008, pp. 47–88.

[73] S. H. Tijs, "Nash equilibria for noncooperative n-person games in normal form," *Siam Review*, vol. 23, no. 2, pp. 225–237, 1981.

[74] E. J. Anderson and H. Xu, "ε-optimal bidding in an electricity market with discontinuous market distribution function," *SIAM journal on control and optimization*, vol. 44, no. 4, pp. 1391–1418, 2005.

[75] S. Impram, S. V. Nese, and B. Oral, "Challenges of renewable energy penetration on power system flexibility: A survey," *Energy Strategy Reviews*, vol. 31, p. 100539, 2020.

[76] H. C. Bloomfield, D. J. Brayshaw, L. C. Shaffrey, P. J. Coker, and H. Thornton, "Quantifying the increasing sensitivity of power systems to climate variability," *Environmental Research Letters*, vol. 11, no. 12, p. 124025, 2016.

[77] G. Mokryani and P. Siano, "Evaluating the integration of wind power into distribution networks by using monte carlo simulation," *International Journal of Electrical Power & Energy Systems*, vol. 53, pp. 244–255, 2013.

[78] S. Ncwane and K. A. Folly, "Power System Transient Stability Considering Wind Power Generation and System Net-Load," in *2023 31st Southern African Universities Power Engineering Conference (SAUPEC)*, 2023, pp. 1–6.

[79] ——, "Impact of load variability modelling on probabilistic power system transient stability," *International Journal of Electrical and Electronic Engineering & Telecommunications*, vol. 11, no. 5, pp. 344–350, 2022.

[80] M. Alhajali, B. Fox, J. Kennedy, and D. J. Morrow, "Impact of wind variability on weakly interconnected power systems," in *IEEE PES General Meeting*. IEEE, 2010, pp. 1–6.

[81] nationalgridESO, "Future energy scenarios," 2021. [Online]. Available: https://www.nationalgrideso.com/future-energy/future-energy-scenarios/fes-2021

[82] Q. Pang, A. De Paola, V. Trovato, and G. Strbac, "Value of interconnectors operating in simultaneous energy-frequency response markets," *IEEE Transactions on Power Systems*, vol. 37, no. 5, pp. 3381–3393, 2021.

[83] C. Yingvivatanapong, W.-J. Lee, and E. Liu, "Multi-area power generation dispatch in competitive markets," *IEEE Transactions on Power Systems*, vol. 23, no. 1, pp. 196–203, 2008.

[84] Entso-e, "Tyndp 2022 - regional investment plan - baltic sea," 2022. [Online]. Available: https://eepublicdownloads.blob.core.windows.net/public-cdn-container/tyndp-documents/TYNDP2022/public/RegIP-2022-BS.pdf

[85] J.-F. Forero-Quintero, R. Villafáfila-Robles, S. Barja-Martinez, I. Munné-Collado, P. Olivella-Rosell, and D. Montesinos-Miracle, "Profitability analysis on demand-side flexibility: A review," *Renewable and Sustainable Energy Reviews*, vol. 169, p. 112906, 2022. [Online]. Available: https://www.sciencedirect.com/science/article/pii/S1364032122007882

[86] F. D'Ettorre, M. Banaei, R. Ebrahimy, S. A. Pourmousavi, E. M. V. Blomgren, J. Kowalski, Z. Bohdanowicz, B. Łopaciuk Gonczaryk, C. Biele, and H. Madsen, "Exploiting demand-side flexibility: State-of-the-art, open issues and social perspective," *Renewable and Sustainable Energy Reviews*, vol. 165, p. 112605, 2022. [Online]. Available: https://www.sciencedirect.com/science/article/pii/S1364032122005007

[87] J. A. Short, D. G. Infield, and L. L. Freris, "Stabilization of grid frequency through dynamic demand control," *IEEE Transactions on power systems*, vol. 22, no. 3, pp. 1284–1293, 2007.

[88] H. Hao, B. M. Sanandaji, K. Poolla, and T. L. Vincent, "Potentials and economics of residential thermal loads providing regulation reserve," *Energy Policy*, vol. 79, pp. 115–126, 2015. [Online]. Available: https://www.sciencedirect.com/science/article/pii/S0301421515000142

[89] ——, "Aggregate flexibility of thermostatically controlled loads," *IEEE Transactions on Power Systems*, vol. 30, no. 1, pp. 189–198, 2014.

[90] V. Trovato, S. H. Tindemans, and G. Strbac, "Leaky storage model for optimal multi-service allocation of thermostatic loads," *IET Generation, Transmission & Distribution*, vol. 10, no. 3, pp. 585–593, 2016. [Online]. Available: https://ietresearch.onlinelibrary.wiley.com/doi/abs/10.1049/iet-gtd.2015.0168

[91] V. Trovato, F. Teng, and G. Strbac, "Role and benefits of flexible thermostatically controlled loads in future low-carbon systems," *IEEE Transactions on Smart Grid*, vol. 9, no. 5, pp. 5067–5079, 2017.

[92] M. Song, W. Sun, Y. Wang, M. Shahidehpour, Z. Li, and C. Gao, "Hierarchical scheduling of aggregated tcl flexibility for transactive energy in power systems," *IEEE Transactions on Smart Grid*, vol. 11, no. 3, pp. 2452–2463, 2019.

[93] S. Córdova, C. A. Cañizares, Á. Lorca, and D. E. Olivares, "Aggregate modeling of thermostatically controlled loads for microgrid energy management systems," *IEEE Transactions on Smart Grid*, vol. 14, no. 6, pp. 4169–4181, 2023.

[94] K. Dehghanpour and S. Afsharnia, "Electrical demand side contribution to frequency control in power systems: a review on technical aspects," *Renewable and Sustainable Energy Reviews*, vol. 41, pp. 1267–1276, 2015.

[95] P. Babahajiani, Q. Shafiee, and H. Bevrani, "Intelligent demand response contribution in frequency control of multi-area power systems," *IEEE Transactions on Smart Grid*, vol. 9, no. 2, pp. 1282–1291, 2016.

[96] W. Zhang, J. Lian, C.-Y. Chang, and K. Kalsi, "Aggregated modeling and control of air conditioning loads for demand response," *IEEE transactions on power systems*, vol. 28, no. 4, pp. 4655–4664, 2013.

[97] J. Hu, J. Cao, M. Z. Chen, J. Yu, J. Yao, S. Yang, and T. Yong, "Load following of multiple heterogeneous tcl aggregators by centralized control," *IEEE Transactions on Power Systems*, vol. 32, no. 4, pp. 3157–3167, 2016.

[98] S. H. Tindemans and G. Strbac, "Low-complexity decentralized algorithm for aggregate load control of thermostatic loads," *IEEE Transactions on Industry Applications*, vol. 57, no. 1, pp. 987–998, 2020.

[99] J. Hu, J. Cao, J. M. Guerrero, T. Yong, and J. Yu, "Improving frequency stability based on distributed control of multiple load aggregators," *IEEE Transactions on Smart Grid*, vol. 8, no. 4, pp. 1553–1567, 2015.

[100] S. H. Tindemans, V. Trovato, and G. Strbac, "Decentralized control of thermostatic loads for flexible demand response," *IEEE Transactions on Control Systems Technology*, vol. 23, no. 5, pp. 1685–1700, 2015.

[101] J. L. Mathieu, M. Kamgarpour, J. Lygeros, G. Andersson, and D. S. Callaway, "Arbitraging intraday wholesale energy market prices with aggregations of thermostatic loads," *IEEE Transactions on Power Systems*, vol. 30, no. 2, pp. 763–772, 2014.

[102] E. Commission, "Trans-european networks for energy," 2022. [Online]. Available: https://energy.ec.europa.eu/topics/infrastructure/trans-european-networks-energy_en

[103] ——, "An eu strategy to harness the potential of offshore renewable energy for a climate neutral future." 2020.

[104] D. Keles, J. Dehler-Holland, M. Densing, E. Panos, and F. Hack, "Cross-border effects in interconnected electricity markets - an analysis of the Swiss electricity prices," *Energy Economics*, vol. 90, p. 104802, 2020. [Online]. Available: https://www.sciencedirect.com/science/article/pii/S0140988320301420

[105] V. Trovato, "The impact of spatial variation of inertial response and flexible inter-area allocation of fast frequency response on power system scheduling," *Electric Power Systems Research*, vol. 198, p. 107354, 2021.

[106] X. Lai, L. Xie, Q. Xia, H. Zhong, and C. Kang, "Decentralized multi-area economic dispatch via dynamic multiplier-based lagrangian relaxation," *IEEE transactions on power systems*, vol. 30, no. 6, pp. 3225–3233, 2014.

[107] A. Ahmadi-Khatir, A. J. Conejo, and R. Cherkaoui, "Multi-area unit scheduling and reserve allocation under wind power uncertainty," *IEEE Transactions on power systems*, vol. 29, no. 4, pp. 1701–1710, 2013.

[108] ENTESO-E, "Tyndp 2022 - regional investment plan - baltic sea," 2022. [Online]. Available: https://eepublicdownloads.blob.core.windows.net/public-cdn-container/tyndp-documents/TYNDP2022/public/RegIP-2022-BS.pdf.

[109] E. GROUP, "Celtic interconnector," 2020. [Online]. Available: https://www.eirgridgroup.com/the-grid/projects/celtic-interconnector/the-project/.

[110] Ofgem, "Interconnector," 2021. [Online]. Available: https://www.ofgem.gov.uk/energy-policy-and-regulation/policy-and-regulatory-programmes/interconnectors

[111] "Eirgrid grid code v12," 2013. [Online]. Available: https://www.eirgridgroup.com/site-files/library/EirGrid/GridCode.pdf.

[112] ENTSO-E, "2022 load-frequency control annual report,," 2023. [Online]. Available: https://eepublicdownloads.entsoe.eu/clean-documents/SOC%20documents/LFC/2022_ALFC_Report_FOR_PUBLISHING.pdf.

[113] J. O'Sullivan, A. Rogers, D. Flynn, P. Smith, A. Mullane, and M. O'Malley, "Studying the maximum instantaneous non-synchronous generation in an island system—frequency stability challenges in ireland," *IEEE Transactions on Power Systems*, vol. 29, no. 6, pp. 2943–2951, 2014.

[114] S. S. Torbaghan, M. Gibescu, B. G. Rawn, and M. Van der Meijden, "A market-based transmission planning for hvdc grid—case study of the north sea," *IEEE Transactions on power systems*, vol. 30, no. 2, pp. 784–794, 2014.